Physics Lib.

OCT 8 - 1935

DO NOT TAKE FROM LIBRARY
DO NOT TAKE FROM LIBRARY
copy 2

THE PHYSICAL REVIEW

VOLUME 48 *Second Series* NUMBER 7

OCTOBER 1, 1935

Published for the

AMERICAN PHYSICAL SOCIETY

by the

AMERICAN INSTITUTE OF PHYSICS
Incorporated

LANCASTER, PA., AND NEW YORK, N. Y.

THE AMERICAN PHYSICAL SOCIETY

OFFICERS OF THE SOCIETY

R. W. WOOD, *President*
The Johns Hopkins University
Baltimore, Maryland

F. K. RICHTMYER, *Vice President*
Cornell University
Ithaca, New York

W. L. SEVERINGHAUS, *Secretary*
Columbia University
New York, New York

G. B. PEGRAM, *Treasurer*
Columbia University
New York, New York

JOHN T. TATE, *Editor*
University of Minnesota
Minneapolis, Minnesota

L. B. LOEB, *Local Secretary for the Pacific Coast*
University of California
Berkeley, California

THE PHYSICAL REVIEW

BOARD OF EDITORS

JOHN T. TATE, *Editor*

J. W. BUCHTA, *Assistant Editor*

Associate Editors

K. K. DARROW
J. C. HUBBARD
A. E. RUARK
A. ELLETT
L. A. TURNER
G. E. UHLENBECK
W. V. HOUSTON
R. S. MULLIKEN
I. I. RABI

THE PHYSICAL REVIEW, which was established in 1893, is a journal of experimental and theoretical physics. It is published for the American Physical Society by the American Institute of Physics Incorporated. There are two volumes annually with twelve issues in each volume.

Manuscripts for publication should be submitted to John T. Tate, University of Minnesota, Minneapolis, Minnesota.

Proof and all correspondence concerning papers in the process of publication, should be addressed to the Editorial Secretary, American Institute of Physics, 11 East 38th Street, New York, New York.

Subscription price: United States and Possessions and Canada, $15.00; Foreign, $16.50. Subscriptions and orders for back numbers should be addressed to Prince and Lemon Streets, Lancaster, Pennsylvania, or to the American Institute of Physics, 11 East 38th Street, New York, New York.

Advertising is not accepted for the *Physical Review* but attention is called to the *Review of Scientific Instruments with Physics News and Views*, a companion publication of the Institute, and a medium through which the field of physics can be reached most effectively. Rates and other information will be furnished on request to the Editorial Secretary.

Changes of address and complaints of failure to receive the *Physical Review*, in the case of members of the American Physical Society, should be addressed to the Treasurer; in the case of other subscribers, to the Editorial Secretary. New copies can be sent free in response to complaints of non-delivery only if notice of non-delivery is received within three months of date of issue.

The Physical Review is published semi-monthly at Prince and Lemon Streets, Lancaster, Pennsylvania.

Entered at the Post Office at Lancaster, Pennsylvania, as second class matter.

Acceptance for mailing at special rate of postage provided for in section 1103, Act of October 3, 1917, authorized September 6, 1926.

THE
PHYSICAL REVIEW
A Journal of Experimental and Theoretical Physics
VOL. 48, NO. 7 OCTOBER 1, 1935 SECOND SERIES

Diffuse Scattering of X-Rays by Conduction Electrons

CLARENCE ZENER,* *Wayman Crow Hall of Physics, Washington University*
(Received July 8, 1935)

A theoretical expression is obtained for the scattering of x-rays from a completely degenerate free electron gas. Both the classical and the Compton methods are used. The modifications introduced by the periodic potential of the lattice are examined. The scattering by the conduction electrons is found to decrease with the first power of the scattering angle. It is shown that the diffuse scattering by the core electrons decreases as the second power of the angle of scattering. Hence the scattering by the conduction electrons will dominate all other diffuse scattering at sufficiently small angles.

§1.

THE QUANTUM-MECHANICAL theory of the scattering of x-rays has been thoroughly investigated.[1] In practice, however, we may wish to use classical concepts. Again, for incoherent scattering, we may find it convenient to think in terms of photons being scattered by single electrons, as in the Compton effect. In the first, the classical method, the interference between two electrons arises from the addition of the amplitudes of the scattered x-rays. In the second, the Compton method, the interference between two electrons arises through the operation of Pauli's exclusion principle. Thus an electron cannot jump into a state already occupied by another electron.

The first method gives the correct *total intensity* of scattered x-rays (relativity and resonance effects neglected). The formula developed by Raman for the ratio S of the actual scattering to that which would occur if the intensities of the scattering from each electron were added, is[2]

$$S=1+\text{time average of } N^{-1}\sum_{r\neq s}\cos k(z_r-z_s). \quad (1)$$

Here N is the total number of electrons, and

$$k=(4\pi/\lambda)\sin\phi/2,$$

where λ is the wave-length of the incident x-rays, and ϕ is the angle of scattering. Wave mechanics gives the formula[3] (relativity and resonance effects neglected)

$$S=1+\int\psi N^{-1}\sum_{r\neq s}\cos k(z_r-z_s)\psi^* dv_1\cdots dv_N. \quad (2)$$

These two expressions for S are identical if we identify the classical time average with the average over $\psi\psi^*$.

If the probability that one electron were at a given position did not depend upon the positions of other electrons, ψ could be written as a product of eigenfunctions of single electrons

$$\psi=\prod_s\psi_s(\mathbf{r}_s,\delta_s),$$

where δ_s denotes the spin variable. In this case (2) reduces to

* The author was aided in part by a grant from the Rockefeller Foundation to Washington University for research in science.

[1] See A. H. Compton, Phys. Rev. **47**, 367 (1935) for a comprehensive review of the literature.

[2] C. V. Raman, Ind. J. Phys. **3**, 359 (1928), Eq. (3).

[3] I. Waller and D. R. Hartree, Proc. Roy. Soc. **A124**, 124 (1929), Eq. (14).

$$S=1+N^{-1}\sum_{n\neq n'} f_{nn}f_{n'n'}.$$

We shall use the notation

$$f_{nn'}=\int \psi_n \cos kz \psi_{n'}^* dv$$

with the convention that the integral is zero when n and n' refer to states with opposite spins. The second term usually represents constructive interference. Thus two electrons bound to the same atom may move independently of one another, but their mere confinement to the same atom gives constructive interference, at least at small angles.

The probability of one electron being at a definite position is dependent upon the presence of the other electrons by virtue of Pauli's exclusion principle. This principle is taken explicitly into account by writing the wave function in the form

$$\psi=\sum_P (-1)^{\sigma_P} P \prod_s \psi_s(\mathbf{r}_s, \delta_s).$$

Here P is an operator which permutes the coordinates (including the spin coordinate) of the electrons, and σ_P is the order of the permutation. With this wave function (2) becomes[3]

$$S=1+N^{-1}\sum_{n\neq n'} (f_{nn}f_{n'n'}-f^2_{nn'}). \qquad (3)$$

The last term is intrinsically negative. Its interpretation depends upon our picture of the scattering process. According to the Raman viewpoint, Pauli's exclusion principle lessens the constructive interference between electrons of like spin. According to the Compton viewpoint, Pauli's exclusion principle prohibits those collisions between photons and electrons in which the recoil electron would find itself in a state already occupied by another electron of like spin.

The first purpose of this paper is to discuss in detail the scattering of x-rays in a case where both methods may be carried out exactly (§2 and §3). This case is the scattering by a free electron gas. The second purpose is to examine the scattering by the conduction electrons of actual metals (§4). Finally, we investigate the conditions where this scattering may be observed (§5).

§2.

From the classical standpoint the scattering of x-rays from a free electron gas presents the same problem as the scattering from a monatomic liquid. In the first problem we must find the interference between the individual electrons, while in the second we must find the interference between the individual atoms. The following analysis for a free electron gas follows step by step the well-known analysis[4] for a monatomic liquid.

The probability that a particular electron lies within the volume element dv_m at the same time that another particular electron lies within the volume element dv_n is

$$P(dv_m/V)(dv_n/V),$$

where V is the total volume of the electron gas. Since the medium is isotropic, P is a function only of the distance r between the two volume elements, i.e., between the two electrons. Eq. (1) may now be transformed to[5]

$$S=1-n4\pi\int_0^\infty (1-P)\frac{\sin kr}{kr} r^2 dr, \qquad (4)$$

where n is the density of electrons.

If the electrons moved independently of one another, then $P=1$, and the interference would average out to zero. Actually, Pauli's exclusion principle tends to keep electrons of like spin apart. Since the configurations favorable to constructive interference are thereby reduced, the average interference will be destructive, at least for small angle scattering.

The function $1-P$ for a free electron gas is[6]

$$1-P=(9/2)\left(\frac{\sin (r/d)-(r/d)\cos (r/d)}{(r/d)^3}\right)^2. \qquad (5)$$

Here $d=\lambda_0/2\pi$, where λ_0 is the wave-length of the fastest electrons, namely, $2(3n/\pi)^{-1/3}$. $1-P$ has been plotted in Fig. 1a. It has the important property that

$$n4\pi\int_0^\infty (1-P)r^2 dr=1,$$

i.e., the integral of the "electron hole" density is equivalent to one positive electron. Hence scattering in the forward direction will be completely destroyed by interference.

[4] Compton and Ellis, *X-Rays in Theory and in Experiment* (1935), pp. 177–185.
[5] Reference 4, Eq. (3.80).
[6] E. Wigner and F. Seitz, Phys. Rev. **43**, 807 (1933).

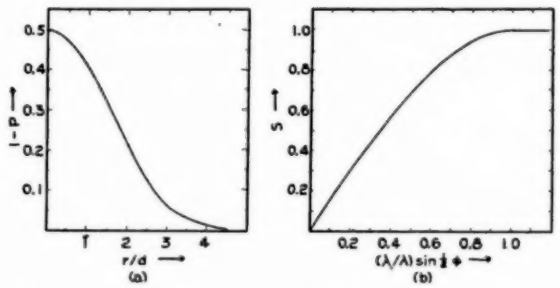

FIG. 1. Classical representation of scattering by free electron gas. The "electron hole" density (a) gives rise by destructive interference to an S value (b) less than unity.

In order to obtain an explicit expression for S, we have merely to substitute (5) into (4). We obtain (see Fig. 1b)

$$S=\begin{cases}(1/2)(3x-x^3), & x<1\\ 1 \qquad\qquad , & x>1,\end{cases} \tag{6}$$

with $x=kd/2=(\lambda_0/\lambda)\sin(\phi/2)$.

The method of performing the integration in (4) will be briefly sketched. We obtain with obvious transformations

$$S=1-\left(\frac{3}{2\pi ix}\right)\int_{-\infty}^{\infty}\left(\frac{\sin z-z\cos z}{z^3}\right)^2 e^{i2xz}z\,dz.$$

Since the integrand has no poles in the complex plane, we may choose any path for the integration, say the path Γ_1 of Fig. 2. Express the integrand as the sum of three terms, containing the factors $\exp 2i(x+1)z$, $\exp 2ixz$, $\exp 2i(x-1)z$, respectively. The integral of the first two terms vanishes, since no pole lies between the path Γ_1 and an infinite semicircle in the upper half-plane, on which the two terms vanish. If $x>1$, the third term likewise vanishes. Now the integral of the third term along Γ_1 is equal to $-2\pi i$ times its residue at $z=0$, plus its integral taken along the path Γ_2. If $x<1$, this integral along Γ_2 vanishes, since the integrand is zero along an infinite semicircle in the lower half-plane. We are thus left with $-2\pi i$ times the residue of the third term at $z=0$. This leads us directly to (6).

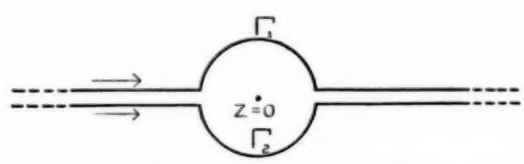

FIG. 2. Paths of integration used in evaluating S.

§3.

In the case of a free electron gas, Eq. (3) reduces to

$$S=1-N^{-1}\sum_{n\neq n'} f_{nn'}{}^2.$$

A simple phenomenological interpretation of this equation is the following.

We regard the scattering of x-rays as the simple Compton scattering of photons by individual electrons. The intensity of scattering in any direction is given by the Thomson formula (apart from relativity corrections). During the collision the scattering electron suffers a change of momentum which is calculable from the principles of conservation of energy and of momentum. Since the wave properties of the photon are not considered, constructive and destructive interference between two electrons does not occur. However, we must recognize that the electrons obey Pauli's exclusion principle. We thus exclude those collisions for which the final quantum state of the electron is already occupied. In the case of a (completely degenerate) Fermi gas, the final momentum must thus lie outside the Fermi surface in momentum space.

The scattering factor S may thus be calculated as follows. We calculate the momentum $\mathbf{\Delta p}$,

$$|\mathbf{\Delta p}|=(2h\nu/c)\sin(\phi/2),$$

which an electron must absorb to scatter a photon through the angle ϕ. Then $S(\phi)$ is equal to that fraction of the volume inside the Fermi

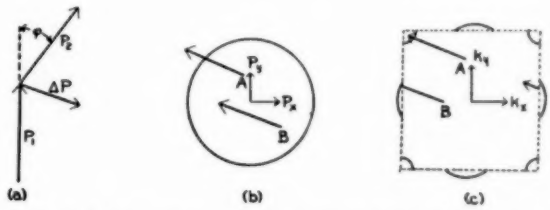

FIG. 3. Compton representation of scattering by a free electron gas. The momentum change of a photon (a) during a collision is accompanied by an opposite change in momentum of the scattering electron (b). Electrons at such positions as A in momentum space are effective, while those in such positions as B are not effective. (c) is a schematic diagram analogous to (b) for the case of conduction electrons. The full lines represent the Fermi surface. The dotted square represents the boundary of the (multiply connected) first zone.

surface for which $\mathbf{\Delta p}+\mathbf{p}$ lies outside the Fermi surface (see Fig. 3). A simple calculation shows that this fraction is given by Eq. (6).

§4.

In an actual metal the conduction electrons are not entirely free. A quantum state may no longer be specified by its momentum. Instead, each quantum state is specified by a vector $\mathbf{k}$ which, however, has many properties analogous to that of momentum.[7] In particular, if a photon changes its momentum by $\mathbf{\Delta p}$ in colliding with an electron, the electron must change its $\mathbf{k}$ vector by an amount $\mathbf{\Delta k}=-\mathbf{\Delta p}$. Thus only those states $\mathbf{k}$ are effective in this particular type of scattering for which the state $\mathbf{k}-\mathbf{\Delta p}$ is unoccupied.

The only difference between conduction and free electrons which we need consider is that in the former the Fermi surface in k space is not necessarily a sphere. In fact, k space is divided into an infinite number of zones, each zone being multiply connected.[8] At small angle scattering only transitions between states in the same zone are important.

As the angle of scattering is decreased it is thus evident that S becomes proportional to the area of the Fermi surface. In divalent metals there are just enough conduction electrons to fill the first zone. Hence as the binding in these metals becomes stronger (case of poor conductors) the area of the Fermi surface, together with S, becomes smaller. For extremely tight binding (case of insulators) the area of this surface vanishes.

[7] An excellent review of the quantum theory of conduction electrons is given by H. Bethe, *Handbuch der Physik* (1933), Vol. 24, No. 2.

[8] For example, see reference 7, Fig. 19.

§5.

It remains to investigate the conditions under which diffuse scattering from conduction electrons may be experimentally observed. It is necessary of course that the scattering due to the conduction electrons be comparable to the scattering due to the core electrons.

The diffuse scattering due to each core is given by[9]

$$I=I_e\{(Z'-f^2/Z')+(1-e^{-2M})f^2\}.$$

Here I_e is the Thomson scattering of a single electron, Z' is the number of electrons per core. The structure factor f is given approximately by

$$(4\pi/k)\int_0^\infty u(r)\sin(kr)rdr,$$

where $u(r)$ is the density of the core electrons, and $k=(4\pi/\lambda)\sin(\phi/2)$. For our present purpose we need only know that the temperature dependent Debye-Waller term M contains k^2 as a factor.

Inspection shows that a Taylor expansion of I starts with k^2. The expansion of the first term starts with k^2 since $f(k)$ is an even function of k, and $f(o)=Z'$. That the expansion of the second term starts with k^2 is evident from the dependence of M upon k.

Hence the diffuse scattering from the core electrons at small angles varies as ϕ^2. From Eq. (6) we see that the diffuse scattering by the conduction electrons varies as ϕ. Hence at sufficiently small angles the latter will become greater than the former. Calculation shows that for the particular case of lithium at room temperature the two types of scattering become equal at scattering angles such that

$$(A/\lambda)\sin(\phi/2)=0.04.$$

[9] G. E. M. Jauncey, Phys. Rev. **37**, 1193 (1931); Y. H. Woo, Phys. Rev. **38**, 6 (1931).

Extra Negative Term in the Incoherent Part of the Diffuse Scattering of X-Rays from Neon-Like Crystals

G. E. M. JAUNCEY* AND J. H. DEMING, *Washington University, St. Louis*

(Received July 8, 1935)

Following the suggestion of Harvey, Williams and Jauncey that experimental evidence for the need of the Waller-Hartree extra negative term which arises from the Pauli exclusion principle can best be obtained in the diffuse scattering of x-rays from crystals, careful measurements of the S_{exp} values for NaF, MgO and SiC have been made at 295°K using the method of Jauncey and Claus. Various precautions are described. Since the theoretical S_{th} values depend somewhat critically upon the characteristic temperature Θ for a given crystal, a discussion of the determination of Θ from specific heat data is given. It is shown that for x-ray purposes the proper value for Θ is that obtained from specific heat data for fairly low temperatures even though the temperature at which x-ray scattering occurs may be fairly high. Tables of quantum-mechanical f and ΣE_r^2 values extend only to $(\sin\phi/2)\lambda = 1.1$. Beyond this the crystals approach neon gas in their scattering and it was found that Brown's analytical formula for neon gives better agreement with experiment than does Froman's extrapolation formula. The experimental results showed excellent agreement with the Waller-Hartree theory and thus give definite evidence for the operation of the Pauli exclusion principle on the outer shell electrons. Some remarks on the classical analog of the extra term are included. A special discussion of the results for SiC is given.

1. INTRODUCTION

THE theory of the diffuse scattering of x-rays from crystals leads to the formula[1]

$$S = S_{\text{coh}} + S_{\text{inc}}/(1+\alpha \text{ vers } \phi)^3, \qquad (1)$$

in which S_{coh} and S_{inc} refer respectively to the coherent and incoherent parts of the scattered rays. For crystals consisting of two kinds of atoms

$$S_{\text{coh}} = \{f_1^2(1-e^{-M_1}) + f_2^2(1-e^{-M_2})\}/(Z_1+Z_2) \quad (2a)$$

and Waller and Hartree's theory of x-ray scattering[2] requires that

$$S_{\text{inc}} = 1 - \{\Sigma(E_{jj}^2)_1 + \Sigma(E_{jj}^2)_2\}/(Z_1+Z_2) - \{\sum_{j\neq k}|E_{jk}|_1^2 + \sum_{j\neq k}|E_{jk}|_2^2\}/(Z_1+Z_2), \quad (2b)$$

in which the symbols have previously been defined[3] and the numerical subscripts refer to the two kinds of atoms. Because of its algebraic sign, the term containing the subscripts jk has been called the extra negative term.[4] Harvey, Williams and Jauncey[3] have pointed out that the most favorable situation for showing the need for the extra negative term is in the diffuse scattering of x-rays from crystals. In addition, they have calculated the values of $\Sigma|E_{jk}|^2$ for neon. Values of f, the atom form factor, and of ΣE_{jj}^2 have been calculated by James and Brindley[5] and by Heisenberg,[6] respectively. Tables of these values are now given by Compton and Allison.[7] We have used the values for Mg^{+2}, Na^+, F^-, O^{-2} in calculating the theoretical values for our crystals of NaF and MgO.

Compton[8] remarks that there seems to be no exact classical analog of the extra negative term, although he suggests that it represents the constraints upon each electron's motion due to the presence of the other electrons in the atom. At a recent symposium on x-ray scattering, Jauncey[9] also suggested this idea of constraints between electrons. In his extension of the Raman-Compton[10, 11] classical theory of x-ray scattering, Jauncey[12] introduced the probability distribution function $p(z_1, z_2, \cdots z_n)dz_1dz_2\cdots dz_n$ for the probability of electrons 1, 2, $\cdots$ n being in dz_1, dz_2 $\cdots$ dz_n at z_1, z_2, $\cdots$ z_n, respectively, from the center of the atom. Jauncey then made the simplifying assumption

* The senior author was aided in part by a grant from the Rockefeller Foundation to Washington University for research in science.

[1] G. E. M. Jauncey, Phys. Rev. **42**, 453 (1932).
[2] I. Waller and D. R. Hartree, Proc. Roy. Soc. **A124**, 119 (1929).
[3] G. G. Harvey, P. S. Williams and G. E. M. Jauncey, Phys. Rev. **46**, 365 (1934).
[4] E. O. Wollan, Phys. Rev. **43**, 955 (1933).
[5] R. W. James and G. W. Brindley, Phil. Mag. **12**, 81 (1931).
[6] W. Heisenberg, Physik. Zeits. **32**, 737 (1931).
[7] A. H. Compton and S. K. Allison, *X-Rays in Theory and Experiment*, pp. 781, 782.
[8] A. H. Compton, Phys. Rev. **47**, 367 (1935).
[9] G. E. M. Jauncey, Phys. Rev. **47**, 196 (1935).
[10] C. V. Raman, Ind. J. Phys. **3**, 357 (1928).
[11] A. H. Compton, Phys. Rev. **35**, 925 (1930).
[12] G. E. M. Jauncey, Phys. Rev. **37**, 1193 (1931).

$$p(z_1, z_2, \cdots z_n) = p_1(z_1) \cdot p_2(z_2) \cdots p_n(z_n). \quad (3)$$

This means that the probability distribution function for any one electron is independent of the position of any other electron in the atom. This assumption leads in the case of crystals consisting of atoms of one kind or of monatomic gases to

$$S_{\text{inc}} = 1 - (\sum_{r=1}^{Z} E_r^2)/Z, \quad (4)$$

where for the rth electron

$$E_r = \int p_r \cos kz_r dz_r \quad (5)$$

and $k = 4\pi(\sin \phi/2)/\lambda$. If, however, the probability distribution function for one electron is not independent of the positions of the other electrons in the atom, the relation (3) no longer holds and S_{inc} is no longer given by (4). As an example of the change in S_{inc} caused by introducing constraints, let us consider the two models of the helium gas atom discussed by Compton.[11] In the first model each electron is at random on a sphere of radius b. In this case

$$p(z_1, z_2) = p_1(z_1) \cdot p_2(z_2), \quad (6)$$

where

$$\begin{aligned} p_1(z_1) = p_2(z_2) &= 1/2b, \quad -b < z < b \\ &= 0, \qquad |z| > b \end{aligned} \quad (7)$$

and we arrive at

$$f = \sum_{r=1}^{Z} E_r = 2(\sin kb)/kb, \quad (8)$$

$$S_{\text{coh}} = f^2/Z = 2(\sin^2 kb)/k^2b^2 \quad (9a)$$

and

$$S_{\text{inc}} = 1 - (\sin^2 kb)/k^2b^2. \quad (9b)$$

In the second model, each electron is again on a sphere of radius b but the two electrons are always at opposite ends of a diameter. Now, although (7) is true, the relation (6) is not true. For the second model, Debye[13] gives

$$S = 1 + (\sin 2kb)/2kb. \quad (10)$$

[13] P. Debye, Ann. d. Physik **46**, 809 (1915).

According to the classical theory the coherent part of the rays scattered from an atom can be eliminated in all directions, except the Laue directions, by assembling many like atoms into a perfect lattice.[14] The scattering which does occur in the non-Laue directions is then incoherent. Using this criterion, we find that

$$S_{\text{inc}} = 1 + (\sin 2kb)/2kb - 2(\sin^2 kb)/k^2b^2. \quad (11)$$

This expression differs from (9b) because of the electrons being constrained to move at the opposite ends of a diameter. Each model has the same atom form factor (8) and so for either model of helium gas S_{coh} is given by (9a).

A comparison of Williams' experimental S values[15] for NaF with theory indicates a better agreement when the extra negative term is included than when not.[3] However, the discrepancy between theory and experiment is too great for comfort; and, in view of the importance of the theory, a more accurate test of the formula was considered necessary, and so this present research was undertaken.

2. Experimental Method

Following the method described by Jauncey and Claus,[16] we used the continuous spectrum from a tungsten target tube operated at 34.3 kv peak and 8 ma. As always, great care was taken in evading Laue spots. The distribution of intensity in the continuous spectrum was obtained by reflection from calcite and is shown in Fig. 1. This curve is uncorrected for change in the reflecting power of the calcite for different wavelengths. Thicknesses of aluminum sufficient to reduce the intensity of the primary rays from 1.00 to 0.86, 0.61, 0.42, and 0.22, respectively, were determined experimentally. The reduction of total intensity in the continuous spectrum due to each of these thicknesses was calculated as previously described[16] and found to agree very well with each of the respective values just

[14] This is evident from the fact that the double summation in Jauncey and Harvey's paper (Phys. Rev. **37**, 1203 (1931)) becomes zero when the atom centers are always exactly at lattice points and there is thus no thermal motion.

[15] P. S. Williams, Phys. Rev. **46**, 83 (1934).

[16] G. E. M. Jauncey and W. D. Claus, Phys. Rev. **46**, 941 (1934).

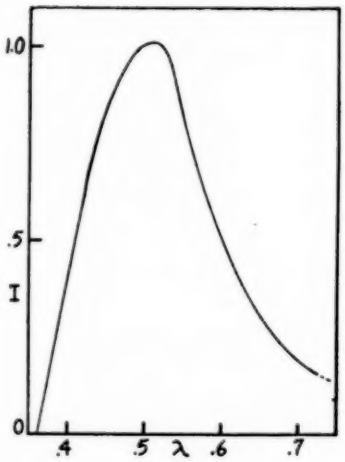

FIG. 1. Spectral distribution curve for the x-rays falling upon, but not penetrating through, the crystals.

given. It seemed better not to attempt any correction of the curve of Fig. 1.

Instead of comparing the intensity of the rays scattered from the crystal under observation with that of the rays scattered from paraffin as was usually done by Jauncey and Claus,[16] we always compared the intensity of the diffusely scattered rays with that of the primary rays penetrating the crystal. To do this we cut off a flash of primary rays of duration 1/60 sec. by means of a pendulum. We then calculated

$$S_{\text{exp}}=(R^2W/ANZ\rho t)\cdot(2\cos\phi/2)/(1+\cos^2\phi)\cdot(m^2c^4/e^4)\cdot D_\phi/D, \quad (12)$$

where D_ϕ is the ion current due to the rays scattered in a direction ϕ, D is that due to the primary rays transmitted through the crystal slab, and the remaining quantities have previously been defined.[17] It is to be noted that the ratio D_ϕ/D is of the order 1/10,000. The disparity in the concentration of the ions in the ionization chamber is even greater than this because of the fact that the primary beam is fairly narrow. It was feared that there might be some unsuspected ion-recombination effect. We therefore reduced D from 1.00 to 0.66, 0.25, and 0.11 and obtained no certain change in the ratio D_ϕ/D, as compared with the corresponding theoretical value of D_ϕ/D, for a scattering angle of 30°. Since D_ϕ/D is not a function of D, we conclude that the experimental D_ϕ and D are saturation values. Of course, we had, in addition, applied the usual test for saturation by varying the voltage across the ionization chamber. We estimate our experimental error at about 0.02 in the S_{exp} values.

[17] G. E. M. Jauncey and Ford Pennell, Phys. Rev. **43**, 505 (1933).

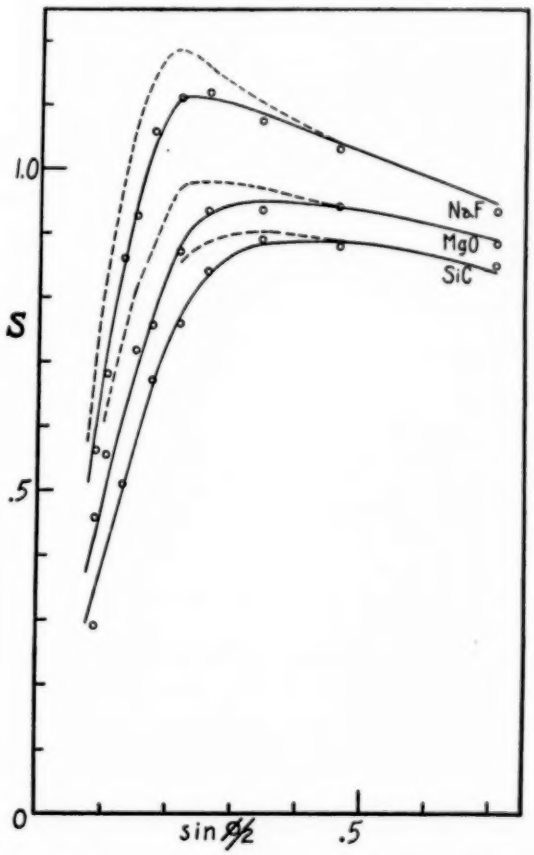

FIG. 2. Comparison of theory and experiment. Full curves include the Waller-Hartree extra negative term; broken curves do not.

The values of S_{exp} for single crystal slabs of NaF, MgO and SiC (carborundum) are given in Table I and are shown as circles in Fig. 2. The

TABLE I. S_{exp} *values.*

sin ϕ/2	NaF	MgO	SiC
0.087	0.56	0.46	0.29
.104	0.68	0.55	—
.130	0.86	—	.51
.148	0.93	.72	—
.174	1.06	.76	.67
.216	1.11	.87	.76
.259	1.12	.93	.84
.342	1.08	.93	.89
.462	1.03	.94	.88
.707	0.93	.88	.85

values of ρt for the crystal slabs were: NaF, 0.349; MgO, 0.681; SiC, 0.326 g/cm^2. It is to be noted that our S_{exp} values are all absolute and that there has been no fitting of the experimental and theoretical values at any point.

3. Comparison with Theory

The theoretical quantity S_{th} is defined by[17]

$$S_{th}=\int\left\{S_{coh}+\frac{S_{inc}K_\phi T_\phi}{K_0(1+\alpha \text{ vers } \phi)^3}\right\}Id\lambda\Big/\int Id\lambda, \tag{13}$$

where I is a function of λ representing the distribution of intensity in the spectrum of the x-rays penetrating the crystal slab, so set that the normal to the slab bisects the angle of scattering. The spectral distribution curve shown in Fig. 1 is not the curve of I *vs.* λ used in (13) but is the distribution curve for the x-rays falling on the slab. Knowing the absorption coefficients for various wave-lengths in a given crystal slab and knowing its effective thickness $t/(\cos\phi/2)$, the curve of I *vs.* λ for the rays penetrating the crystal can easily be calculated from Fig. 1. There is a separate curve for each angle of scattering and for each crystal.

From (2a) we see that it is necessary to know the Debye-Waller exponents M_1 and M_2. In the case of cubic crystals consisting of atoms of nearly equal mass, M_1 may be taken as equal to M_2. This is the case for NaF. Also $M_1\sim M_2$ when the experimental temperature, which for our experiments was 295°K, is considerably lower than the characteristic temperature of the crystal. This is the case for MgO and SiC. Waller's theory[18] shows that at temperatures below the characteristic temperature it is the mass per unit volume[19] which is involved in the formula for M, and so we have used the average atomic weight in this formula. But, before M can be calculated, the characteristic temperature Θ must be known. Shonka[20] has obtained $\Theta=442$°K for NaF by comparing the intensities of the various Debye-Scherrer circles for the powdered crystal at 295°K with the intensities of the corresponding circles for 86°K. Unfortunately, we are unaware of any x-ray determination of Θ for MgO or SiC. We find that the uncertainties in the values of Θ as calculated from specific heat data lead to variations in S_{th} which are greater than our experimental error in S_{exp} and are a considerable fraction of the change in S_{th} expected as the result of the inclusion or otherwise of the Waller-Hartree extra negative term.

In order to obtain a method of calculating Θ from specific heat data which will be valid for x-ray purposes, we have taken the tabulated specific heat values for NaCl and KCl[21] and for NaF.[22] We have changed these values from C_p to C_v by means of the formulas[23]

$$C_p-C_v=C_p^2T\times.0214/T_m, \tag{14}$$

where T_m is the melting point, and

$$C_p-C_v=\beta^2MT/K\rho, \tag{15}$$

where β is the coefficient of volume expansion, M the molecular weight, K the compressibility and ρ the density of the crystal. The values of C_v for our crystals determined by either formula are in good agreement, but lack of extensive thermal data makes (14) the more useful. We then compared the C_v values with a table of Debye's specific heat function[24] and found the corresponding Θ/T values. Knowing the temperature for each of these values, we have calculated values of Θ and have then plotted curves of Θ *vs.* Θ/T as shown in Fig. 3. It is seen that the points give evidence of falling on curves which approach a constant value. The dotted lines show the values of Θ which are satisfactory for x-ray purposes as found by Shonka for NaF, by James and Brindley[25] for KCl, and by James and Firth[26] for NaCl. It is seen that the x-ray value of Θ for each of these crystals corresponds to the constant value which is obtained from specific heat data at fairly low temperatures. The specific heat values of Θ for MgO[21] are also shown

[18] I. Waller, Diss. Uppsala (1925).
[19] Dr. C. Zener of this laboratory has informed us of this interesting theoretical fact.
[20] J. J. Shonka, Phys. Rev. **43**, 947 (1933).
[21] Int. Crit. Tables, V, 91.
[22] Int. Crit. Tables, V, 100.
[23] See F. K. Richtmyer, *Introduction to Modern Physics*, (first edition) pp. 244, 245.
[24] See J. K. Roberts, *Heat and Thermodynamics*, p. 404.
[25] R. W. James and G. W. Brindley, Proc. Roy. Soc. **A121**, 155 (1928).
[26] R. W. James and E. Firth, Proc. Roy. Soc. **A117**, 62 (1927).

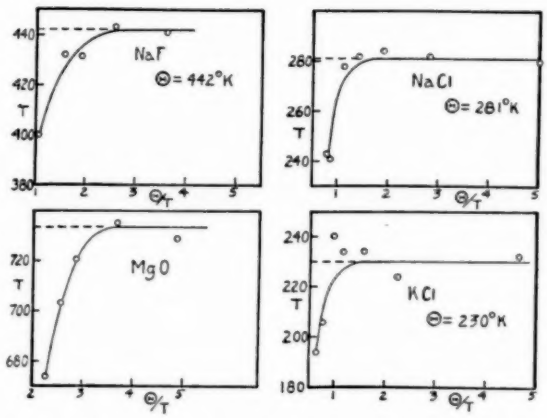

FIG. 3. Characteristic temperature curves obtained from specific heat data. The value of Θ shown in the body of each graph is that most suitable for x-ray purposes. Errata: The ordinates should be labeled Θ instead of T.

in Fig. 3. It seems, therefore, that the x-ray value of Θ for MgO should be 734°K.

The rest of the calculation of the S_{th} values was done as described by Jauncey and Claus,[16] these values being averaged for ionization chamber window width and height and for cross-sectional area of the primary beam of x-rays at small angles of scattering. The full curves of Fig. 2 show the S_{th} values in which the Waller-Hartree extra negative term has been included, while the broken curves are for the omission of this term. The agreement of experiment with the Waller-Hartree theory is remarkably good. It should be noted that it is necessary in the case of MgO to use Θ = 734°K and not 674°K (shown as the lowest value in Fig. 3) in order to get an agreement between theory and experiment. If one assumes the Waller-Hartree theory to be correct, this means that the x-ray value of Θ for MgO is about 734°K. Our results also imply the excellence of the quantum-mechanical f and ΣE_r^2 values as calculated approximately by James and Brindley and by Heisenberg.[27]

[27] These values do not extend beyond $(\sin\phi/2)/\lambda = 1.1$ and some kind of extrapolation becomes necessary at the larger angles of scattering. We have found that Brown's (Phys. Rev. **44**, 214 (1933)) analytical formula for neon gives much better agreement with experiment for all three crystals than does Froman's extrapolation formula (Phys. Rev. **36**, 1339 (1930)).

The experimental points and theoretical curves for SiC are worthy of comment. The ions in NaF and MgO are neon-like, but there is no certainty that the Si and C atoms become quadruply ionized and therefore neon-like. Also we were hard put to it to determine Θ for SiC. The structure of this crystal is more complicated than that of NaF or MgO. Perhaps for this reason, when we tried to determine Θ by the method of Fig. 3, we found no tendency for the points to fall on a curve similar to those of Fig. 3. We therefore resorted to an average value which we took as 1023°K. Using this value and assuming the ions C^{-4} and Si^{+4}, we obtained the theoretical curves shown.[28] The numerical values of the Waller-Hartree extra negative term as worked out by Harvey, Williams and Jauncey[3] are for neon, and in this paper we have assumed these neon values to be valid for neon-like ions. The formulas given by Waller and Hartree only apply to cases where the outer shell of electrons is complete. We do not know how to correct for the operation of the Pauli exclusion principle in other cases, and so we have made no attempt to calculate values of S_{th} for SiC for possibilities other than Si^{+4} and C^{-4}. It is probably a coincidence, but it is possibly of interest, that the experimental points for SiC fall so well on the Waller-Hartree curve for the quadruply ionized atoms.

The authors wish to thank Dr. Preston Harris, Chemistry Department, Ohio State University for the crystal of MgO and Mr. R. C. Brenner, Director of the Research Laboratory, Carborundum Company for the large crystals of SiC.

[28] The following f and ΣE_r^2 values were necessary for our calculation of S_{th} values but were not available in the literature. Using the information contained in James and Brindley's paper[5] we have obtained

$(\sin\phi/2)/\lambda$	0.0	0.1	0.2	0.3	0.4	0.5	0.6	0.7	0.8	0.9	1.0	1.1
$f(C^{-4})$	10.0	6.2	3.7	2.6	1.9	1.7	1.6	1.4	1.3	1.2	1.0	0.9
$\Sigma E_r^2(C^{-4})$	10.0	5.8	3.1	1.65	1.4	1.3	1.0	0.8	0.7	0.6	0.5	0.4
$\Sigma E_r^2(Si^{+4})$	10.0	9.4	8.3	6.8	5.2	4.0	3.1	2.5	2.0	1.8	1.65	1.5

These values should be useful to other workers in this field.

On the Structure and Interpretation of the Infrared Absorption Spectra of Crystals

R. BOWLING BARNES, R. ROBERT BRATTAIN, *Palmer Physical Laboratory, Princeton University,*
AND
FREDERICK SEITZ, *Physics Department, University of Rochester*

(Received July 19, 1935)

An experimental and theoretical investigation of the absorption spectrum of MgO in the near infrared is reported. Part A is devoted to the experimental results, which were obtained by use of a rocksalt spectrometer. They show that the fundamental absorption is accompanied by a great deal of secondary structure. In Part B an interpretation of the results of A is undertaken on the basis of a quantum-mechanical treatment of anharmonic potential forces. On this basis, it is shown that a cubic crystal of the MgO type should not possess but a single near infrared absorption as previous calculations had indicated, but should possess an extremely complicated secondary structure. In Part C the possibilities of obtaining a quantitative correlation between experiment and theory are discussed and it is concluded that the former must be made the object of additional refinements.

INTRODUCTION*

IN the work to be described in the following paper, both experimental and theoretical investigations were carried on and are published here simultaneously. In order to keep them somewhat apart, we have decided to present the details of the first in Part A and those of the second in Part B, and to present a general account of their connection in the introduction and the conclusion.

As a result of conclusions drawn from the classical theory of crystal structure of Madelung, Born, von Kármán and other workers in the field,[1] it was generally believed until the past few years, that a cubic crystal possessed but one absorption frequency, corresponding to a motion in which like ions move together and unlike ions are 180° out of phase. For the alkali-halide crystals, this fundamental should be expected to vary inversely as the effective mass $m_1m_2/(m_1+m_2)$ of the two ions, and in fact, it was found that those corresponding to LiF, NaCl and KBr are at wave-lengths 32.6, 61.1 and 83.3μ, respectively. It is as a result of this fact that these crystals show a large transparency in the near infrared, KI being transparent as far out as 33μ.

Because of the supposed simplicity of their spectra, it was concluded that they should be ideal substances on which to test the classical theory of dispersion in the infrared, and in 1930 Czerny[2] presented the results of his attempt to use NaCl for this purpose. He reported the presence of a weak secondary maximum of absorption upon the short wave-length side of the fundamental. A similar result was obtained for KCl. In a second paper[3] it was shown that these crystals possessed not one but several secondary maxima, giving rise to absorption curves which differed considerably from those predicted on the basis of the previously mentioned theories, and only by using a layer of crystal 0.17μ thick were the authors able to obtain a curve of the theoretical type. Fig. 1, taken directly from the above paper shows the type of curve obtained for NaCl. Continuing this work, Barnes[4] showed that some fifteen crystals of this type possessed similar secondary maxima. At this time a good deal of structure was observed, but since the resolving power was very low, the work published was to be regarded as being essentially envelopes of possible additional structure.

Following this, Born and Blackman[5] sought an explanation of these results on the basis of anharmonic terms in the potential function of interaction of the lattice atoms, and handled the problem of a linear diatomic chain along classical mechanical lines. Their results showed that such terms would give rise to additional maxima, one on the short wave-length side of the fundamental

* The experimental section of this paper (Part A) is principally due to R. B. Barnes and R. R. Brattain, and the theoretical section (Part B) was developed principally by F. Seitz while a fellow in theoretical physics at Princeton University.

[1] E. Madelung, Nachr. Gött. M. P. Klasse, March 1909 and Jan. 1910; Physik. Zeits. **11**, 898 (1910); M. Born and Th. von Kármán, Physik. Zeits. **13**, 297 (1912); M. Born and M. Goeppert-Mayer, *Geiger-Scheel Handbuch der Physik*, Vol. 24b.

[2] M. Czerny, Zeits. f. Physik **65**, 600 (1930).

[3] R. Bowling Barnes and M. Czerny, Zeits. f. Physik **72**, 447 (1931).

[4] R. Bowling Barnes, Zeits. f. Physik **75**, 723 (1932).

[5] M. Born and M. Blackman, Zeits. f. Physik **82**, 551 (1933); M. Blackman, Zeits. f. Physik **86**, 421 (1933).

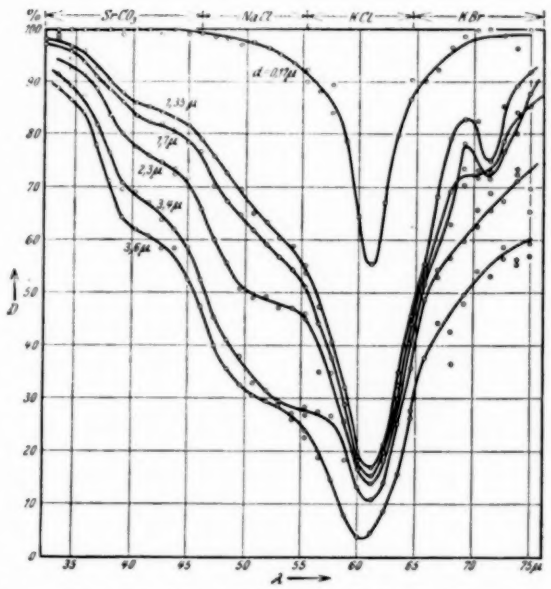

FIG. 1. Transmission of thin films of NaCl. (Barnes and Czerny.)

and one on the long wave-length side (the former agreeing reasonably well with the experimental values), so that a qualitative check of the validity of this assumption was obtained.

When good specimens of MgO became available, it was decided that a more thorough investigation of the structure of the absorption spectrum of a cubic crystal could be carried through than had been done previously.[6] This crystal is particularly suitable for near infrared investigation since its spectrum lies closer to the visible than does that of any other cubic crystal, and, moreover, it may be obtained in perfect crystalline as well as powdered form. Under these favorable circumstances an investigation was carried through and the principal experimental results may be tabulated as follows:

1. The absorption spectra of (a) powdered, (b) evaporated films and (c) cleavage plates of crystalline MgO are identical as far as maxima are concerned as long as the particle size of the powder is not such as to give rise to anomalous scattering or refracting effects.

2. The fine structure is reproducible on various thicknesses of material and indicates that there are more than forty absorption peaks on the near infrared side of the largest absorption peak when the crystal is at room temperature.

3. The fundamental absorption line does not lie at 14.2μ as has been previously supposed, but is further in the infrared.

[6] R. Bowling Barnes and R. Robert Brattain, Phys. Rev. **47**, 416 (1935).

From this work, it was concluded that the results of Born and Blackman were not general enough to handle the case at hand and another approach to the theoretical side of the problem was undertaken. For this purpose it was assumed that the crystal could be handled as a three-dimensional quantum-mechanical system of interacting particles arranged at the mesh points of the NaCl type lattice and a general potential function of interaction was set up using only the group theoretical restrictions required by symmetry. This is to be contrasted with the type of potential function employed in the Born treatment of ionic crystals in which central forces are assumed between particles. The recent high precision work on the elastic coefficients by Quimby, Balamuth, Rose and Durand[7] indicates conclusively that the Cauchy-Poisson relations are not valid, the c_{12} of Voigt being only about half of the corresponding c_{44} for divalent ionic crystals of the type of MgO, while for monovalent crystals of the type of NaCl, c_{12} is ten percent larger than c_{44} in the neighborhood of absolute zero. Since equality of c_{12} and c_{44} was essential for the validity of the Born theory these facts point to a basic lack of generality in it and for this reason it is found necessary, for the time being, to employ a phenomenological description of potential fields in much the same way that is done in handling molecular potential functions.

By employing the anharmonic terms as perturbations, normal coordinates were introduced so as to afford a suitable system of quantum-mechanical variables and from these the first-order energy spectrum arising from the harmonic terms was determined. It is of course identical with the classical energy spectrum and for the diatomic face-centered lattice is included inside of two zones, in each of which there are three branches corresponding to the three directions of polarization of waves. The perturbing terms were then regarded as being such as to alter the selection rules for transitions without appreciably affecting the energy spectrum, and it was found that this effect can be regarded as important only for transitions in which two waves whose momentum vectors lie in the neighborhood of the sur-

[7] L. Balamuth, Phys. Rev. **45**, 721 (1934); we are deeply indebted to these people for the use of results of their work that is as yet unpublished.

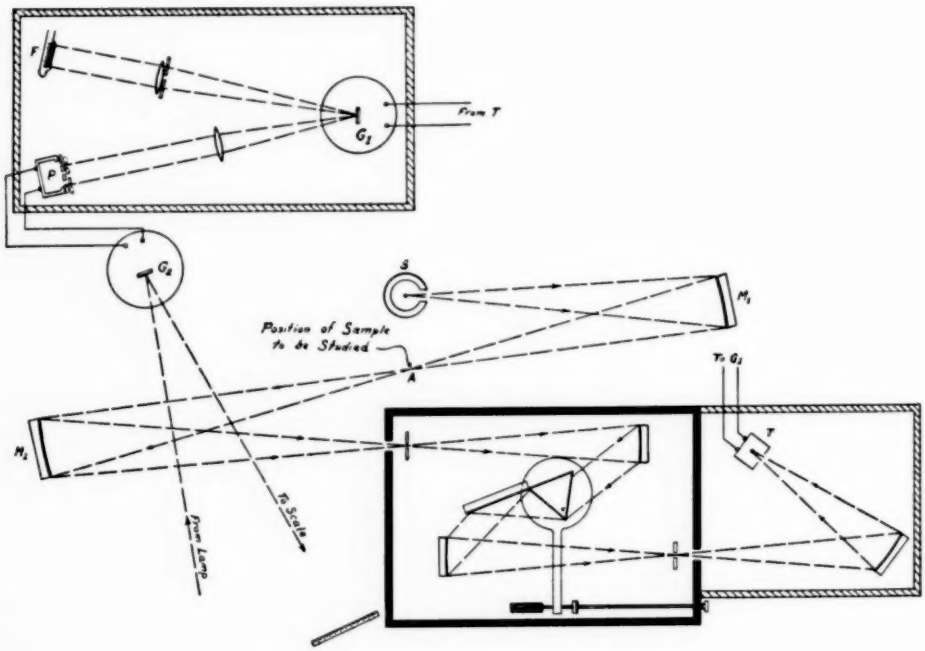

FIG. 2. Rocksalt spectrometer and amplifier.

faces of the zones and at regions near these surfaces where the energy gradient is zero, are simultaneously excited, since in this case the integrated effect of many insignificant absorption lines is appreciable in the vicinity of one wave-length. In this case both the sum and difference energies of the two waves will give rise to absorption peaks. The conclusions drawn were as follows:

1. The first-order anharmonic terms give rise to a large number of absorption lines of types to be described in a later section.

2. Any attempt at determining correlations between the experiment and theory at this stage of the development of the former is premature since the conditions under which the theory is presented are such that they will be realized best at low temperatures and it is only when such experiments are carried out that correlations may be sought for. There is no reason for expecting that such correlations do not exist, however.

PART A. EXPERIMENTAL SECTION. THE NEAR INFRARED SPECTRUM OF MgO

In order to be able to obtain better experimental results, a cubic crystal was sought whose fundamental corresponded to a wave-length in the near infrared where higher resolution could be employed. Consequently, the authors were pleased to learn that The Norton Company, using an electric furnace which operated at a temperature above 2500°C were able to fuse MgO, and prepare large flawless single crystals from the molten material. The samples obtained possessed almost every property which would make them suited for this purpose. They were clear, hard, easy to cleave (down to 0.075 mm), were not affected by water, were obtainable in sizes up to $3\times4\times1$ cm, possessed almost perfect cleavage planes so that no polishing or grinding was necessary, were very tough and resistant to acids and heat, and the material had its fundamental in the near infrared. Both transmission and reflection measurements were made throughout the region from 1μ to 15.6μ. Previous x-ray investigations have shown that MgO crystals are cubic in their structure being of the NaCl or face-centered type.[8]

§1. Apparatus and procedure

For this investigation in which it was desired to be able to study the absorption of the samples throughout the near infrared, the experimental set-up shown in Fig. 2 proved very satisfactory. The radiation from a hot platinum strip (S),

[8] P. P. Ewald and C. Hermann, *Structurbericht* (Leipzig, 1931).

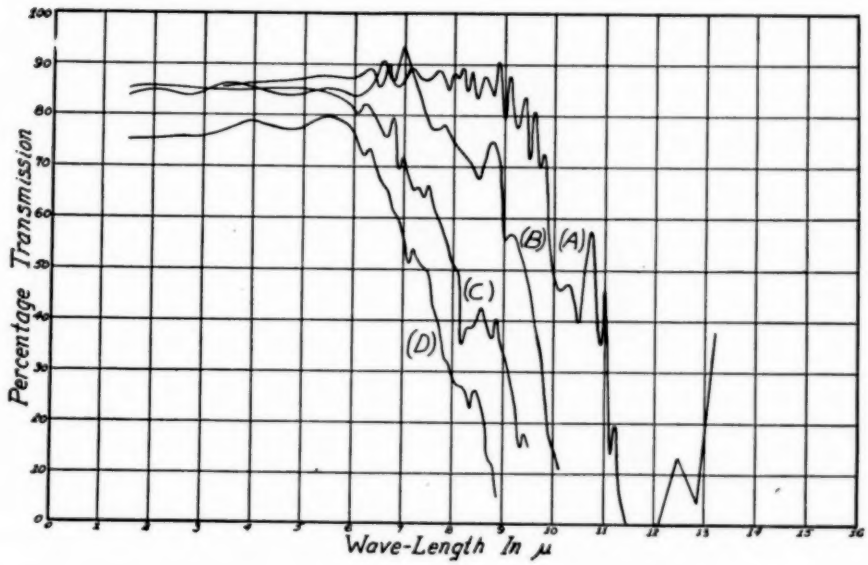

FIG. 3. Transmissions of cleaved plates of MgO. (a) 0.12 mm; (b) 0.47 mm; (c) 1.75 mm; (d) 3.05 mm.

which was operated from a 22-volt transformer at a current of 20 amperes, was brought to a focus upon the sample by M_1, and after diverging was focused upon the slit of the spectrometer by the mirror M_2. After emerging from the spectrometer which contained a rocksalt prism and a Wadsworth mirror, this radiation was then concentrated upon a Moll linear thermopile. The latter was connected as shown to an original Moll galvanometer (55 ohms internal resistance), the deflections of which were then amplified by means of the photoelectric relay[9] system. The filament F (4 volts, 4 amperes) was focused by the two lenses over the galvanometer mirror to the photoelectric cell, P, which was a selenium cell of the blocking layer type and had an active surface 3×3 cm. The use of the grids as shown increased the sensitivity threefold. An H.S. Leeds and Northrup 16.4-ohm galvanometer was then used to read the currents produced by the photoelectric cell. After taking extreme precautions to avoid any unsteadiness due to fluctuations in the temperature and pressure of the room, the relay system was set and used at a magnification of about 150-fold. The thermocouple, although not of the vacuum type, was placed in an evacuated container in order to avoid the pressure effects referred to just above. The scale distance was 2.5 meters.

The calibration of the instrument was determined empirically, by mapping the positions on the scale of many well-known sharp bands such as those of H_2O, the emission and absorption bands of CO_2, the reflection bands of quartz, the absorption bands of benzene, toluene and cyclohexane. Points were thus obtained at rather close intervals out to 15.2μ. The transmission curves obtained were accurately reproducible as far out as the measurements were made. The authors realize that the extreme wave-lengths may be uncertain, due to errors in the calibration curve, by as much as $\pm0.05\mu$. The calibration curve was checked frequently, and aside from a shift back and forth from time to time of less than $\pm0.01\mu$ due to changes in the temperature of the prism, was found to be constant.

At the position marked A in Fig. 2, a sliding tower was built which enabled the sample to be moved in and out of the light beam, several measurements being taken in each of these two positions. The curves plotted below are in every case the actual percentage transmissions as measured, no corrections having been made for the losses of energy at the two surfaces of the crystal. The accuracy of the curves with regard to the ordinates is about ±2 percent.

[9] R. Bowling Barnes and F. Matossi, Zeits. f. Physik **76**, 24 (1932); L. Bergmann, Physik. Zeits. **32**, 688 (1931).

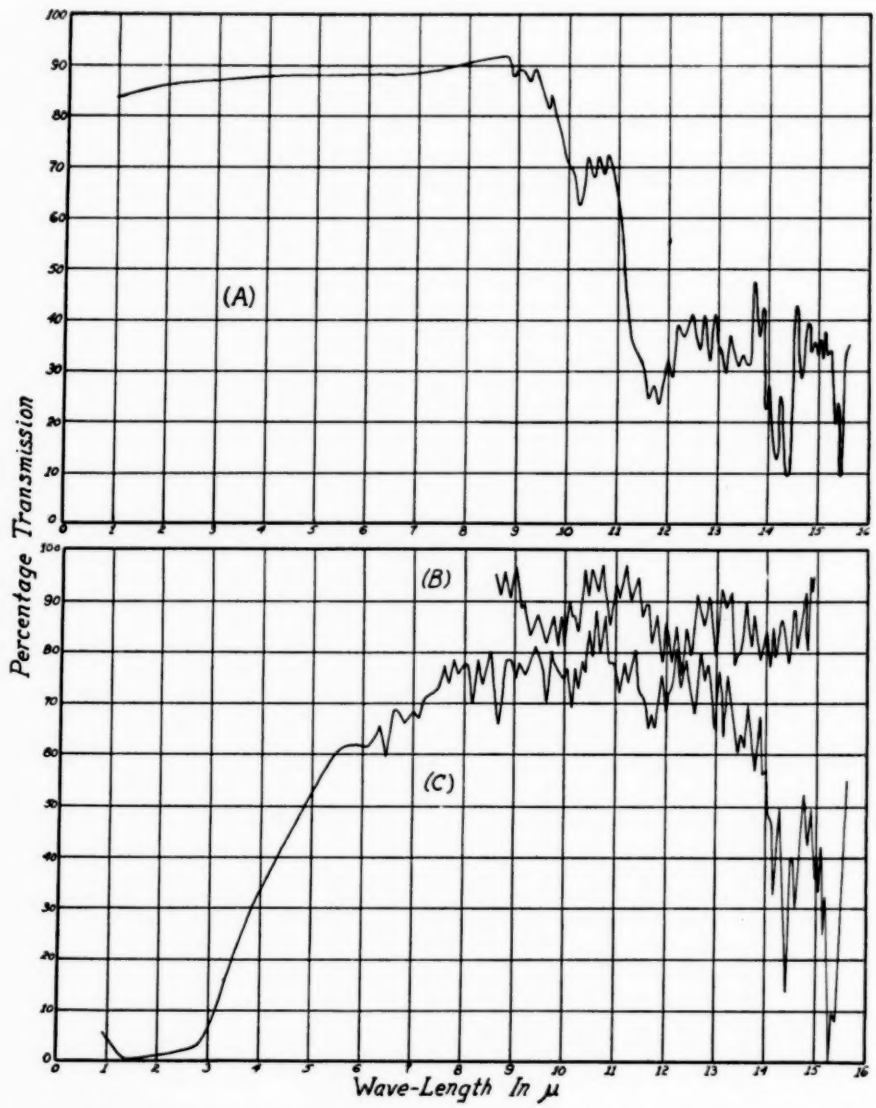

FIG. 4. (a) Transmission of a thin cleaved plate, $t=0.075$ mm. (b) Transmission of a 1μ layer of MgO evaporated onto a nitrocellulose film. (c) Transmission of a layer of MgO fumed onto a plate of NaCl.

§2. Results

(a) Fig. 3 shows the results plotted to a μ scale for different thicknesses of MgO prepared by cleaving plates from one of the large single crystals. The similarity between the curves will be noted. The agreement of the secondary structure in the various plates is good considering the resolving power of the instrument and the fact that as we proceed to greater thicknesses, the relative strengths and breadths of the absorption lines vary giving rise to absorption peaks of new shapes.

In Fig. 4 curve (a) the composite curve resulting from many separate runs on a cleaved plate 0.075 mm is given. No experimental points are indicated but each of the minima shown has been checked in at least two or three of the individual sets of measurements. The structure is quite complicated, yielding some 40 absorption lines between 6μ and 15.5μ.

(b) In the work of Czerny and Barnes[3] thin films of the alkali halides were prepared by heating the salts in a vacuum by means of a tungsten spiral and allowing them to condense onto a film

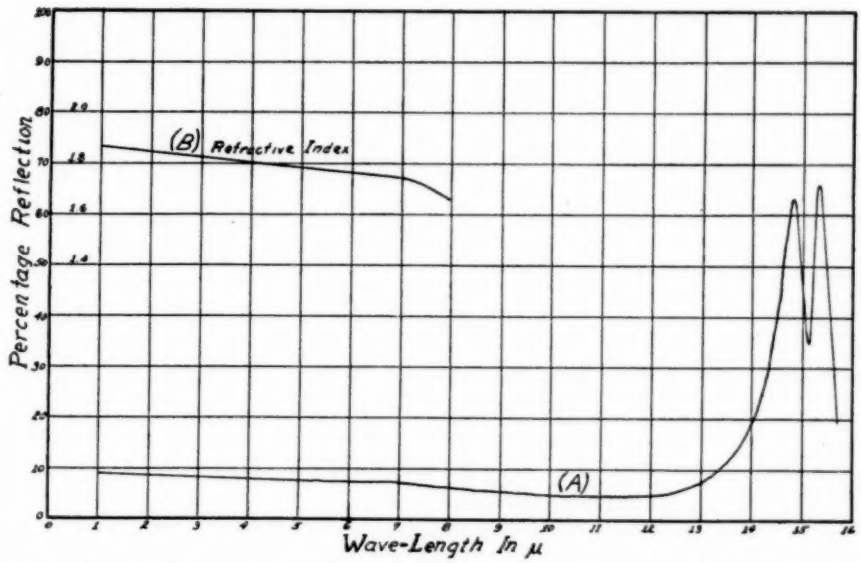

FIG. 5. (a) Reflection power of a crystal of MgO. (b) Dispersion curve of MgO calculated by use of the relation $R=(n-1)^2/(n+1)^2$.

of nitrocellulose. It was shown in their paper that the optical constants of a NaCl film prepared in this manner were identical with those of a massive plate of salt. Hilsch and Pohl[10] and their coworkers have also obtained results which showed that films prepared in this manner were really single crystals. Further proof that such films are really crystalline has been obtained by Kirchner,[11] using electron diffraction.

Curve (b) in Fig. 4 shows the result of a series of measurements upon such a thin film of approximately 1μ thickness. It is immediately obvious that the wave-lengths of the fine structure lines agree in almost every detail with those of the composite curve for the thin cleavage plate shown above in curve (a).

(c) In order to obtain still another check upon the existence of this secondary structure the transmissions of several thin films of finely powdered MgO were studied. The powders were prepared by two different methods, namely, by grinding up pieces of the large single crystals and by burning a piece of magnesium ribbon and allowing oxide to deposit upon a thin plate of NaCl. Curve (c) Fig. 4. shows the results of these measurements from which it is at once evident that the secondary structure is the same as that found for the thin cleaved plate and the evaporated film.

(d) The positions of the source and M_1 were now changed and an extra plane reflection put in at the focus A in order to be able to study the reflection power of one of the large crystals. At each wave-length the crystal was interchanged with the plane silvered mirror and the ratios of the deflections from the two taken as the percent reflection power of MgO. These results are shown by curve (a) of Fig. 5. A double reflection maximum is seen at 14.8μ and 15.3μ. From the values of R for the region below say 8μ, the refractive indices of MgO may be obtained by using the simple equation $R=(n-1)^2/(n+1)^2$. The dispersion curve thus arrived at is shown by curve (b). The value of $n=1.86$ at 1μ is in fair agreement with the value $n_F=1.747$ reported by Brice and Strong.[12]

§3. Discussion of results

(a) MgO has been the subject of several investigations. Ångström in 1889 studied its absorption, while Coblentz in 1913 reported that with increasing wave-lengths its reflection power increased. In the latter investigation measurements were made at only 6 wave-lengths. In 1928, Fräulein S. Tolksdorf[13] made a study of

[10] R. Hilsch and R. W. Pohl, Zeits. f. Physik **57**, 145 (1929). See later papers.
[11] F. Kirchner, Ann. d. Physik **11**, 741 (1932); Zeits. f. Physik **76**, 576 (1932).
[12] R. T. Brice and J. Strong, Phys. Rev. **47**, 255 (1935).
[13] S. Tolksdorf, Zeits. f. physik. Chemie **132**, 161 (1928).

MgO from 2 to 15μ by means of a prism spectrometer. Following a method suggested by herself and Fräulein Laski,[14] she studied the transmission of a thin film of finely powdered MgO held between two plates of NaCl. A transmission curve was obtained which ranged from about 40 percent at 2μ to 95 percent at 15μ and which showed three distinct minima, located at 3.85, 7.65 and 14.2μ. These she mistook for 4ν, 2ν and ν, respectively. In view of the predictions of the classical theories mentioned in the introduction, she called these supposed overtones "anharmonic" vibrations.

Comparison of her results with those shown in Fig. 4, shows that Fräulein Tolksdorf had mistaken the 14.2μ secondary maximum for the fundamental, and had not measured any further out in the infrared.

In 1931, Strong,[15] using reststrahlen, showed that a layer of MgO fumed onto a NaCl plate showed a very strong absorption in the neighborhood of 23μ. A crystal of β-MgO showed 80 percent reflection at this same wave-length. He offered these results to show that the maximum found by Tolksdorf at 14.2μ could not be the fundamental of MgO.

In a short note, two of us reported the preliminary results of this investigation.[16] At that time we stated that we had found a strong absorption around 14μ which we identified with the fundamental reported by Tolksdorf, the results of Strong not being known to us. In view, however, of the absorption band which we later observed at 15.4μ and the work of Strong the identification of any one absorption band as the fundamental is quite uncertain. At present we are not in a position to say, for example, whether the reflection maxima of Fig. 5 are due to strong secondary maxima or to the fundamental. This question must be decided at a later date. From our present results one can only say that the fundamental absorption of MgO is accompanied by many secondary maxima.

(b) The curves shown in Fig. 4 show very conclusively that the infrared spectrum of a solid may be studied successfully in either of the three forms, namely, cleavage plates, powder or evaporated films. The last two methods require great care and sometimes lead to spurious results.

Before using the powder method the investigator should be familiar with the authors' paper and those of Pfund on the infrared of powders.[17] In the light of these papers, the increasing transparency of the powdered MgO found by Tolksdorf as longer wave-lengths were reached, is readily understood. In all cases where powders are used the particle size of the powder must be smaller than the wave-lengths of the regions being studied in order to avoid spurious effects, and shifts in the wave-lengths.

Hirsekorn[18] measured the transmission of films of NaCl evaporated at atmospheric pressure, and found spurious effects due to the particles. These evaporated films must be prepared in the very highest vacuum obtainable.

These last-named methods have been used to advantage by many people, and it is therefore very gratifying to see that all three methods when applied to the same substance yield results strictly comparable in every detail.

(c) In conclusion it must be mentioned that, since these secondary maxima are probably due to anharmonic terms in the force equation, they should be sensitive to changes of temperature, as will be discussed in Part B. Accordingly, preparations are under way to repeat these measurements first at liquid air then at liquid hydrogen temperatures. Then and only then could a complete correlation with theory be expected.

§4. Experiments on other crystals

From time to time the complex structure of the infrared absorption bands of various crystals, as evidenced by reflection as well as transmission measurements has surprised experimenters. As increasingly higher resolving power has been employed, it has become more and more evident that these bands possessed a real fine structure the exact interpretation of which is unknown.

No attempt will be made at this point to give a complete list of papers bearing upon the above statements, however it is felt that several investigations should be cited.

[14] G. Laski and S. Tolksdorf, Naturwiss. **14**, 21 (1926).
[15] J. Strong, Phys. Rev. **37**, 1565 (1931).
[16] R. Bowling Barnes and R. Robert Brattain, Phys. Rev. **47**, 416 (1935).
[17] R. Bowling Barnes, R. Robert Brattain and R. S. Firestone, Phys. Rev. **47**, 792A (1935); A. H. Pfund, Phys. Rev. **36**, 71 (1930); J. Opt. Soc. Am. **24**, 143 (1934); J. Opt. Soc. Am. **23**, 375 (1933).
[18] H. G. Hirsekorn, Ann. d. Physik **6**, 985 (1930).

In addition to MgO Tolksdorf studied CaO, BeO, ZnO, CdO and HgO. For the first three she found the spectra to consist of several distinct maxima of absorption where only one or two were expected. For CdO and HgO, she was unable to locate the fundamentals because they were beyond 22μ, the limit of her spectrometer; however, she did find in the near infrared, several weak absorptions which are probably analogous to the secondary maxima reported above for MgO. A complete account of this work, and an attempt to identify these secondary maxima as harmonics and combinations will be found in the book of Schaefer and Matossi, *Das Ultrarote Spektrum*.

Silverman[19] measured, in the neighborhood of the 7μ band, the reflection and transmission of calcite, and found between 6.4μ and 7.4μ some 33 lines in each case. This unexpected fine structure he suggested was possibly due either to the disturbing effects of imperfections in the crystal, or to combinations with the far infrared bands of calcite.

Silverman and Hardy[20] showed that the 9μ quartz band also possessed an extremely complicated structure.

Recent papers from the laboratory of Schaefer and Matossi also point to the presence of complicated structure in the cases of many crystals.

Besides the original work discussed above, other investigators[21] have studied the alkali halides and verified the existence of the secondary maxima in every case.

Although the absorptions of all types of crystals seem to possess this fine structure, or secondary structure, the most important thing to be done right now is undoubtedly to obtain very accurate measurements on cubic crystals. Experiments performed at low temperatures, with polarized radiation, or with the radiation traversing the crystal in directions other than normal to the 100 plane, will yield results which will be of the greatest theoretical importance with regard to the study of the solid state.

[19] S. Silverman, Phys. Rev. **39**, 72 (1932).
[20] J. D. Hardy and S. Silverman, Phys. Rev. **37**, 176 (1931); S. Silverman, Phys. Rev. **45**, 158 (1933).
[21] K. Korth, Nachr. d. Ges. d. Wiss. zu Gött. Math-Phys. Kl. 1932, p. 576; A. Mentzel, Zeits. f. Physik **88**, 178 (1934).

Part B. Theoretical Interpretation

§1. Previous developments: a criticism of the Born approximation

A sketch of the general scheme followed in an attempt to approach a theoretical interpretation of the previous results was presented in the introduction, and before proceeding with a detailed discussion of this, we shall pause to review some of the previous developments.

In the earliest period of observation of the reflection spectra of solids, it was found[22] that for cubic crystals the spectra could be accounted for by assuming that they possessed one fundamental absorption frequency and that the reflection properties were related to this by means of the well-known formulae of optics. In noncubic crystals, it was necessary to assume the presence of several absorption maxima. Following this, a number of dimensional equations relating this frequency for cubic crystals to other physical properties were suggested by Einstein, Lindemann, Braunbeck and others, and were found to give rough agreement with the established facts.

On the basis of some remarkably good assumptions concerning the arrangements of atoms in the alkali halides, Madelung[23] succeeded in relating the fundamental absorption frequency to the interaction forces and connected these with the elastic coefficients. This was followed by a paper of Born and von Kármán[24] in which the ideas behind Madelung's work were placed upon a firmer basis for analytical treatment. Although the conclusions which they drew from their development are not strictly correct when viewed in the light of modern knowledge, their treatment of vibrational waves has continued to be of service in many fields. In addition, this work gave an indication of the weaknesses of the Debye theory of specific heats in which the crystal was treated as a continuous solid—a question which has been the object of considerable qualitative and semi-quantitative investigation in recent times.[25]

[22] A complete sketch of the work discussed in this paragraph is to be found in Schaeffer and Matossi, *Das Ultrarote Spektrum* (Berlin, 1930).
[23] E. Madelung, Nachr. d. Ges. d. Wiss. zu Gött. M. P. Klasse, March 1909, Jan. 1910; Physik. Zeits. **11**, 898 (1910).
[24] M. Born and Th. von Kármán, Physik. Zeits. **13**, 297 (1912).
[25] M. Blackman, Proc. Roy. Soc. **A148**, 365, 389 (1935); **A149**, 117, 126 (1935).

During a subsequent period, Born and coworkers succeeded in developing a theory of ionic crystals,[26] based upon the assumption of central force interaction of ions, by means of which a number of properties of such crystals such as dielectric constant and fundamental frequency could be correlated. Such correlations are to be regarded as first approximation connections which are valid when the assumptions made are correct to within factors that are essentially refinements. The principal assumption which is made is that of central force interaction of ions. For the purpose of many property-correlations, such as those mentioned previously, considerable inaccuracy in these assumptions may not lead to wide discrepancies in results, simply because the quantities correlated are not sensitive to alterations in the fundamental assumptions; that is, for example, neither the dielectric constant nor the fundamental frequency of a crystal will be greatly affected by small deviations of the interaction potential from one of the central type. This is not true of many other properties of crystals, however, particularly those which are the differences of relatively insensitive quantities. This question is of considerable importance when the problem of determining the positions of the secondary absorption maxima of crystals relative to the fundamental is raised, as will be shown in the following sections, and for this reason it is important that the extent to which the results of the assumptions of Born are valid be known. If they are found to be incorrect to a sufficient degree, it will be necessary to proceed from an entirely phenomenological standpoint, as will be shown to be the case.

One of the principal results of the assumption of central forces when dealing with arbitrary crystals is the so-called Cauchy-Poisson relations[27] between the components of the stress-strain tensor. For cubic crystals, with which we are principally concerned, these relations are such that equality is to be expected between the coefficients c_{12} and c_{44} of Voigt, the first of which connects the transverse stress to the strain along a given crystallographic axis, while the second relates the shearing stress in a plane orthogonal to one of the principal axes to a shearing strain in the same plane. A number of results concerning these relations for valence crystals and metals[28] revealed that they are not nearly satisfied. Previous[29] to some very recent work by Quimby, Balamuth, Rose and Durand[7] using oscillating circuit methods, the only measurements carried on for the determination of the constants for ionic crystals dealt with the monovalent alkali halides and were performed at ordinary temperatures. In these earlier cases the relationships were found to be valid to within an experimental error which we judge to be about 5 percent. The room temperature values are not particularly valuable for the present discussion, however, since the elastic coefficients are known to vary considerably with temperature and we are really interested in the absolute zero values. The work of reference 7, however, has furnished a good deal of information for both monovalent (NaCl) and divalent ionic crystals (MgO) over a temperature range extending down to 80 degrees Kelvin with an accuracy exceeding that previously obtained by about one power of 10. A sample set of values of the adiabatic coefficients of both of these crystals are given in Table I. The isothermal values may be determined from these by adequate small corrections which are always such as to lower c_{44} and leave c_{12} unchanged.

TABLE I.

	$c_{11}10^{-11}$		$c_{12}10^{-11}$		$c_{44}10^{-11}$	
°K	NaCl	MgO	NaCl	MgO	NaCl	MgO
273.1	5.035	28.841	1.277	15.350	1.279	8.705
210	5.284	29.128	1.298	15.421	1.253	8.585
150	5.508	29.396	1.315	15.472	1.127	8.535
80	5.754	—	1.332	—	1.159	—
77.4	—	29.547	—	15.501	—	8.462

From these results it is clear that in the vicinity of absolute zero the c_{44} coefficient will be about 15 percent less than c_{12} for NaCl, while in the case of MgO the ratio is almost 2 to 1. This presents conclusive evidence that the Born approximation is a rather rough one for ionic crystals.

[26] A thorough review of this work is given by M. Born and M. Goeppert-Mayer in the *Geiger-Scheel Handbuch der Physik*, Vol. 24b.

[27] W. Voigt, *Lehrbuch der Kristallphysik* (Teubner, 1910), p. 607.

[28] A review of the work of Voigt on this subject may be found in M. Born's *Atomtheorie des Festenzustands* (Teubner, 1923), Chapter I.

[29] W. Voigt, reference 26, p. 741; P. W. Bridgman, Proc. Am. Acad. **64**, 19 (1929). We are indebted to Professor Bridgman for correspondence concerning details of this work.

With the discovery of secondary maxima, Born and Blackman,[5] as we have stated in the introduction, sought an explanation of this phenomena on the basis of anharmonic potential terms and solved the problem of the diatomic linear chain, considering such terms to be small perturbations, as a classical mechanical one. As is well known, the frequency spectrum for this problem as a function of the variable $\sigma=2\pi/\lambda$, λ being the wave-length, is represented by a curve of the type shown in Fig. 6 in which the discontinuity occurring for $\sigma=\pm\pi/Na$, where a is the distance between nearest like atoms, is a characteristic of the diatomic lattice that disappears when the masses of the particles are equal and $2N$ is the total number of atoms. The results of Born and Blackman show that on the basis of their classical reasoning one would expect frequencies $\nu_1+\nu_2$ and $\nu_1-\nu_2$ as well as the fundamental frequency ν to be absorbing. These results were then extended to the three-dimensional case again on a classical basis, but with neglect of a suitable analysis of the discontinuous zone structure that must exist by analogy with the results of the theory of metals. This last point represents a serious omission, even if the use of classical mechanics and the use of central forces were valid, and will be discussed more thoroughly in §3.

In view of these facts, the problem will be handled entirely anew in the following sections and with a view toward eventually obtaining correlations between experimental and theoretical results.

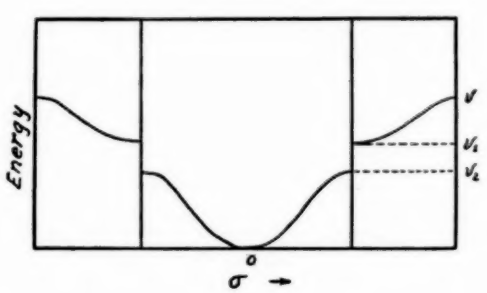

FIG. 6. A representative energy-wave number distribution for the linear chain. In the classical case the energy is proportional to the square of the frequency, while in the quantum case it is proportional to it. In the three-dimensional lattice, this is characteristic of the energy spectrum for one polarization and a line passing through the origin in σ-space. The discontinuities occur when this line intersects the zones.

§2. The symmetry restrictions induced on a general potential form

As a basis for a phenomenological discussion of the interaction potential of atoms, we shall assume that they are regularly arranged in a lattice at points

$$l\tau_1+m\tau_2+n\tau_3+\rho_a \tag{1}$$

where l, m and n are integers, τ_1, τ_2, τ_3 are the primitive translations of the lattice, and ρ_a is a vector independent of lmn which gives the position of the ath atom in a unit cell. For a diatomic face-centered lattice of the cubic type, τ_1, τ_2, τ_3 may be taken in the form

$$\begin{pmatrix} a \\ a \\ 0 \end{pmatrix}, \quad \begin{pmatrix} a \\ 0 \\ a \end{pmatrix}, \quad \begin{pmatrix} 0 \\ a \\ a \end{pmatrix}, \tag{2}$$

respectively,[30] while ρ_a may be chosen to be zero for one atom (type a, say) and

$$\begin{pmatrix} a \\ 0 \\ 0 \end{pmatrix} \tag{3}$$

for the other (type b), so that a is the closest distance between unlike atoms. Thus when the atoms are in their equilibrium positions, the lattice will be invariant under one of the 230 space groups and we must expect the equilibrium potential function to be likewise invariant (i.e., to belong to the unit representation of the space group). When the atoms are displaced from their equilibrium positions, so that the new position of an atom of type a, say, in the lmn-th cell relative to its old is given by the vector of component $x_a^i(lmn)(i=1, 2, 3)$, the potential of the lattice will be altered, but we shall assume that it may be expressed as a power series expansion in these displacement variables in such a manner that all terms of a given degree are invariant under the group. As is well known, the constant term in this expansion need not be considered, while the linear terms will vanish as the condition of equilibrium. We shall regard the quadratic terms as being of principal importance and treat the cubic terms as small perturbations. For this purpose, we shall

[30] For a presentation of the theory of crystal symmetry in terms of the notation to be presented here see F. Seitz, Zeits. f. Krist. **88**, 433 (1934), et seq.

begin by neglecting the latter and choose a set of normal coordinates for which the quadratic is in normal form, which must be taken to be real since we will want to quantize the entire system. We shall consider the crystal to be fixed, so that the process of choosing normal coordinates is essentially one of resolving all of the x's into Fourier-like components and treating the amplitude-coefficients as a set of variables. Since one of these will correspond to pure translations, it is important that the potential be invariant under infinitesimal translations, and we must express it as a function of differences

$$x_a{}^i(l'm'n') - x_c{}^i(lmn) = \xi_{ac}{}^i(l'm'n', lmn) \quad (4)$$

of displacements, which will also allow us to express the potential change going with a homogeneous deformation of the lattice. It is implied that the coefficients in the power series expansion are so defined that the entire expression is invariant under infinitesimal rotations because we are dealing with a scalar form, so that we shall be concerned with all quadratic and cubic forms in the differences that belong to the unit representation of the space group. Of these a very large number may be neglected since they are considered to be physically unimportant, and we will actually consider but a very small fraction of the possible terms.

For simple crystals in which each atom is at a center of symmetry of the type for which the corresponding point group is that of the class to which the space group belongs, the problem of finding the desired form is comparatively easy. In this case the translational symmetry may be handled completely apart from the rotational, and we need only take the sum of the equivalent potentials of equivalent cells, these potentials being determined by mere rotation group considerations (i.e., screw operations and glide planes do not play a role).

In the lattice of the NaCl type (Fig. 7) with which we shall be entirely concerned, each atom possesses the symmetry O^h for which the ten irreducible representations have been given by Bethe.[31] The character system going with these is listed in Table II, in which Γ^+ and Γ^- are written together with the corresponding signs for the elements of determinant 1 and -1.

[31] H. Bethe, Ann. d. Physik **3**, 133 (1929).

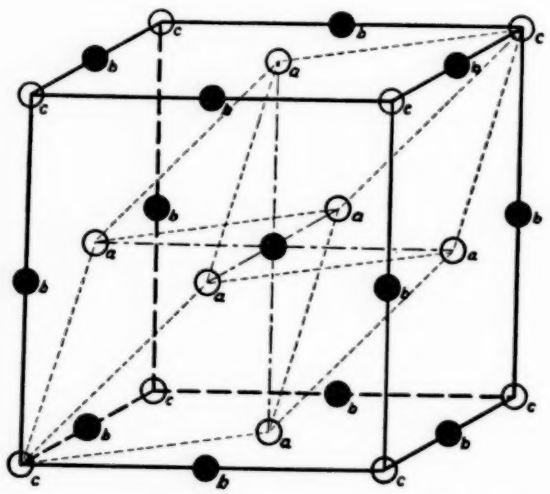

FIG. 7. Face-centered cubic lattice of the NaCl type.

Although the translation group is of the type Γ_c', it is convenient to designate each atom by the integers lmn which specify its position vector of components la, ma, na, since these lie at all mesh points of a simple cubic lattice. Of the possible interaction terms of each atom with its neighbors, we shall consider only those between a given one and its twenty-six neighbors. Moreover, of these we shall be concerned only with quadratic terms of the type

$$\xi^i(l'm'n', lmn)\xi^j(l'm'n', lmn) \quad (5)$$

and with cubic terms of the type

$$\xi^i(l'm'n', lmn)\xi^j(l'm'n', lmn)\xi^k(l'm'n', lmn) \quad (5a)$$

and discard those in which the indices of the

TABLE II. *Character system for crystallographic group O^h.*

	E	$6C_2'$	$8C_3$	$3C_2$	$6C_4$	I	$6R_d$	$8S_6$	$3R_h$	$6S_4$
Γ_1	1	1	1	1	1	±1	±1	±1	±1	±1
Γ_2	1	1	−1	−1	1	±1	±1	∓1	∓1	±1
Γ_3	2	2	0	0	−1	±2	±2	0	0	∓1
Γ_4	3	−1	1	−1	0	±3	∓1	±1	∓1	0
Γ_5	3	−1	−1	1	0	±3	∓1	∓1	±1	0

where: E is the unit element;
$6C_2'$ is the class of 6 two-fold rotations about axes of the (110) type;
$8C_3$ is the class of 8 three-fold rotations about axes of the (111) type;
$3C_2$ is the class of 3 two-fold rotations about axes of the (100) type;
$6C_4$ is the class of 6 four-fold rotations about axes of the (100) type;
I is the inversion;
$6R_d$ is the class of 6 reflection planes orthogonal to axes of (110) type;
$8S_6$ is the class of 6 six-fold rotary reflections about axes of (111) type;
$3R_h$ is the class of 3 planes orthogonal to axes of the (100) type;
$6S_4$ is the class of 6 rotary reflections about axes of the (100) type.

type $l'm'n'$ in these differ among themselves. This simplification has the effect of reducing the total number of terms for the twenty-six neighbors to about a fourth. Of the terms considered, those which describe the interaction between unlike atoms are the same regardless of which type of atom is at the center of neighbors, and need to be counted but once for each cell, while those which describe the interaction of like particles appear with different coefficients depending upon the type of atom concerned.

The problem of analyzing the character system of the quadratic and cubic terms will not be gone into here, and it will suffice to tabulate the results. Regarding the former, it is found that there are ten forms to be considered as these may be classed as follows. In all cases the variables ξ, η, ζ will be considered in place of ξ^1, ξ^2, ξ^3, and because of the restriction (5) we may write $\xi\eta(l'm'n', lmn)$ in place of $\xi(l'm'n', lmn) \cdot \eta(l'm'n', lmn)$, etc. The summation indicated will always imply that two terms in which a cyclic permutation of the variables that appear are to be added. The character system of the various cases is listed in Table III.

I Interaction of given atom with 6 unlike neighbors

1. $\Sigma\{\xi^2(l+1mn)+\xi^2(l-1mn)\}$;

2. $\Sigma\{\xi^2(lmn+1)+\xi^2(lmn-1)+\xi^2(lm+1n)+\xi^2(lm-1n)\}$.

II Interaction of given atom with 12 nearest like neighbors

3. $\Sigma\{\xi^2(lm+1n+1)+\xi^2(lm+1n-1)+\xi^2(lm-1n-1)+\xi^2(lm-1n+1)\}$;

4. $\Sigma\{\xi^2(l+1m+1n)+\xi^2(l+1m-1n)+\xi^2(l+1mn+1)+\xi^2(l+1mn-1)\}$;

5. $\Sigma\{\xi\eta(l+1m+1n)+\xi\zeta(l+1mn+1)-\xi\eta(l+1m-1n)+\xi\zeta(l+1mn-1)\}$;

6, 7 and 8 duplicate 3, 4, 5 for atoms of other type.

III Next nearest unlike neighbors

9. $\Sigma\{\sum_{\pm 1}\xi^2(l\pm 1, m\pm 1, n\pm 1)\}$;

10. $\Sigma\{(\eta+\zeta)\xi(l+1m+1n+1)-(\eta-\zeta)\xi(l+1m-1n+1)-(\eta+\zeta)\xi(l+1m-1n-1)+(\eta+\zeta)\xi(l+1m+1n-1);-(\eta+\zeta)\xi(l-1m+1m+1)+(\eta-\zeta)\xi(l-1m-1n-1)+(\eta+\zeta)\xi(l-1m-1n-1)-(\eta-\zeta)\xi(l-1m+1n+1)\}$.

In the following we shall designate the coefficient of each of the ten quadratic terms by $\alpha(1), \cdots, \alpha(10)$, respectively.

Since we shall employ the cubic terms only insofar as they are able to break down the selection rules for optical transitions, and we shall assume that they do not affect the energy spectrum given by the quadratic terms, it will not be necessary to go farther than to write down the set of terms arising from (5a) when only the six nearest neighbors are considered for reasons that will become apparent in §5. The character system is given in Table IV.

TABLE III. *Character system for quadratic terms considered.*

Type of neighbor	Conditions (5)	E	$6C_2'$	$8C_3$	$3C_2$	$6C_4$	I	$6R_d$	$8S_6$	$3R_h$	$6S_4$	No.
I	$i=j$	18	0	0	6	2	0	2	0	12	0	2
I	$i\neq j$	18	0	0	−2	−2	0	2	0	−4	0	0
II	$i=j$	36	2	0	0	0	0	2	0	12	0	2
II	$i\neq j$	36	2	0	0	0	0	2	0	−4	0	1
III	$i=j$	24	0	0	0	0	0	4	0	0	0	1
III	$i\neq j$	24	0	0	0	0	0	4	0	0	0	1

The corresponding cubic forms are

1. $\Sigma\{\xi^3(l+1mn)-\xi^3(l-1mn)\}$

2. $\Sigma\{\xi^2\eta(lm+1n)-\xi^2\eta(lm-1n)+\xi^2\zeta(lmn+1)-\xi^2(lmn-1)\}$.

TABLE IV. *Character system for cubic terms considered.*

Relations in (5a)	E	$6C_2'$	$8C_3$	$3C_2$	$6C_4$	I	$6R_d$	$8S_6$	$3R_h$	$6S_4$	
$i=j=k$	18	0	0	−2	2	0	2	0	4	0	1
$i\neq j=k$	36	0	0	−4	0	0	0	0	8	0	1
$i\neq j\neq k$	6	0	0	2	−2	0	2	0	4	0	0

§3. Normal coordinates: the energy spectrum

The process of reducing the quadratic expression, corresponding to the sum of the possible invariant terms introduced in §2, to normal form is essentially one of reducing a matrix to diagonal form, and since this matrix is invariant under an entire space group, we know that the normal coordinate system will be one in which the space group is reduced. When the Born-von Kármán boundary conditions are employed, it may be shown[32] that for all crystals these coordinates may be taken to be of the Fourier type

$$\chi_\sigma \exp(i\sigma\cdot\mathbf{r}) \tag{6}$$

where χ_σ is invariant under the primitive translations of the lattice and σ is a vector such that

[32] F. Bloch, Zeits. f. Physik **52**, 555 (1929); F. Seitz, *On the Reduction of Space Groups* to appear in Annals of Mathematics, January (1936).

$$\sigma \cdot \mathbf{T}_i = 2\pi n_i. \qquad (7)$$

In this, $\mathbf{T}_i$ are the three vectors defining the polyhedron at the surface of which the boundary conditions are satisfied. For a simple cubic lattice of type Γ_c, for example, this polyhedron may be taken to be a cube so that these vectors lie along each of the three axes. In the case at hand in which we are dealing with lattice vibrations, χ_σ will be periodic in the primitive translations and will be a vector function which takes values only at the positions of the atoms. In other words, for a lattice of the type considered here, the functions (6) will represent waves in which the atom of type 1 at la, ma, na has the displacement

$$\chi_\sigma(1, lmn)\mathbf{f}_1(\sigma, lmn) \exp\left[i\sigma \cdot \mathbf{r}(lmn)\right] \qquad (8)$$

where χ_σ is the scalar amplitude of the wave, $\mathbf{f}_1$ is the unit vector in the direction of displacement and $\mathbf{r}(lmn)$ is the position vector of the atom, while atoms of type 2 at the other mesh points will have displacements of scalar amplitude $\chi(2)$ and direction $\mathbf{f}_2$, both of which will generally differ from $\chi(1)$ and $\mathbf{f}_1$. For an arbitrary, allowable σ, the three values of $\mathbf{f}_1$ and $\mathbf{f}_2$ which reduce the terms of type σ to normal form may be determined by solving an appropriate secular equation to be described later.

For a face-centered lattice in which the primitive translations are given by (2), the allowable form of σ is

$$\frac{2\pi}{2Na}\begin{pmatrix} n_1+n_2-n_3 \\ -n_1+n_2+n_3 \\ n_1-n_2+n_3 \end{pmatrix} \qquad (9)$$

corresponding to the boundary conditions being satisfied at the surface of the rhombic dodecahedron of height $2Na$ (Fig. 8), where n_1, n_2, n_3 and N are integers. The lattice defined by allowing n_1, n_2 and n_3 to take on all integer values is the inverse lattice to the face-centered one and is seen to be a body-centered one having a unit cell of volume $4\pi/N^3a^3$. Not all values of the n's correspond to independent modes of vibration, however, and it is readily seen that the only ones which need to be considered are those contained in a cube whose corners are at the eight points corresponding to n_1, n_2, n_3 equal to $\pm N/2$. Within this there are $2N^3$ unit cells so that when the three directions of polarization are taken into account, it corresponds to $6N^3$ degrees of freedom, which is in agreement with the fact that there are $2N^3$ atoms in the rhombic dedocahedron containing N^3 unit cells of the crystals, and each atom possesses three degrees of freedom.

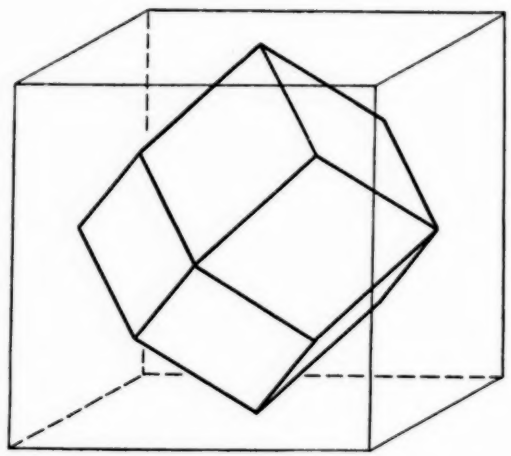

FIG. 8. The rhombic dodecahedron at the surface of which the boundary conditions are satisfied. It possesses one-fourth of the volume of the enclosing cube.

From the standpoint of the energy spectrum, we may expect three energies going with each point in the cube described above corresponding to the generally different energies going with the three directions of polarization of a wave of given σ. It is to be expected that these energy functions $E^i(\sigma)$, where i ranges over the three polarization vectors, will generally vary smoothly from point to point except at the surfaces of definite polyhedra, or *zones*, where they will have discontinuities analogous to those met with[33] in describing electron waves in solids. The space between two zones will generally contain as many points of σ space as there are unit cells in the polyhedron at the surface of which the boundary conditions are to be satisfied—N^3 in this case, so that we may expect that there will be two zones in the problem at hand, and, in fact, for the lattice Γ_c', these correspond to the cube and truncated octahedron shown in Fig. 9. Since we do not consider regions outside of this cube to be different from that inside, the energy surfaces will end at the

[33] L. Brillouin, *Quantenstatistik* (Berlin, 1931), Chap. VIII. The basis for examining the connection between these zones and crystal symmetry is laid in the second of the references 32, and will be extended for presentation in this journal in the near future.

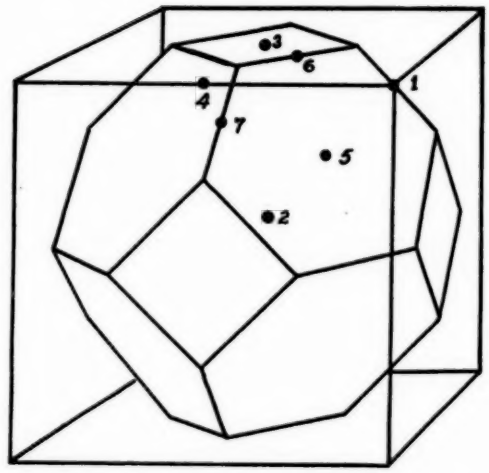

FIG. 9. First two zones for a face-centered diatomic crystal of the NaCl type (translation group Γ_c'). The inner zone is a truncated octahedron and the second is a cube. The difference in volume between the first and second is equal to that of the first. The numbers indicate particular points to be discussed in the text. (Note no. 2 is the center.)

cube, but may be expected to possess a vanishing gradient normal to the surface,[34] while at the surface of the truncated octahedron they will possess definite discontinuities, being continuous on each side of the surface, and will have a vanishing normal gradient there. Fig. 6 represents the characteristic behavior of $E(\sigma)$ for one direction of polarization as σ varies along a line passing through the origin. The discontinuity occurs when σ reaches the truncated octahedron, and the curve ends at the cube.

It is a general characteristic of this zone structure that each of the points in one zone may be viewed as being associated with a definite point in another zone in the sense that the waves going with the two have exactly the same symmetry properties (belong to the same irreducible representation), and in the present case these two points are connected by a vector of the same length as one of the vectors

$$\mathbf{s}^i=\frac{2\pi}{2a}\begin{pmatrix}\pm 1\\ \pm 1\\ \pm 1\end{pmatrix} \tag{10}$$

joining the origin with a cube corner. These vectors are the only members of the $2N^3$ considered (aside from the origin), that possess the property that their scalar product with each of the primitive translations is 2π, or 0. It is readily seen that to each point between the cube and the truncated octahedron, the vector $\sigma+\mathbf{s}^i$ lies either outside of the cube (and is not to be considered) or inside of the truncated octahedron, the only ambiguous cases being those in which σ lies on the surface of the latter polyhedron, and this difficulty, which is never of physical importance, may be removed by assuming that one of any two such points that are connected by a vector $\mathbf{s}$ belongs to the inner zone and the other to the outer. Because of this fact and the fact that $\sigma\pm\mathbf{s}^i$ possesses the same properties as σ under the translation group, we need only consider points belonging to the truncated octahedron, and it will turn out that the correct multiplicity of solutions corresponding to the double-valuedness of each point inside will automatically follow. These two solutions are, in fact, the modes of vibrations in which neighboring atoms are out of phase by more or less than 90 degrees, respectively. Later on, we shall return to the characterization by use of all points in the cube, and consider the three energies going with the wave in which unlike neighboring atoms are most out of phase to be outside of the truncated octahedron.

Finally, it must be borne in mind that we want all waves to be real for the purposes of quantization, and for this reason, we shall replace $\exp(i\sigma\cdot\mathbf{r})$ in the preceding by both $\sin\sigma\cdot\mathbf{r}$ and $\cos\sigma\cdot\mathbf{r}$, and have for the Fourier resolution of the displacement vector $x^i(lmn)$ of atoms of type a and b:

(1) Atoms of type 1

$$x^i(lmn)=\sum_\sigma\sum_\alpha\left\{\frac{\chi_\alpha(\sigma,c)}{\sqrt{m_1}}f_\alpha{}^i(\sigma,c)\cos\sigma\cdot r(lmn)+\frac{\chi_\alpha(\sigma,s)}{\sqrt{m_1}}f_\alpha{}^i(\sigma,s)\sin\sigma\cdot r(lmn)\right\} \tag{11}$$

where $\chi_\alpha(\sigma,c)$ is the amplitude of the cosine wave polarized in the direction $f_\alpha{}^i$ ($\alpha=1,2,3$), etc. The allowed vectors $\mathbf{f}^i$ are to be determined by an appropriate set of equations.

[34] A proof of this may be derived from the work of H. Jones and C. Zener, Proc. Roy. Soc. **A144**, 101 (1934) by means of group-theoretical extensions that will be discussed in this journal in the near future.

(2) Atoms of other type

$$x^i(l'm'n')=\sum_\sigma\sum_\alpha\left\{\frac{\psi_\alpha(\sigma,c)}{\sqrt{m_2}}g_\alpha{}^i(\sigma,c)\cos\sigma\cdot\mathbf{r}(l'm'n')\right.$$

$$\left.+\frac{\psi_\alpha(\sigma,s)}{\sqrt{m_2}}g^i(\sigma,s)\sin\sigma\cdot\mathbf{r}(l'm'n')\right\}\quad(11a)$$

where ψ and $\mathbf{g}$ have the same significance as χ and $\mathbf{f}$ in (1) and ψ_α accompanies χ_α.

The introduction of the factor $1/\sqrt{m_1}$ and $1/\sqrt{m_2}$ has the effect of reducing the kinetic energy form to one in which $\dot\chi^2$ and $\dot\psi^2$ have the same coefficient and it is only necessary to consider the potential form in determining the normal coordinates.

It may be readily shown that in all cases in which the atoms occupy points of inversional symmetry:

$$\begin{pmatrix}-1&&\\&-1&\\&&-1\end{pmatrix},$$

the sine and cosine waves separate completely in all of the sums that will be taken so that we need only consider the latter and designate $\chi(\sigma,c)$ and $\psi(\sigma,c)$ by $\chi(\sigma)$ and $\psi(\sigma)$ for the present. In considering the cubic terms, it will be necessary to return to the previous notation. From this it is readily seen that for a given σ the six quantities $\chi_\alpha(\sigma)$, $\psi_\beta(\sigma)$ $(\alpha,\beta=1,2,3)$ will give rise to a secular equation of the sixth degree unless one or more of the polarization pairs is known beforehand, in which case the secular determinant may be reduced to a two- and a four-, or to three two-dimensional ones, depending upon whether one or two pairs is known. If they are not known, the solution of the secular equation will determine these directions in terms of the set of f_α and g_β that have been assumed at the start in (11) and (11a). It is clear from the symmetry of the quadratic form that the $\mathbf{f}$'s will be mutually orthogonal, as will be the $\mathbf{g}$.

§4. Wave quantization and selection rules

The process of quantizing the waves once the reduction to normal form has taken place is simply one of writing the Schrödinger equation corresponding to the Hamiltonian function

$$\sum_\sigma\sum_\alpha\tfrac{1}{2}\{(\dot q^2(\sigma,c)+\kappa_\lambda{}^2(\sigma)q^2(\sigma,c))$$

$$+(\dot q^2(\sigma,s)+\kappa_\lambda{}^2(\sigma)q^2(\sigma,s))\}\quad(12)$$

where it assumed that the q_λ's are the amplitudes of the normal variables of given σ so that the total energy is the sum over σ and λ of terms of the type (12), the former taking on all values corresponding to the cube. The $\kappa_\lambda{}^2(\sigma)$ are the roots of the secular equation discussed in the last section. The Schrödinger equation for this problem is simply

$$\frac{h^2}{8\pi^2}\frac{\partial^2\psi(q_\lambda(\sigma),n_\lambda(\sigma))}{\partial q_\lambda{}^2(\sigma)}+\frac{\kappa_\lambda{}^2(\sigma)}{2}q_\lambda{}^2(\sigma)\,\psi(q_\lambda(\sigma),n_\lambda(\sigma))$$

$$-E(n_\lambda(\sigma))\psi(q_\lambda(\sigma),n_\lambda(\sigma))=0\quad(13)$$

for which the energy of the stationary state $\psi(q_\lambda(\sigma),n_\lambda(\sigma))(n_\lambda(\sigma)=0,1,2,\cdots)$ is given by

$$\frac{h}{2\pi}(n+1/2)\kappa_\lambda(\sigma),\qquad(13a)$$

$\kappa_\lambda(\sigma)$ being the classical oscillator frequency.

The probability of optical transitions from a state ψ_n to $\psi_{n'}$ will be proportional to the square of the dipole moment matrix component connecting these two states, and this matrix will be zero for all σ except $\sigma=\mathbf{s}^i$ in which case the three waves of equal energy corresponding to a normal mode in which unlike neighbors are 180 degrees out of phase (i.e., the mode going with $\sigma=\mathbf{s}^i$ of the last section which we shall designate simply by $\mathbf{s}$ in the future) possess a nonvanishing matrix.[35] This matrix $\mathbf{p}_\tau(\mathbf{s})$ $(\tau=1,2,3)$ will be of the form

$$\mathbf{p}_\tau(\mathbf{s})=e(s)\mathbf{q}_\tau(\mathbf{s})/\sqrt{M}\qquad(14)$$

where $M=m_1m_2/(m_1+m_2)$ and $e(s^i)$ is the effective ionic charge to be determined from precise theoretical considerations. If the ions were rigid spherical structures, which the evidence of §1 indicates to be only roughly true, this would be the absolute value of the electronic charge for the alkali halides and twice this for MgO. In the present paper, however, we are interested only in the possibility of absorption and not in the intensity of the absorption lines so that this point

[35] C. J. Brester, *Kristallsymmetrie und Reststrahlen, Diss.* (Utrecht, 1923).

is not a critical one. Since $\mathbf{p}_r(\mathbf{s})$ is proportional to $\mathbf{q}_r(\mathbf{s})$ it will have nonvanishing matrix components only if $n'=n\pm 1$, so that only light quanta of frequency $\nu(\mathbf{s})$ may be emitted or absorbed in the quadratic approximation. This is of course just the classical result as was to be expected.

§5. Alterations induced by the presence of the cubic terms

As we have stated previously, we shall assume that the results of the presence of the cubic terms will be such as to leave the energy spectrum unaltered, but will affect the wave functions enough so that the selection rules of §4 are no longer strictly valid. These cubic terms will be of the form

$$\sum_l \{\sum_{ijk} \sum_{l'l''l'''} \alpha_{ijk}^{l'l''l'''} \xi^i(l'l)\xi^i(l''l)\xi^k(l'''l)\}, \quad (15)$$

where l, l', l'', l''' designate triples lmn, etc. and the $\alpha^{l'l''l'''}$ are the coefficients upon which the proper symmetry restrictions have been placed. If the values of the x^i's are substituted, it is readily seen that this reduces to the form

$$\sum_{\alpha\beta\gamma} \beta_{\alpha\beta\gamma}(\sigma_1\sigma_2\sigma_3) q_\alpha(\sigma_1) q_\beta(\sigma_2) q_\gamma(\sigma_3), \quad (15a)$$

in which σ_1, σ_2, σ_3 in a given term are subject to the condition

$$\sigma_1 \pm \sigma_2 \pm \sigma_3 = \mathbf{s}', \quad (16)$$

where s' is any vector such that

$$\mathbf{s}' \cdot \tau^i = 2\pi n_i, \quad (16a)$$

τ_i being one of the primitive translations (2) and n_i an integer. There are rather important restrictions upon the β's as we shall see later, but we shall not be interested in these at the present time.

If we now add the sum of terms (15) to the Hamiltonian function, we may obtain the new stationary states by use of an appropriate perturbation scheme such as that of Schrödinger or Brillouin-Wigner.[36] The unperturbed eigenfunctions of the system will be of the form

$$\Psi_o = \Pi_{\sigma,\ \alpha} \psi(q_\alpha(\sigma), n_\alpha(\sigma)) \quad (17)$$

corresponding to a state in which the coordinate $q_\alpha(\sigma)$ is in the $n_\alpha(\sigma)$th quantum state. The corresponding perturbed function will be of the form

$$\Psi(\cdots, q_i(\sigma), \cdots; \cdots n_i(\sigma)) = \Pi_{\alpha\sigma}\psi(q_\alpha(\sigma), n_\alpha(\sigma)) + \sum_{\sigma_1\sigma_2\sigma_3} \sum_{\alpha\beta\gamma} \gamma(n'_\alpha(\sigma_1), n'_\beta(\sigma_2) n'_\gamma(\sigma_3))$$

$$\times \psi(q_\alpha(\sigma_1), n_\alpha'(\sigma_1))\psi(q_\beta(\sigma_2), n_\beta'(\sigma_2))\psi(q_\gamma(\sigma_3), n_\gamma'(\sigma_3)) \cdot \Pi'_{\sigma\alpha,\ \alpha}\psi(q_\alpha(\sigma); n_\alpha'(\sigma)), \quad (18)$$

in which σ_1, σ_2, σ_3 satisfy the rule (16), Π' does not include the wave functions of the variables $q_\alpha(\sigma_1)$, $q_\beta(\sigma_2)$, $q_\gamma(\sigma_3)$ and

$$\begin{aligned} n_\alpha'(\sigma_1) &= n_\alpha(\sigma_1) \pm 1, \\ n_\beta'(\sigma_2) &= n_\beta(\sigma_2) \pm 1, \\ n_\gamma'(\sigma_3) &= n_\gamma(\sigma_3) \pm 1. \end{aligned} \quad (19)$$

The coefficients γ are proportional to matrix components of the cubic perturbation term (15), which we need only assume to be small. The conditions (19) follow from the harmonic oscillator nature of the unperturbed problem and it is to be understood that n' cannot be negative. In order to find the transition probability two states of the type (18), it is necessary to examine the matrix components of $\mathbf{p}(\mathbf{s})$ given by (14) since, as was pointed out there, this represents the dipole moment for the entire crystal, and from the remarks made in §4 it follows that $\nu(\mathbf{s})$ will still be the principal frequency because Ψ_0 is the prominent term in Ψ. Because of the presence of the higher order terms in (18), this may possess nonvanishing dipole moment components with other states Ψ' arising from nonvanishing components between the first-order term of Ψ and the second-order terms of Ψ' and *vice versa*.

There are several prominent cases that we shall handle separately:

Case I. Let us assume that in Ψ the various waves of $q_\alpha(\sigma)$ are in states given by the quantum numbers $n_\alpha(\sigma)$. Then among the higher order terms, which will be a linear combination of other states, there will be characteristic terms in which the states corresponding to $q_\alpha(\sigma_1)$, $q_\beta(\sigma_2)$,

[36] The Schrödinger perturbation scheme may be found in any textbook on quantum mechanics. L. Brillouin, J. de phys. et rad. (III) **1**, 373 (1932); E. P. Wigner Bull., Hung. Acad. (to appear shortly).

$q_\gamma(\sigma_3)$, $q_\delta(\mathbf{s})$ are given by

$$n_\alpha(\sigma_1)\pm 1, \quad n_\beta(\sigma_2)\pm 1, \quad n_\gamma(\sigma_3)\pm 1, \quad n_\delta(s), \quad (20)$$

where σ_1, σ_2, σ_3 must satisfy the condition (16). There will clearly be 2^3 such states, unless some of the n's are zero in which case only the positive sign may appear. These higher order terms will possess important nonvanishing components only with that state Ψ' in which the zero-order term has quantum numbers $n_\alpha(\sigma)$, excluding those going with $q_\alpha(\sigma_1)$, $q_\beta(\sigma_2)$, $q_\gamma(\sigma_3)$, $q_\delta(\mathbf{s})$ in which cases the quantum numbers must be

$$n_\alpha(\sigma_1)\pm 1, \quad n_\alpha(\sigma_2)\pm 1, \quad n_\alpha(\sigma_3)\pm 1, \quad n_\gamma(\mathbf{s})\pm 1, \quad (21)$$

in which the signs of the first three terms must agree with those of (20), so that the energy difference between Ψ and Ψ' is

$$h(\pm\nu_\alpha(\sigma_1)\pm\nu_\beta(\sigma_2)\pm\nu_\gamma(\sigma_3)\pm\nu_\delta(\mathbf{s})), \quad (22)$$

that is, all energies corresponding to the sum (22) may be absorbed or emitted, the first case being that in which the resultant quantity is positive and the second that in which it is negative. If the matrix components between the zero-order term of Ψ and the higher order terms of Ψ' are considered, it is readily seen that they introduce no new possibilities, while the terms arising from interconnection of the higher order term of both Ψ and Ψ' will be cast aside as negligible.

Case II. If σ_1 (or either of the other two σ's) is equal to s, the argument of case I is practically repeatable, the only difference being that but three waves $q_\beta(\sigma_2)$, $q_\gamma(\sigma_3)$, $q_\delta(\mathbf{s})$ need be considered. The energies that may be absorbed or emitted are now given by

$$\pm\nu_\beta(\sigma_2)\pm\nu_\gamma(\sigma_3) \quad (23)$$

or

$$\pm\nu_\beta(\sigma_2)\pm\nu_\gamma(\sigma_3)\pm 2\nu(\mathbf{s}), \quad (23a)$$

which are just the results one would obtain from (22) by setting $\nu_\alpha(\sigma_1)=\nu(\mathbf{s})$.

Case III. If either of the σ's were equal to zero, difficulty would arise from the fact that the corresponding states belong to a continuous spectrum, and a special treatment would be required, but we may safely assume that the absorption involved in any single transition of this type is negligible and that the cases in which σ is practically, but not quite zero (see below) are the really important ones. For these, the discussion given above is valid, and the frequencies absorbed or emitted are practically

$$\pm\nu_\alpha(\sigma_2)\pm\nu_\beta(\sigma_3)\pm\nu(\mathbf{s}). \quad (23b)$$

The additional cases in which all of the σ's are equal to s or zero do not occur as will be seen later.

It is perhaps wise to repeat that the negative signs in (22), (23), (23a) are valid only if the corresponding states are excited in Ψ, since this fact will give rise to much of the temperature dependent effects; that is, at sufficiently low temperatures only the positive signs will be important.

The absorption (or emission) coefficient for any given frequency of the allowed type will necessarily be small if the assumptions made here are essentially correct, and in order to obtain a region of strong absorption, it is necessary that there be a large number of allowable combinations of σ in the equations of Case I and II for which the energy absorbed is practically constant and the relation (16) is maintained.[37] This implies that the energy spectrum in the neighborhood of each of the combining σ's must be such that its gradient is practically zero, which can only occur when the σ's are in the vicinity of those regions of the zone for which the gradient actually does vanish. This implies the need for precise knowledge of the zone structure of each lattice dealt with, and an examination of the zones described previously for the face-centered lattice shows that there are seven values of σ for which the gradient vanishes. (σ's which are sent into one another by symmetry operations are not counted as different). As may be expected, these points correspond to the interaction of the zones with symmetry axes, so that the polarization direction of the waves may be determined at once. Thus in the (100) direction, it is evident that there will be one wave polarized in this direction (longitudinal wave), and two waves of equal energy (differing from that of the longitudinal wave) for which the polarization directions are orthogonal to this. These points are listed below along with the number of different energies going with the three direction of

[37] The importance of this was realized by Born and Blackman in their work.

polarization. The actual energies in terms of the parameters $\alpha(1), \cdots, \alpha(10)$ of the potential energy expression will not be given at this time since correlations have not yet been obtained.

1. Intercept of the (111) axes with the cube; there are three equal energies.
2. The origin corresponds to three equal energies.
3. Intercept of (100) axis with cube. The two transverse waves have equal energies differing from that of the longitudinal wave.
4. Intercept of the (110) type of axis with the cube. There are two different energies corresponding to a wave polarized in the (100) direction and two polarized in the plane orthogonal to this, the latter two being degenerate.
5. The center of the hexagonal faces of the truncated octahedron. The longitudinal wave is polarized perpendicular to the face, and has a different energy from that of the two degenerate transverse waves.
6. The center of the edge of a square face of the truncated octahedron (say the (100) face). There are three waves of different energy, one of which is polarized in a direction orthogonal to the plane passing through the (100) axis and the point. The other two polarization directions lie in the (011) and the $(0\bar{1}1)$ directions.
7. The intercept of the (011) axis with the truncated octahedron, bisecting one of the edges of a hexagonal face; the three waves are of different energies and their polarization axes lie along this axis and in the two symmetry planes which intersect it, respectively.

The points corresponding to these cases are indicated by the appropriate number in Fig. 9.

Of these seven cases, it is to be noted that 1 and 2, 3 and 4, and 6 and 7, respectively, possess σ's which differ by a vector of the type $\mathbf{s}^i$, so that of these three pairs, one member may be assumed to have the three, possibly degenerate, energies going with the lower part of the discontinuity and the other the energies going with the upper part. In case 5, for which $2\sigma = s^i$, the discontinuity is such that both upper and lower branches have values at the same point; that is, the discontinuity arises from an actual double-valuedness of the energy surfaces at this point—a property that is intimately tied up with the symmetry properties.

Were the β's in (15) all nonvanishing, it would be safe to say that the spectrum would possess as its most prominent secondary lines, those transitions of the type (23), (23a) and (23b) in which σ_2 belongs to the lower side of the discontinuity and σ_3 to the upper, or *vice versa*, and in which the signs before both of these are positive. For in these cases $\nu(\sigma_1)+\nu(\sigma_2)$ would vary very slowly as σ_2 and σ_3 take on values permitted by the relation $\sigma_2 \pm \sigma_3 = \mathbf{s}^i$ since one of these decreases as the other increases, and there would be a large accumulation of transitions of nearly constant energy. It is readily seen that there would be 17 possible combinations of this type, namely, those listed below:

3 and 4—four lines (two different polarization energies);
5 and 5—four lines (two different polarization energies);
6 and 7—nine lines (three different polarization energies).

Designating these 17 sums, $\nu_\beta(\sigma_2)+\nu_\gamma(\sigma_3)$, as multiplet A, the 17 lines corresponding to (23) would appear on the large frequency side of the fundamental, $\nu(\mathbf{s})$, since they are all found to be greater than it. Similarly, this same multiplet will appear at an equal interval on the large frequency side of $2\nu(\mathbf{s})$ and $3\nu(\mathbf{s})$ corresponding to (23b) and (23a), respectively.

The 17 difference frequencies $|\nu_\beta(\sigma_2)-\nu_\gamma(\sigma_3)|$ which we shall designate as multiplet B, would also be prominent at high temperatures and, corresponding to the cases (23), (23b) and (23a) we should have the cases

$$B, \quad \nu(\mathbf{s})+B, \quad 2\nu(\mathbf{s})+B.$$

Similarly, if we designate $-A$ by $\bar{A}$ and $-B$ by $\bar{B}$, the cases

$$-\nu(\mathbf{s})+A, \quad \nu(\mathbf{s})+\bar{B}, \quad 2\nu(\mathbf{s})+\bar{B}, \quad 2\nu(\mathbf{s})+\bar{A}$$

would be of importance, and indicate that the multiplet A would appear between 0 and $\nu(\mathbf{s})$, that the inverted multiplet $\bar{B}$ would appear be-

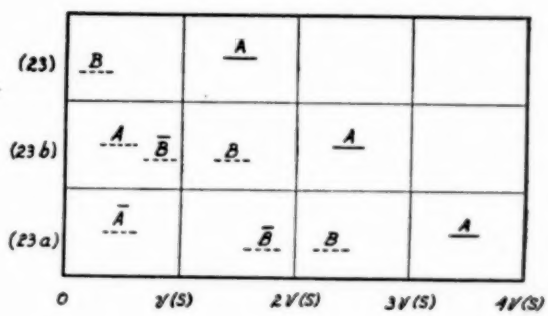

FIG. 10a. A schematic representation of the disposition of multiplets A, B and their inverses. The dotted lines represent lines that will disappear at very low temperatures. The three rows correspond to results arising from the three equations indicated.

tween 0 and $\nu(\mathbf{s})$ and $\nu(\mathbf{s})$ and $2\nu(\mathbf{s})$, respectively, and that the inverted multiplet $\bar{A}$ would appear between 0 and $\nu(\mathbf{s})$ (see Fig. 10a).

The restrictions on the β's, however, do not allow all of the 6×17 possible sums and differences of (23), (23a) and (23b) to appear, and in fact, the cases excluded are those corresponding to transitions in which states involving 1, 2, 3 and 4 are excited in any combination. This of course, excludes the 4×3 transitions involving 3 and 4 mentioned above and also some others not yet discussed. This restriction may be brought out only by a detailed investigation of the type of trinomial expressions in the q's that may occur, the argument being essentially as follows.

In terms of the normal coordinates $q_\alpha(\sigma, c)$ and $q_\beta(\sigma, s)$ the displacement vector for the atom of type 1 or 2 situated at lmn is given by

$$x^i(lmn)=\sum_\alpha\sum_\sigma\{q_\alpha(\sigma, c)f_\alpha{}^i(\sigma)p_\alpha(\sigma, lmn)\cos\sigma\cdot\mathbf{r}(lmn)+q_\alpha(\sigma, s)f_\alpha{}^i(\sigma)p_\alpha(\sigma, lmn)\sin\sigma\cdot\mathbf{r}(lmn)\}, \quad (24)$$

where $q_\alpha(\sigma)$ are the final normal coordinates, and σ extends throughout the entire cube in σ-space, $f_\alpha{}^i(\sigma)$, is the αth polarization vector going with the σth wave, which will be identical for like atoms, while $p_\alpha(\sigma, lmn)/p_\beta(\sigma, l'm'n')$ gives the relative amplitudes of the atoms at lmn and $l'm'n'$, assuming they have the same phase (this will be 1 if the atoms are identical). For the prominent values of σ in which we are interested, the polarization directions are identical for unlike atoms, so that we need not carry the indices lmn in these quantities.

Using (24), the quantity $\xi^1(l_im_in_i, lmn)$ is

$$\sum_\sigma\sum_\alpha\{q_\alpha(\sigma, c)f_\alpha{}^i(\sigma)(p(\sigma, l_im_in_i)\cos\sigma\cdot\mathbf{r}(l_im_in_i)-p(\sigma, lmn)\cos\sigma\cdot\mathbf{r}(lmn))$$
$$+q_\alpha(\sigma, s)f_\alpha{}^i(\sigma)(p(\sigma, l_im_in_i)\sin\sigma\cdot\mathbf{r}(l_im_im_i)-p(lmn)\sin\sigma\cdot\mathbf{r}(lmn))\} \quad (25)$$

and if we set $\mathbf{r}(l_im_in_i)=\mathbf{r}(lmn)+\rho(l_im_in_i)$, this becomes

$$\xi^i=\sum_\sigma\sum_\alpha\{[q_\alpha(\sigma, c)f_\alpha{}^i(\sigma)A(\sigma, l_im_in_i)-q_\alpha(\sigma, s)f_\alpha{}^i(\sigma)B(\sigma, l_im_in_i)]\cos\sigma\cdot\mathbf{r}(lmn)$$
$$+[q_\alpha(\sigma, s)f_\alpha{}^i(\sigma)A(\sigma, l_im_in_i)+q_\alpha(\sigma, s)f_\alpha{}^i(\sigma)B(\sigma; l_im_in_i)]\sin\sigma\cdot\mathbf{r}(l_im_in_i)\} \quad (26)$$

where

$$\begin{aligned}A(\sigma, l_im_in_i)&=-(p(\sigma, lmn)-p(\sigma, l_im_in_i)\cos\sigma\cdot\rho(l_im_in_i))\\ B(\sigma, l_im_in_i)&=-p(\sigma, l_im_in_i)\sin\sigma\cdot\rho(l_im_in_i)\end{aligned} \quad (27)$$

so that A is invariant under an inversion in lmn, while B goes into its negative. If terms of this type are substituted in one of the invariant forms of §2 and the result is summed over all values of lmn corresponding to like atoms, the result may be written in the form

$$\sum_{l_im_in_i}\gamma(l_im_in_i)\sum_{\sigma_1\sigma_2\sigma_3}\{a(\sigma_1, l_im_in_i)a(\sigma_2, l_im_in_i)a(\sigma_3, l_im_in_i)-a(\sigma_1, l_im_in_i)b(\sigma_2, l_im_in_i)b(\sigma_3, l_im_in_i)$$
$$-b(\sigma_1, l_im_in_i)a(\sigma_2, l_im_in_i)b(\sigma_3, l_im_in_i)-b(\sigma_1, l_im_in_i)b(\sigma_2, l_im_in_i)a(\sigma_3, l_im_in_i)\} \quad (28)$$

where σ_1, σ_2, σ_3 must satisfy the relation (16), $l_im_in_i$ are summed over the values occurring in a given form with the proper coefficients γ, and

$$\begin{aligned}a(\sigma, l_im_in_i=)\sum_\alpha\{q_\alpha(\sigma, c)f_\alpha{}^iA(\sigma, l_im_in_i)-q_\alpha(\sigma, s)f_\alpha{}^iB(\sigma, l_im_in_i)\},\\ b(\sigma, l_im_in_i)=\sum_\alpha\{q_\alpha(\sigma, s)f_\alpha{}^iA(\sigma, l_im_in_i)+q_\alpha(\sigma, c)f_\alpha{}^iB(\sigma, l_im_in_i)\}.\end{aligned} \quad (29)$$

Now since $\xi^i\xi^j\xi^k(l+\lambda_1m+\mu, n+\nu)$ goes into $-\xi^i\xi^j\xi^k(l-\lambda, m-\mu, n-\nu)$ under inversion in the point lmn, the expression

$$\xi^i\xi^j\xi^k(l+\lambda, m+\mu, n+\nu)-\xi^i\xi^j\xi^k(l-\lambda, m-\mu, n-\nu) \quad (30)$$

must occur in each cubic invariant form if the first term does. As a result of this, it follows at once that in the result (28), when (29) is substituted, all terms not containing $B(\sigma, l_i m_i n_i)$ an odd number of times will vanish. Closer inspection shows quite readily that this fact does not depend upon the assumption that all three products in a given trinomial possess the same lmn and $l_i m_i n_i$.

Now in the cases 1, 2, 3 and 4 described previously, $\sin \sigma \cdot \rho(l_i m_i n_i) = 0$ for all values of ρ so that all intercombinations of these can give rise to no secondary maxima since the necessary combination of q's do not appear in (15).

For the combination of 5 and 1, and 6, 7, and 1, in the manner described above, this does not occur and all possible transitions are allowed, so that there are 13 frequencies $\nu_\beta(\sigma_2) + \nu_\gamma(\sigma_3)$ arising from these two cases, and the multiplets A and B as well as their inverses will contain this number of terms.

From the restriction discussed in the previous paragraph, it follows that the frequencies $2\nu(\mathbf{s})$, $3\nu(\mathbf{s})$ and $4\nu(\mathbf{s})$ may not occur as a combination of cases 1 and 2, as far as the cubic terms are concerned; moreover, it is easily seen that the case in which $\sigma_1 \neq \mathbf{s}$ cannot lead to anything new if all restrictions are taken account of properly.

There is one additional possible source of secondary maxima, namely, those cases in which $\sigma_2 = -\sigma_3$ (and $\sigma_1 = \mathbf{s}$), so that only transitions in which waves on the lower side or on the upper side play a role along with s are concerned. Such transitions undoubtedly have probabilities comparable with those considered above, but will probably not lead to maxima of the same intensity since the $\nu(\sigma_2) \pm \nu(\sigma_3)$ will not be constant for as large a range of σ_1 as in the preceding cases. It follows as before that only cases 5, 6 and 7 may occur along with 1.

At low temperatures, which means temperatures well below the characteristic temperature of the crystal, the peaks corresponding to cases in which negative signs occur in (23), (23a), (23b) (dotted lines in Figs. 10a and b) will disappear and only those in which all are positive will remain. The number of lines corresponding to these is 93 as compared with 260 in the high temperature case.

Part C. On the Correlation Between Experimental and Theoretical Results

If an attempt is made to find a satisfactory correlation between the preceding experimental and theoretical results, it is readily seen that the former is not complete enough either to confirm or deny the correctness of the latter. In the first place, it is essential that the fundamental frequency be unmistakably identified, and this is seen to be impossible at present because of the limitations on the long wave-length side of the spectrometer; that is, the absorption peak at 15.3μ would be the fundamental if it were definitely known that there were no additional high absorption regions beyond this, but that cannot be definitely stated. If the work of Strong can be accepted as correct, it would indicate that another region of absorption exists in the vicinity of 23μ. This difficulty may be removed by using another prism, such as one of KCl, or by using a grating spectrometer.

Second, the resolving power in the short wave-length region (5 to 10μ) of the present instrument is not sufficiently great to guarantee that the secondary structure has been determined to the same degree of accuracy as that in the region from 10 to 15μ; and, as a result, the position and number of peaks in the former region is not sufficient to test the symmetry about ν and 2ν, assuming the 15.3μ line is the fundamental.

Third, the broadening of all of the lines, because of the influence of high temperature on the coupling between waves, makes the precise position of the maxima very difficult to determine. This difficulty could be considerably reduced by

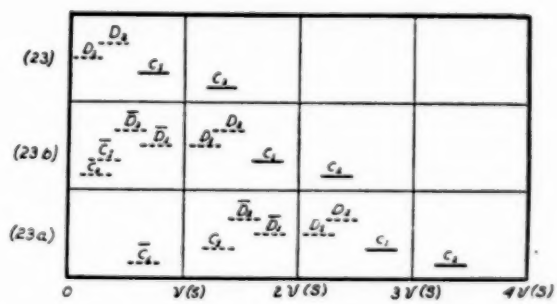

FIG. 10b. The plan is the same as that of Fig. 10a, the difference being that the multiplets arising from transitions involving waves on but one side of a discontinuity are shown.

cooling the observed sample to sufficiently low temperatures.

Concerning the precise position of the fundamental the following theoretical remarks may be made. If we make the very rough assumption that $\alpha(1)$ and $\alpha(2)$ are predominantly larger than any of the other 10 coefficients in B §2, and that these are related to the components of the stress-strain tensor, the fundamental frequency is found to be

$$\nu=(1/\sqrt{2}\pi)(A/M)^{\frac{1}{2}},$$

where

$$M=m_1m_2/(m_1+m_2), \quad A=a(c_{11}+c_{44}),$$

a is the nearest distance between unlike atoms, and c_{11} and c_{44} are the usual elastic coefficients. If the corresponding wave-lengths are determined using the results for the elastic coefficients discussed above, it is found that for NaCl and MgO the fundamental is at 49.5μ and 17.5μ respectively. Since the former is actually at 61.1μ, this suggests that the theoretical results are definitely low and indicates that the true value for MgO may be somewhat farther in the infrared.

In order to obtain experimental data that are capable of being compared with the preceding theoretical considerations, we are undertaking a thorough study of the absorption of the MgO crystal at low temperatures by means of an echelette grating spectrometer.

OCTOBER 1, 1935 PHYSICAL REVIEW VOLUME 48

The Spectra of Strontium Hydride

W. R. FREDERICKSON AND M. E. HOGAN, JR., *Syracuse University* AND WILLIAM W. WATSON, *Yale University*

(Received July 25, 1935)

New SrH band systems photographed at high dispersion include: (1) an abbreviated $C\,^2\Sigma\rightarrow N\,^2\Sigma$ system with (0,0) band head at 3808A, (2) a many-lined $D\,^2\Sigma\rightarrow N\,^2\Sigma$ system between 5000A and 6700A, (3) an $E\,^2\Pi\rightarrow N\,^2\Sigma$ system consisting of a $\Delta v=0$ sequence only with the (0,0) band at 5323A. The (0,0) and (0,1) C bands have three violent perturbations and a sharp cut-off due to predissociation at $K'=19$. The form and magnitude of the perturbations are computed. Quantum analyses give $B_0=3.930$ and $D_0=-9.31\times10^{-4}$ for the C state, $B_1=3.56$ for the normal state. Quantum assignments of the lines of the six principal branches of the (0,0) band of the E system are presented. For the E state $A=117$, $B^*_{0,-\frac{1}{2}}=3.6388$, $B^*_{0,+\frac{1}{2}}=3.8687$ and perturbations at small J values distort the Λ-doubling curve for the $^2\Pi_{\frac{1}{2}}$ state.

INTRODUCTION

IT has previously been observed[1] that strontium hydride exhibits two band systems in the red region of the spectrum, a $^2\Sigma\rightarrow{}^2\Sigma$ system with principal head at 7020A and a $^2\Pi\rightarrow{}^2\Sigma$ system whose (0,0) band has heads at 7347A and 7508A. These bands lie slightly towards longer wave-lengths from the analogous systems of the CaH molecule. Since the lowest electronic levels of Sr and Ca are so very similar one would expect a fairly complete correspondence between the hydride spectra of these two elements.

In addition to the two CaH systems in the red there are three other systems[2] in the visible and near ultraviolet. An interesting $^2\Sigma\rightarrow{}^2\Sigma$ system consisting normally of but two bands, (0,0) at 3534A and (0,1) at 3696A, exhibits a sharp cut-off at $K=9$ of the $v'=0$ level due to predissociation. There is also in the range 4000A–5800A a weak $^2\Sigma\rightarrow{}^2\Sigma$ system whose bands have no marked heads and whose upper vibrational levels all display violent perturbations. Finally, the existence of a $^2\Pi\rightarrow{}^2\Sigma$ band at 4900A with Q branches having very closely spaced rotational lines has been noted. SrH band systems corresponding to all of these have been located by the writers. In each instance the system is displaced slightly towards the red from the position of the similar CaH system. We shall discuss in this paper the abbreviated $^2\Sigma\rightarrow{}^2\Sigma$ bands in the near ultraviolet and the $^2\Pi\rightarrow{}^2\Sigma$ system in the green region only.

[1] W. W. Watson and W. R. Fredrickson, Phys. Rev. **39**, 765 (1932).

[2] Cf. W. Jevons, *Report on Band Spectra of Diatomic Molecules* for references.

FIG. 1. Microphotometer trace of the (0, 0) C band of SrH at 3808A. Note the multiple perturbations and the sharp cut-off due to predissociation at $K'=19$.

For the sake of brevity and to emphasize the similarity between the spectra of these two molecules, we shall adopt the same alphabetical designation of states as used for CaH. The normal state, common to all the band systems, is $N\,^2\Sigma^+$. The upper states of the red bands are $A\,^2\Pi$ and $B\,^2\Sigma$, that of the near ultraviolet system is $C\,^2\Sigma$, for the many-lined spectrum from 5000A to 6700A the upper state is $D\,^2\Sigma$, and for the green bands $E\,^2\Pi$.

TABLE I. *Assignment of frequencies in the* $C\,^2\Sigma \rightarrow N\,^2\Sigma(0, 0)$ *band of SrH* (cm^{-1} units).

Int.	ν (obs)	$R(K'')$	Int.	ν (obs)	$P(K'')$
3	26548.88	18	1	26291.72	1
3	47.64	18	2	84.88	2
1	39.49	17	3	78.68	3
1	38.03	17	1	77.36	19
4	11.76	16	2	75.31	19, 13
4	10.68	16	4	73.07	4, 20
4	497.16	15	1	71.85	20
4	95.22	15	0	70.09	14
2	76.32	14	3	68.30	5
2	74.40	14	0	65.33	8
1	72.20	12	6	63.38	6, 18
1	63.69	12	6	62.14	17, 18
5	61.79	13	6	59.96	8, 17
5	60.85	13	8	58.63	7
5	46.81	12	4	56.96	9, 10
6	45.58	12	5	55.04	8, 10
6	31.88	11		53.56	15, 16
0	25.70	10	7	53.56	11, 12, 12
4	18.19	10		51.40	13, 13, 14, 16
4	17.09	10	0	35.44	9
1	08.32	9			
1	06.23	9			
4	03.85	9			
4	392.18	8			
4	91.85	8			
3	81.44	7			
3	79.78	7			
0	74.94	6			
1	68.32	6			
1	62.42	6			
0	58.19	7			
3	53.22	5			
4	43.12	4			
3	33.21	3			
3	23.91	2			
2	15.15	1			
1	06.94	0			

Preliminary spectrograms were made with a small 120-cm grating, while the spectrograms from which measurements were taken were obtained in the second order of the 21-foot grating in a stigmatic mounting, the average dispersion being 2.4A per mm. The light source was a d.c. arc carrying 2 amperes between a water-cooled copper cathode and a hollow copper anode filled with metallic strontium in an atmosphere of hydrogen at about 7 cm of Hg pressure. Eastman 40 plates were used for the C system, Eastman I–C plates for the E bands. The exposure time for each group was two hours.

THE C SYSTEM

The C system of SrH consists merely of a (0,0) band with its head at 3808A, exhibiting multiple perturbations and a sharp cut-off at $K'=19$, together with a considerably weaker (0,1) band at 3984A, both bands degrading towards the violet. The sudden cessation of lines in these bands is undoubtedly caused by predissociation into the continuum of the less stable $D\,^2\Sigma$ state. In Table I are listed the intensities, wave numbers and quantum assignments of the lines of the (0,0) band. These assignments are made with the aid of lower state combination differences known from the earlier work on the red band systems. The nature of the perturbations may be seen by inspection of Fig. 1 which is a microphotometer trace of this band. The complex structure of this band is in decided contrast with the simplicity of the corresponding CaH C

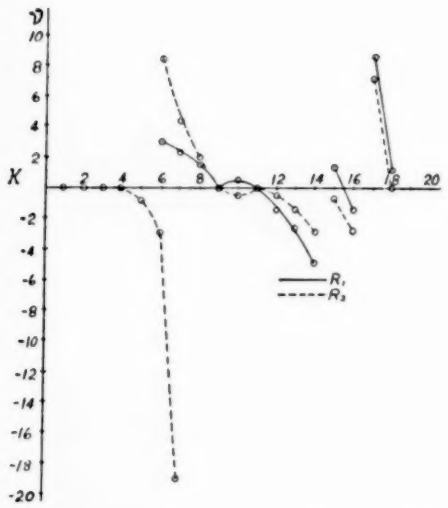

FIG. 2. Graph showing departures of observed R branch lines of the (0, 0) C band from positions predicted by fourth degree least-squares equation for the unperturbed lines. + indicates observed line has a larger wave number than the predicted value.

band. Whereas the lines in the CaH band are single, most of those in the SrH band are close doublets due to the larger coefficient $\gamma=0.122$ of the spin doubling in the normal state. The first perturbation appears at $K'=7$ although the lines belonging to $K'=6$ are broad and somewhat displaced. Therefore in evaluating the constants of the upper state it is possible to use only the first five of the appropriate combination differences. This somewhat lessens the accuracy of this calculation. From these five differences we compute $B_0'=3.930$ and $D_0'=-9.31\times10^{-4}$.

If one substitutes the B_0 constants in the usual expression for R-branch frequencies (neglecting the terms involving the D constants since K is small), the wave numbers of these first five lines may be calculated. In order to get agreement with the observed frequencies, it is evident that an extra linear term $-0.21K'$ must be included. This term is considerably smaller than the corresponding extra term $-2.22K'$ in the CaH C band.[3]

The nature and magnitude of the perturbations have been determined in the following manner. We observe that the R branch lines for $K''=9$ and 11 are intense and single while $R(10)$ has the splitting required by the spin doubling in the $K''=10$ level. Assuming, then, that these three lines (taking the mean of the two $R(10)$ lines) are practically in their normal position, and by using them in conjunction with the first six lines of the R branch, the following fourth degree equation representing these frequencies has been determined by the method of least squares:

$$\nu=26300.00+6.719M+0.3958M^2 -0.00329M^3+7.32\times10^{-6}M^4.$$

The variation of the position of each of the other R branch lines from that calculated with this equation is shown in Fig. 2. These variations which yield curves of the "anomalous dispersion" type indicate the presence of three perturbations.

In the construction of Fig. 2 the assignment of the perturbed lines to either the R_1 or R_2 branch has been made so as to give the best agreement with the known $\Delta_2F_1''(J)$ and $\Delta_2F_2''(J)$ values, using P branch lines of about the same intensity. This assignment accounts for every line on the low wave number side of the origin, including even a weak line lying some 15 cm^{-1} beyond the head of the band. In the region of R branch lines but one line at 26,413.82 remains unassigned. The characteristic assignment of the weaker, greatly perturbed lines to transitions already represented by stronger, less perturbed lines is to be noted.

Since the corresponding band of CaD has so many perturbations[4] in contrast to the simplicity of the CaH band, the study of the hydrogen

TABLE II. *Assignment of frequencies in the $C^2\Sigma\rightarrow N^2\Sigma(0, 1)$ band of SrH* (cm^{-1} units).

K''	R	P	K''	R	P
3	25165.11	25110.20	11	269.86	90.00
4	75.10	04.93	12	285.27	91.32
				86.48	92.59
5	Masked	01.13	13	302.82	94.57
6	"	096.42		04.02	
7	211.50	Masked	14	319.51	97.31
	13.20			21.29	98.65
8	225.62	087.56	15	25341.95	25099.95
	24.48	92.59		43.86	101.13
9	238.07	91.32	16	59.70	02.19
		92.59		61.19	
10	253.13	90.26	17	89.88	12.07
	54.05			91.67	14.26

[3] B. Grundström, Zeits. f. Physik **69**, 235 (1931).

[4] W. W. Watson, Phys. Rev. **47**, 27 (1935).

TABLE III. *Assignment of frequencies in the* $E\,^2\Pi \rightarrow N\,^2\Sigma(0, 0)$ *band of SrH* (cm^{-1} units).

$J''+\frac{1}{2}$	P_1	Q_1	R_1	P_2	Q_2	R_2
1						18972.59
2		18868.95	18883.22		18958.56	77.53
3	18850.98	72.11	95.04	18936.64	56.35	82.71
4	47.20	75.17	905.04	26.98	53.98	89.30
5	43.74	78.30	15.77	17.17	52.80	96.25
6	39.49	81.47	26.86	09.48	52.00	19002.97
7	36.11	84.81	38.23	02.45	52.00	10.28
8	32.57	88.35	49.10	894.27	52.50	
9	29.58	91.49	59.81	87.50	53.12	26.38
10	26.16	95.04	69.18	81.47	53.98	34.98
11	22.41	98.99	81.56	75.15	55.38	43.79
12	17.56	902.45	91.99	69.56	56.94	53.00
13	15.84	05.88	19002.97	64.42	58.86	62.48
14	12.76	09.48	13.84	59.56	61.28	72.11
15	09.23	13.22	24.88	55.12	63.69	82.09
16	06.23	17.17	36.38	50.98	66.38	92.23
17	03.43	20.50	46.96	47.20	69.18	102.48
18	00.10	25.41	58.20	43.74	72.59	12.88
19	798.27	29.43	69.48	40.56	76.27	23.62
20	96.20	33.71	80.78	37.54	79.55	
21	93.86	38.23	92.23	34.94	83.58	45.22
22	91.96	42.62	103.60	32.57	87.67	56.24
23	90.09	47.07	15.07	30.41	91.99	67.62
24	88.67	52.00	26.45	28.60	96.25	78.39
25	87.11	56.77	38.03	27.20	19000.76	89.70
26	85.91	61.57	49.42	26.16	05.22	200.96
27	84.80	67.15	60.97	25.35	09.43	12.27
28	83.81	71.68	72.62	24.23	14.84	23.44
29	83.13		84.05	23.50		34.72
30	82.58		95.16			45.80
31	82.00		206.70			57.07
32	81.40		17.96			68.05
	81.00		29.02			
			40.06			
			51.17			
			61.58			
			73.77			
			84.45			

isotope effect in this SrH band should prove interesting. This investigation will be reported in a forthcoming paper.

In Table II are listed the frequencies and quantum assignments of the (0,1) C band. The analysis of this band is somewhat hindered by the low intensity of its lines and by the presence of several strong atomic lines. Perturbations identical with those of the (0,0) band are of course present. The few final state combination differences yield the values $B_1''=3.56$ and $D_1''=-1.7\times10^{-4}$.

THE E SYSTEM

The $\Delta v=0$ sequence of the E system of SrH has a principal head at 5323A, the bands degrading to the violet. Because of the near equality of the rotational B constants in the two electronic states involved, other sequences are apparently of negligible intensity. Analysis shows the bands to be of the $^2\Pi\rightarrow{}^2\Sigma$ type. Since the lines in the P and R branches are very distinct at a distance from the origin, quantum assignments are easily made for these lines with the help of the combination differences for the final $N\,^2\Sigma$ state. These assignments show the $E\,^2\Pi$ state to be regular.

Below $J''=8$ the assignment of lines becomes very uncertain. This uncertainty is caused by the presence of the numerous lines of the (1,1) and (2,2) bands as well as lines of the D system which extend into this region. Also there are undoubtedly perturbations at the low J values. It is quite evident that in the $^2\Pi_{\frac{1}{2}}$ sub-state with $v=0$ perturbations occur at $J'=16\frac{1}{2}$ and $10\frac{1}{2}$. In Table III are listed the assignments of frequencies for the P_1, P_2, Q_1, Q_2, R_1 and R_2 branches of the (0,0) band.

The assignment of quantum numbers to the Q_1 and Q_2 branches is based on Λ-doubling considerations. Since $A/B\leqq31$ and since the nature of the doubling indicates that the p constant must be positive, it is assumed that the Λ-doubling of the $E\,^2\Pi$ state should lie somewhat between that exhibited by SiH and ZnH.[5] Fig. 3 shows the Λ-doubling for the assignments chosen. Due to the uncertainty of the P_1- and R_1-branch assignments for J values below $J=8$, the Λ-doubling curve in this range for the $\Pi_{\frac{1}{2}}$ levels

[5] R. S. Mulliken and A. Christy, Phys. Rev. **38**, 105 (1931).

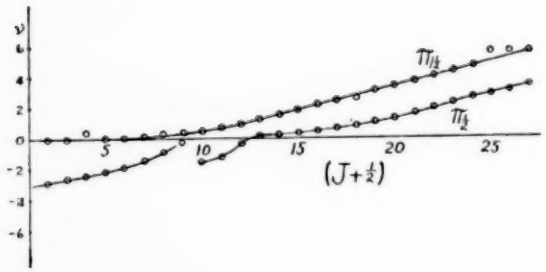

FIG. 3. Λ-doubling curves for the $E\,^2\Pi$ state of SrH.

may not be accurate. If it is correct as given, the failure of the curve to return to zero at $J=0$ must be attributed to another perturbation. Because of this possibility of error in the P_1 and R_1 branches at low J values, however, we do not evaluate the usual p_0 and q_0 quantities involved in the Λ-doubling. The other molecular constants, determined from the $\Delta_2 F$ values in the customary manner,[2] are presented in Table IV.

Satellite branches should be observed in this band. We have located the ${}^RQ_{21}$ branch at large J values but the other satellite branches cannot be definitely established because of the many weaker lines of the other bands present in this region.

TABLE IV. *Rotational constants of the* $E\,^2\Pi \rightarrow N\,^2\Sigma(0, 0)$ *SrII band at 5323A.*

$N\,^2\Sigma$ state: $B_0=3.6198$	$D_0=-1.287\times10^{-4}$
$E\,^2\Pi$ state: $B_0{}^*-\frac{1}{2}=3.6388$	$D_0=-1.03\times10^{-4}$
$B_0{}^*+\frac{1}{2}=3.8687$	$D_0=-1.95\times10^{-4}$
$A=117$	

ELECTRONIC STATES OF SrH

In our earlier work[1] on the red bands of SrH we noted that the $A\,^2\Pi$ and $B\,^2\Sigma$ states stand to each other in the relation of "pure precession," being undoubtedly $5p\sigma^2 5p\pi\,^2\Pi$ and $5p\sigma^2 5p\sigma\,^2\Sigma$ respectively. The $N\,^2\Sigma^+$ normal state is probably $5s\sigma^2 4d\sigma\,^2\Sigma$. The E state may be either $5s\sigma^2 4d\pi\,^2\Pi$ or $5s\sigma 5p\sigma 5p\pi\,^2\Pi$. The D state might then well be $5s\sigma 5p\sigma^2\,^2\Sigma$, and the lack of strong interaction with the E state could be due to the large difference in the B constant of the D state from that of all other states. For our analysis of one of the bands of the D system, with v' as yet unknown, indicates B' to be only 1.91. The lack of strong interaction may also be due to the presence of the $C\,^2\Sigma$ state above the E state, thus neutralizing in part the effect of the D state.

The D system of SrH as well as the C and B systems of SrD will be discussed in a further paper.

OCTOBER 1, 1935 PHYSICAL REVIEW VOLUME 48

The $3p^3\Sigma \rightarrow 2s^3\Sigma$ Bands of HD and D_2

G. H. DIEKE, *The Johns Hopkins University*

(Received July 18, 1935)

The $3p^3\Sigma \rightarrow 2s^3\Sigma$ bands of HD and D_2 which form the most conspicious regularities in the near infrared are given and the band constants calculated.

IN a previous communication[1] the so-called Fulcher bands ($3p^3\Pi \rightarrow 2s^3\Sigma$) of the isotopes HD and D_2 of the hydrogen molecule were given. There is a band system $3p^3\Sigma \rightarrow 2s^3\Sigma$ chiefly lying in the extreme red and near infrared closely connected with the Fulcher bands. It has the same final state, and the initial states belong to the same complex, i.e., they differ only by the value of the projection Λ of the orbital momentum on the internuclear axis.

[1] G. H. Dieke and R. W. Blue, Phys. Rev. **47**, 261 (1935).

The present paper contains chiefly the empirical data of the $3p^3\Sigma \rightarrow 2s^3\Sigma$ system. A theoretical discussion of the $3p$ complex is given in the following paper, which will also contain an account of the perturbations in both systems. The general remarks about the production of the spectrum, the wave-length measurements, etc., made in the previous paper[1] apply also to the present investigation.

In the far red and infrared the sensitivity of the photographic plates varies rapidly with the

TABLE I. *The $3p^3\Sigma \rightarrow 2s^3\Sigma$ bands of HD.*

J	P BRANCH ν	I	R BRANCH ν	I	
			0→0		
0	—	—	11 664.67	2	
1	11 574.34	1	694.49	4	
2	514.36	3	713.90	4	
3	444.97	3	722.78	4	
4	366.59	2	721.22	2	
5	279.73	1	709.06	0	
			1→0		
0	—	—	13 465.77	2	
1	13 377.31	4	491.64	10	
2	315.37	5c	505.20	10	
3	242.09	5	506.34	10	
4	157.88	6c	495.14	10	
5	063.27	5	471.79	0	
6	12 958.84	5	436.34	1	
7	845.16	4	388.39	0	
8	722.88	2c			
9	592.63	3			$+D_2$
			1→1		
0			11 262.98	0	
1			290.98	1	
2			308.77	0	
3			316.41	0	
4			313.49	00	
5					
			2→0		
0	—	—	15 165.34	6	
1	15 078.98	6	187.32	6	
2	015.02	7	195.00	8	
3	14 937 79	6	188.37	6	
4	847.70	7	167.47	7r	
5	745.23	7	132.56	6	
6	631.14	5	083.85	5	
7	505.88	5	021.64	4	
8	370.28	3	14 946.35	3	
	225.81	1			
			2→1		
0	—	—	12 962.60	7	
1	12 878.32	6	986.71	8	
2	818.64	8	998.65	5	$+D_2$
3	747.76	9	998.15	4r	
4	666.08	9	985.87	5	
5	574.12	9	961.41	4	
6	472.42	7	925.10	3	
7	361.56	5			
8	242.21	3			
9	114.83	1			
			3→1		
0	—	—	14 559.84	7	
1	14 477.34	0	580.96	8	
2	415.97	5	590.42	6b	
3	342.07	6	569.03	5	
4	257.98	4	551.11	6	
5	144.89	5	516.13	5r	
6	037.72	4			
7	13 916.10	2c			
			3→2		
0	—	—	12 459.88	7	
1	12 379.33	7	483.05	7	
2	322.13	8	496.62	9	$+D_2$
3	254.43	9	481.43	6	
4	178.46	6	471.69	6	
5	075.59	5	446.90	4	
6	980.54	4			
7					
			4→1		
0	—	—	16 050.74	2	
1	15 970.62	2	066.61	3	
2	906.81	2	066.24	3	
3	827.66	2	049.70	2	
4	733.67	1	017.18	3bv	
5	625.53	0			
6	503.70	00			
			4→2		
0	—	—	13 950.71	5	
1	13 872.65	6	968.64	9	
2	812.95	7	972.41	9	
3	740.00	6	962.05	9	α_{34}, Q_6
4	654.22	7	937.64	4	
5	556.18	4	899.34	4	$+D_2$
6	446.43	2	847.43	1	
7	325.66	1	781.62	2	
8	194.85	1			$+D_2$
			4→3		
0	—	—	11 950.77	4	
1	11 874.62	3	970.71	5	
2	819.05	1	978.51	5	
3	752.12	2	974.16	4	
4	674.32	1	957.75	3	
5	586.21	0	929.41	2	
6			889.33	0	
			5→2		
0	—	—	15 330.13	4	
1	15 254.16	4	343.93	5	
2	192.39	4	341.43	5	
3	115.32	4	322.68	4	
4	023.30	3	287.72	4	
5			coincides with D_α		
6			169.93	2	
			5→3		
0	—	—	13 330.16	2	
1	13 256.17	3	345.97	2	
2	198.48	3	347.51	3	
3	127.41	4	334.78	2	
4	043.38	4	307.80	2	
5	12 946.87	5	266.77	1	
6			838.43	3	
			6→3		
0	—	—	14 586.93	4	
1	14 615.05	3	598.37	5c	
2	455.29	4	593.49	6	
3	379.80	4	571.55	7	
4	289.31	4	534.70	5	
5	183.63	2			
6	065.32	1			
			6→4		
0	—	—	12 684.92	4	
1			698.35	3	
2	12 559.18	4	697.34	3	$+D_2$
3	489.62	5	681.37	3	
4	406.90	5	652.33	3d	
5	310.38	3			
6					

wave-length. The photographic intensities depend very much on the plate used and the sensitization employed. Relative intensities appear sometimes completely distorted even over a comparatively narrow region. This accounts for almost all the apparent intensity anomalies found in the tables.

The frequencies and intensities of the bands are given in the Tables I for HD and II for D_2. The bands contain a large part of the strongest lines in the infrared and are the most prominent feature in that part of the spectrum. Only those bands which are fairly complete are listed. There are several weaker bands, the position of which can be calculated and of which a number of lines can be found. They, as well as bands with higher values of V', are left for a later occasion as undoubtedly their identification will be much more certain when the other strong lines in this region have been classified.

The rotational constants were calculated in the usual way,[1] and they are listed in Table III. The spaces left open are the vibrational levels which are so strongly perturbed that no reliable values can be obtained.

As shown more in detail in the following paper, the B_v values calculated directly from the observations cannot be used for the calculation of the moment of inertia or other constants which have to do with the vibration and rotationless state of the molecule. It is necessary to take into account the influence of the interaction with the $3p^3\Pi$ state. If we correct for this in the way indicated in the following paper the new values for B_v are

	HD	D_2
B_0	20.257	13.553
B_1	19.259	13.045
B_2	18.236	12.504.

This includes the B_v of all those levels which are far enough from any $3p\Pi$ level, so that only the regular Λ doubling has to be taken into account.

B_e can then be calculated from $B_v = B_e$

TABLE II. *The $3p^3\Sigma \rightarrow 2s^3\Sigma$ bands of D_2.*

J	P BRANCH ν	I		R BRANCH ν	I	
			0→0			
0	—	—		11 676.15	0	
1				696.39	0	
2	11 575.39	1		709.82	3	
3	528.90	0		716.39	1	
4	476.25	1		716.14	2	
5	417.65	00		709.29	1	
6	353.38	0		695.27	0	
			1→0			
0	—	—		13 163.44	3	
1	13 103.88	2		181.55	3c	
2	062.67	4		191.80	4	
3	014.06	3c		194.21	4d	
4	12 958.25	6		188.66	4	
5	895.44	5		175.35	1	
6	825.92	8		154.26	2	
7	749.94	3		125.61	0	
8	667.80	3		089.43	0	
9	579.79	5				
10	486.28	2				
			2→0			
0	—	—		14 583.13	3c	
1	14 524.61	3		599.13	4	
2	482.36	6		606.22	5	
3	431.64	4		604.40	4	
4	372.66	4		593.66	5r	
5	305.66	3		574.07	2	
6	230.89	4		545.71	4	
7	148.93	(10)	+HD	508.76	1	
8	059.22	1		463.43	(4)	α_{34}, Q_1
9						
10						
			2→1			
0	—	—		12 768.25	6	
1	12 710.91	4		785.42	5	
2	670.95	7		794.83	8	
3	623.74	7		796.49	6	
4	569.38	9		790.37	7	
5	508.12	7		776.54	3	
6	440.23	6		755.09	4	
7	365.94	4		726.14	3	
8	285.57	4		689.73	2	
9	199.43	2		646.08	1d	
10	107.74	2				
			3→0			
0	—	—		15 934.99	0	
1	15 877.57	0		948.84	0	
2	834.23	3		952.75	1	
3	781.35	1		946.68	0	
4	719.16	2		930.64	3	
5	647.91	0		904.74	1	
6	567.86	1		869.05	1	
7	479.29	00				
8	382.55	00				
			3→1			
0	—	—		14 120.06	4	
1	14 063.78	3		135.10	5	
2	022.79	10		141.33	8	
3	13 973.42	5		138.73	5	
4	915.86	10		127.31	5	
5	850.34	5		107.16	3	
6	777.16	3		078.35	3	
7	696.56	2		040.90	3d	+HD
8	608.85	3		13 995.33	1	
9	514.39	2c				
10	413.50	0r				
			3→2			
0	—	—		12 374.23	6	
1	12 318.99	8		390.40	5	
2	280.39	7		398.91	8	
3	234.45	6		399.71	6	
4	181.41	7		392.83	7	
5	121.54	5		378.27	5	
6	055.06	7		356.20	5	
7	11 982.25	3		326.65	2d	
8	903.36	3		289.75	3	

J	P BRANCH ν	I		R BRANCH ν	I	
			4→1			
0	—	—		15 402.94	2	
1	15 347.75	1		415.83	2	
2	305.68	3		418.84	4	
3	254.16	2		411.95	2	
4	193.39	3		395.20	4	
5	123.61	1		368.66	1	
6	045.09	0		332.44	2	
7	958.12	0		286.68	0	
8	862.88	1		231.56	0d	
9	759.97	0				
10	649.58	00				
			4→2			
0	—	—		13 657.08	4	
1	13 603.08	3		671.16	4	
2	563.27	9		676.43	6	
3	515.18	10		672.95	3	
4	458.94	5		660.71	6	
5	394.74	2		639.80	3	
6	322.80	6		610.28	3	
7	243.74	2		572.32	0	
8	157.50	1d		526.04	1	
9	064.32	0				
10	964.79	1				
			4→3			
0	—	—		11 978.87	3	
1	11 925.94	2		994.00	3	
2	888.39	5		12 001.52	5c	
3	843.56	1		001.35	3c	
4	791.73	2		11 993.54	4	
5	733.11	0		978.14	1	
6	667.83	0		955.22	2	
7	—	—		924.86	0	
8	—	—		887.25	00	
			5→2			
0	—	—		14 869.00	4	
1	14 815.99	3		881.02	5	α_{01}, R_0
2	775.22	5		883.28	6	
3	725.04	4		876.25	5	
4	665.83	5		861.98	5	
5	598.10	3		823.48	1	
6	524.23	1				
7	427.32	3	+HD			
			5→3			
0	—	—		13 190.79	2	
1	13 138.91	0		203.86	4r	
2	100.29	4		208.44	4c	
3	053.46	3		204.71	3	
4	12 998.65	5	+HD	194.85	1	
5	936.46	3		161.74	0	
6	869.16	3				
7	779.89	1				
			6→2			
0	—	—		16 006.34	0	
1	15 954.63	0		015.70	0	
2	912.52	4		014.00	3	
3	859.70	2		001.26	0	
4	796.48	3		15 977.62	(4)	α_{23}, P_3
5	723.15	0		942.88	00	
6	639.74	1		897.36	2	
			6→3			
0	—	—		14 328.03	4	
1	14 277.47	2		338.60	(10)	α_{45}, Q_2 +HD
2	237.50	10	+HD	339.05	4	
3	188.08	4		329.65	4	
4	129.28	5		310.34	5	
5	061.36	3		281.20	2	
6	984.63	4		242.23	2	
7	899.34	4	+HD	193.58	1	
			6→4			
0	—	—		12 715.98	3	
1	12 666.44	3		727.54	3	
2	628.74	7b		730.27	5	
3	582.55	4	9→6, R_1	724.14	3	
4	528.10	7		709.18	5	

J	P BRANCH ν	I		R BRANCH ν	I	
5	465.60	4		685.42	4	
6	395.27	6		652.89	2	
7	317.43	1				
8	233.36	4				
9	140.57	0				
			7→3			
0	—	—		15 385.52	2	
1	15 336.14	1		393.59	1	
2	295.01	2		390.78	3	
3	243.15	2		375.96	2	
4	181.02	2		350.49	3	
5	107.72	0		313.84	1v	
6	024.80	0		266.09	1	
7	931.81	0		207.16	0dc	
			7→4			
0	—	—		13 773.41	2	
1	13 725.11	1		782.60	1	
2	686.18	4		781.96	2	
3	637.59	3		770.44	2	
4	579.80	3		749.27	2	
5	511.93	5		717.84	3	
6	435.44	1		676.83	3	
			7→5			
0	—	—		12 226.45	2	
1	12 179.25	1		236.70	1	
2	238.22	2		142.43	3	
3	097.06	1		229.91	1	
4	043.55	3		213.05	2	
5	11 980.99	2		187.11	1	
6	910.89	2		152.15	1	
			8→3			
0	—	—		16 354.17	00	
1	16 306.03	00		359.57	00	
2	263.60	0		352.46	0	
3	209.25	1D		332.93	00	
4	142.76	2		301.22	00	
5	064.67	00				
	15 975.54	0				
			8→4			
0	—	—		14 742.04	3	
1	14 695.06			748.53	3	
2	654.81	3		743.63	5	
3	603.54	3		727.35	4	
4	541.44	4		700.00	5	
5	468.86	2dc				
6	386.18	1				
			8→5			
0	—	—		13 195.18	1d	+HD
1	13 149.22	0		202.66	0	
2	111.09	1		199.97	1	
3	063.27	(5)	+HD	186.84	0	
4	005.24	2		163.78	0	
5	12 937.96	1				
6	861.63	2				
			9→4			
0	—	—		15 607.40	1	
1	15 562.27	0		610.26	1	
2	520.17	1		599.88	2	
3	465.27	1		576.22	1	
4	397.72	1		539.19	2	
5	317.69	0		488.72	0	
6	225.36	0				
			9→5			
0	—	—		14 060.33	1	
1	14 016.33	0		064.33	1	
2	13 976.39	2		056.09	3	
3	924.65	4d		035.64	1	
4	861.43	3		002.98	3d	
5	786.74	0		957.84	0	
6						
			9→6			
0	—	—		12 577.78	5	
1	12 534.67	0		582.55	4	6→4, P_3
2	496.87	3		576.58	3	
3	448.35	1		559.18	4	
4	389.29	4		530.79	2	
5	319.86	1		490.82	0b	
6						
7						
8						

TABLE III. *Rotational constants of the $3p^3\Sigma$ level.*

v	HD B_v	HD D	D_2 B_v	D_2 D
0	20.077	0.0089	13.475	
1	19.100	87	12.974	0.0042
2	18.095	77	12.440	39
3	+		11.910	39
4	16.044	71	11.367	37
5	15.011	77	+	
6	+		10.201	34
7			+	
8			8.920	27
9			8.024	39

$-\alpha(V+1/2)$. In evaluating these constants the B_0 value of D_2 which is less reliable than the others was disregarded.

We find then

	HD	D_2
B_e	20.766	13.856
α	1.010	0.541
I_e	$1.3319\cdot10^{-40}$	$1.9961\cdot10^{-40}$
r_e	$1.09662\cdot10^{-8}$	$1.09649\cdot10^{-8}$

average $r_0=1.09655\cdot10^{-8}$.

The ratio of the B_e values is 0.6672 which compares well with the theoretical value 0.6671. The ratio 0.534 of the α is lower than the theoretical value 0.544, but the accuracy with which the α can be determined in this case is hardly better than this agreement.

If the constants would be calculated in the same way from the observed B_v without the correction, the ratio of the B_e values would be 0.6692 which is considerably different from the theoretical value 0.6671.

With the rotational energy of initial and final states known, the origins of all the bands can be calculated and they are given in the Tables IV and V. The values marked with a + are the origins of those bands which have strong perturbations. They are obtained only from the P(1) line as the $J'=0$ level cannot be perturbed.[2] As they are calculated from one line only they are less accurate than the other values.

The constants in the formula for the vibrational energy

$$\omega v-xv^2+yv^3-zv^4+\cdots(v=V+1/2)$$

[2] G. H. Dieke, Phys. Rev. **47**, 870 (1935).

TABLE IV. *Zero lines of the $3p^3\Sigma\rightarrow2s^3\Sigma$ bands of HD.*

V' \ V''	0	1	2	3
0	11 624.55			
1	13 427.56	11 224.80		
2	15 129.24	12 926.46		
3		14 525.41+	12 525.41+	
4		16 018.66	13 918.64	11 918.67
5		17 400.16	15 300.16	13 300.18
6				14 521.32

TABLE V. *Zero lines of the $3p^3\Sigma\rightarrow2s^3\Sigma$ bands of D_2*

V' \ V''	0	1	2	3	4	5
0	11 649.14					
1	13 137.49					
2	14 558.24	12 743.35				
3	15 911.16	14 096.23	12 350.41			
4		15 380.22	13 634.40	11 956.15		
5			14 847.31+	13 169.12+		
6			15 985.94	14 307.64	12 695.57	
7				15 366.35+	13 754.23+	12 207.29+
8				16 336.30	14 724.19	13 177.25
9					15 591.37	14 044.37

are

	ω	x	y	z	ν_e
H_2	2196.13	65.80	−0.433		11 838.91
HD	1905.17	51.70	0.522	−0.091	11 825.68
D_2	1556.64	34.51	0.287	0.04	11 813.40
D_2 : HD	0.81706	0.6675	0.550	−0.44	—
ρ^n	.81675	0.6671	0.544	0.445	—

The values for H_2 are obtained from the formula given by Richardson and Das.[3] They cannot be compared directly with the constants for HD and D_2 as they were calculated in a different way from less complete data.

The ratio of the constants for D_2 and HD, which is given in the fourth row, is again approximately equal to the theoretical ρ^n values calculated from the mass ratios. The remarks about the agreement in the Fulcher bands[1] apply also here. In another paper[2] it was shown that the agreement cannot be expected to be better, and that if a higher accuracy is desired, various corrections must be applied. In that paper also the shifts between the origins ν_e of the band systems were discussed.

I wish to thank Dr. C. R. Jeppesen for his help with the measurements of the lines.

[3] O. W. Richardson and K. Das, Proc. Roy. Soc. **A122**, 688 (1929).

The Triplet $3p$ Complex of the Hydrogen Molecule

G. H. DIEKE, *Johns Hopkins University*

(Received July 18, 1935)

Many peculiarities first observed in the Fulcher bands of the hydrogen molecule can be explained by the interaction of the $3p^3\Pi$ with the $3p^3\Sigma$ level. Such peculiarities are: irregular Λ-doublings, perturbations in the $3p^3\Pi$ and $3p^3\Sigma$ state, and the absence of P and R branches for large values of the vibrational quantum numbers. This last phenomenon is due to the predissociation of the $3p^3\Pi$ state.

§1

THE present investigation is concerned with the interaction of the $3p^3\Sigma$ and $3p^3\Pi$ levels of the hydrogen molecule. The $3p^3\Pi \rightarrow 2s^3\Sigma$ bands, the so-called Fulcher bands were the first known regularities in the H_2 spectrum. Richardson and Das[1] to whom the complete analysis of the Fulcher bands is due, noted that the P and R branches of the bands showed marked irregularities and were completely absent if the vibrational quantum number of the initial state exceeded the value three, whereas the Q branches had a perfectly regular structure.

The study[2] of the analogous bands of HD and D_2 led to an explanation of these phenomena as being due to the interaction of the $3p^3\Sigma$ and the $3p^3\Pi$ levels and the analysis of the $3p^3\Sigma \rightarrow 2s^3\Sigma$ bands[3] confirmed this view completely. The present paper is concerned with a closer investigation of this interaction. As examples of interaction between molecular levels which give rise to perturbations in which both levels are completely known are extremely rare, the present case is of considerable general interest, especially as the same kind of interaction can be studied for the three different isotopic molecules.

The empirical material for HD and D_2 is given in two previous papers[2, 3, 4] and the data for H_2 are taken from Richardson and Das.[1]

The theoretical background for the treatment of such interaction has been summarized in a previous paper[5] to which frequent reference will have to be made as "theoretical part."

[1] O. W. Richardson and K. Das, Proc. Roy. Soc. **A122**, 688 (1929).

[2] G. H. Dieke and R. W. Blue, Phys. Rev. **47**, 261 (1935).

[3] See the preceding article.

[4] As more extended measurements have become available the analysis of the Fulcher bands of HD and D_2 could be considerably amplified. Also the $3p^3\Sigma \rightarrow 2s^3\Sigma$ bands of H_2 could be extended.

§2. EMPIRICAL FACTS

It is perhaps most convenient to begin with a summary of the observed empirical facts which require an explanation. They are:

1. All the Q branches are quite regular.
2. The Λ-doubling of the $3p^3\Pi$ state depends in a very erratic way on the vibrational quantum number, and is quite abnormal for some vibrational levels.
3. Whereas the dependence of the Λ-doubling on the rotational quantum number J is only slightly abnormal in most cases, there are pronounced perturbations for certain levels.
4. The H_2, HD and D_2 levels show the same general behavior, but the irregularities are found at different places for the three molecules.
5. For $V'>3$ for H_2 and HD and $V'>4$ for D_2 the P and R branches are completely absent in the Fulcher bands.
6. The $3p^3\Sigma$ levels show also irregularities, but only the big perturbations are easily recognized, as there is no Λ-doubling which registers abnormalities with much greater precision.

§3

If we consider Fig. 1 which is a plot of the vibrational levels of the two electronic states, the explanation of many of the points mentioned above becomes apparent. In the first place we note that there are certain pairs of levels which lie very close together. Such pairs are $3p^3\Sigma$, $V=4$ and $3p^3\Pi$, $V=1$ for H_2, $3p^3\Sigma$, $V=3$ and $3p^3\Pi$, $V=0$ for HD, and $3p^3\Sigma$, $V=5$ and $3p^3\Pi$, $V=1$ for D_2. All these levels show big perturbations which makes it practically certain that the abnormalities listed in §2 are due to the interaction of the $3p^3\Sigma$ and $3p^3\Pi$ levels, and a closer investigation confirms this.

For the notation, etc., reference must be made to the theoretical part.[5] As the interaction is between a Π and Σ level it must be of type A, i.e.,

[5] G. H. Dieke, Phys. Rev. **47**, 870 (1935).

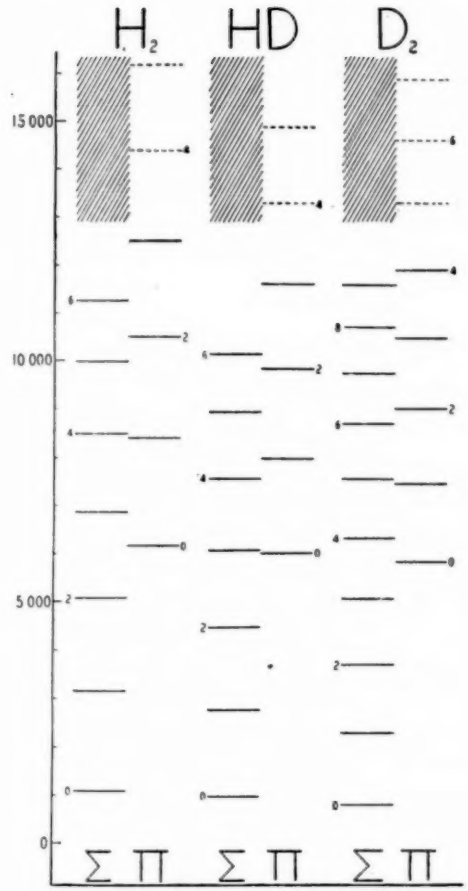

FIG. 1. The vibrational levels of $3p^3\Sigma$ and $3p^3\Pi$. The relative positions of the H_2, HD and D_2 levels are adjusted so that the vibrationless (electronic) level of $3p^3\Sigma$ has the same value for all three molecules.

the coupling of the two states is due to the rotation of the molecule.

The $p\Pi$ state is always split up into a $p\Pi^+$ and a $p\Pi^-$ state[6] due to the rotation of the molecule (Λ-doubling) and of these only the $p\Pi^+$ state can interact with the $p\Sigma^+$ levels. The $p\Pi^-$ level is the initial state for the Q branches and is completely unaffected by the interaction. This explains point 1 of §2, that all the Q branches are completely regular.

If there were no interaction the $p\Pi^-$ level would coincide exactly with the $p\Pi^+$ levels, so that the amount of the Λ-doubling is a direct measure for the magnitude of the interaction. We have seen in the theoretical part that the interaction between two levels is by far the greatest if they have the same vibrational quantum number, and we call the effect of this kind of interaction the regular Λ-doubling. If the vibrational quantum numbers differ, the interaction is much smaller and its effect on the energies is of any consequence only if the levels are close together. This gives us the irregularities in the Λ-doubling.

[6] Usually the $p\Pi^-$ state is called $p\Pi_a$ or $p\Pi_c$ and the $p\Pi^+$ state $p\Pi_b$ or $p\Pi_d$.

§4. The Regular Λ-Doubling

According to (16) and (24) of the theoretical part the regular doubling is in first approximation given by

$$2B_v^2J(J+1)/\delta,$$

in which δ is the distance between the $p\Sigma$ level and the corresponding $p\Pi$ level with the same rotational quantum number J and the same vibrational quantum number V. As the equilibrium distances are different for the two interacting levels, a better approximation is obtained if we substitute $B_{vv}=\int RBR'r^2dr$ for $B_v=\int RBRr^2dr$. (R is the vibrational wave function.) This follows from (17) if the second small and uncertain term is omitted. This correction is very small in our case. With harmonic binding we get, e.g.,

$$B_{00}=(2a/1+a^2)^{\frac{1}{2}}e^{-b^2/2(1+a^2)}B_0,$$

in which

$$a=(\omega_e'/\omega_e)^{\frac{1}{2}},\quad b^2=4\pi^2c\omega_e'\mu(r_0-r_0')^2/h$$

and the values of the constants are for D_2

$$3p^3\Pi\quad r_0=1.047\cdot10^{-8},\quad \omega_e=1678.22$$

$$3p^3\Sigma\quad r_0'=1.096\cdot10^{-8},\quad \omega_e'=1556.64.$$

This gives for D_2 $B_{00}=0.941\ B_0$, and similarly small corrections for the two other molecules.

The regular doubling for the $V=0$ vibrational level is found to be in this way $0.321\ J(J+1)$ for H_2, $0.180\ J(J+1)$ for HD, and $0.078\ J(J+1)$ for D_2.

In Figs. 2, 3 and 4 these calculated regular doublings are compared with some of the observed values. Table I gives all the observed doublings.[7] It is seen that the order of magnitude

[7] As a $p\Pi^+$ and a $p\Pi^-$ level with the same J never can combine with the same lower state, it is not possible to obtain the values of the doubling directly from the observations by using only the combination principle. However, as the structure of the lower ($2s^3\Sigma$) state is very regular,

TABLE I. *Λ-doubling of the $3p^3\Pi$-level.*

	H_2				HD				D_2				
J	$V=0$	1	2	3	0	1	2	3	0	1	2	3	4
1	0.46	−0.31	0.92	1.89	−0.04	0.48	0.29	0.67	0.13	0.09	0.18	0.13	0.23
2	1.25	−1.63	2.68	4.43	−0.43	1.34	0.84	1.89	0.35	0.20	0.62	0.37	0.74
3	2.54	−6.50	4.76	6.46	−3.26	2.45	1.46	3.34	0.50	0.21	1.23	0.70	1.36
4	3.90		6.87	8.28	+9.06	3.83	1.95	4.88	1.00	−0.17	1.97	0.98	2.04
5	5.19		8.36		7.67	5.33	1.75	6.10	1.49	−3.08	2.71	0.75	2.62
6	6.06				7.49	6.59		6.55	1.86	+8.60	3.54	−0.87	2.96
7									2.18	6.22			

of the observed doubling is well represented by the theoretical curves,[8] but that the individual values show considerable systematic deviations from the curves, positive in some cases, negative in others.

§5. IRREGULAR Λ-DOUBLING

These deviations must be due, for the greatest part,[9] at least, to the interaction of the $p\Pi$ level with that $p\Sigma$ level which is its closest neighbor. We take first the case where the interacting levels are not so close that we have typical perturbations. The interaction of two levels with different vibrational quantum numbers is given in first approximation by (17) of the theoretical part in which we can omit again the uncertain second part.

The quantity $B_{vv'}$ can be calculated easily if we make use of the well-known properties of the Hermitian polynomials.[10] We get, e.g., $B_{04}=0.02B_0$ for D_2. This is much too small to account for the empirical deviations of the $V=0$ level of $3p\Pi$ from the theoretical curve (Fig. 2) which would require B_{04} to be of the order of magnitude 0.1 B_0 to 0.2 B_0.

The explanation for this discrepancy must be sought in the fact that the calculations are made under the assumption that the binding is harmonic.[11] They are, however, very sensitive for deviations from the harmonic law. The calculations could be carried out also with a general anharmonic law of force but would be much more cumbersome, and the present state of affairs would hardly justify going into them. Possibly also the neglected term in (17) may be appreciable. We hope to come back to this in a later paper but restrict ourselves now to some qualitative considerations.

Whether the Λ-doubling of a given $p\Pi$ level is diminished or increased depends on whether the $p\Sigma$ level which is its nearest neighbor lies just above or below the $p\Pi$ level. There is no simple law which governs the distance of a given $p\Pi$ level from the closest $p\Sigma$ level, therefore the relative position of such pairs can be considered to be regulated more or less by chance. This accounts for the erratic way in which the irregularities of the Λ-doubling depend on the vibrational quantum number (point 2 of §2). Also there is absolutely no connection between the relative arrangement of such pairs in H_2, HD and D_2 which can be verified by a glance at Fig. 1. This explains point 4 of §2.

If the $3p\Sigma$ level lies just *above* the neighboring $3p\Pi$ level, the effect of this will be that the $3p\Pi$ level will be depressed, i.e., the Λ-doubling diminished. We have such a state of affairs, e.g., for $V=0$ in D_2, $V=2$ in HD and $V=0$ in H_2. These are the levels represented by an x in the Figs. 2–4, and the Λ-doubling lies in all these cases below the theoretical value, as it should.

the differences between successive rotational levels of it can be calculated with any desired accuracy. In fact it is necessary only to calculate the difference between the $J=0$ and $J=1$ levels of $2s^3\Sigma$ with the help of the term formula, and all the rest including the Λ-doublings can be calculated with the help of the combination principle only. The values in the table were obtained in this way.

[8] It may be good to emphasize that no adjustable constant was used for the calculation of the theoretical curves.

[9] There are, of course, other reasons why there should be deviations of the observed Λ-doublings from the theoretical curves. The formula used is only a first approximation and can be expected to hold only for small J. The figures show that for all levels the observed values for the larger values of J seem to have a tendency to be too low, and this kind of deviation must be due to the insufficiency of the formula used.

[10] The calculations necessary for this are of the same kind as those used for the calculations of band intensities in electronic band systems. As the calculations do not give the right magnitude anyway they are omitted here.

[11] Some of the effects of the deviations from the anharmonic binding have been taken into account; e.g., if we use $B_v=B_e-\alpha(V+\frac{1}{2})$, the empirical value of α is used. If the binding is regarded purely harmonic, α would have the same order of magnitude but opposite sign.

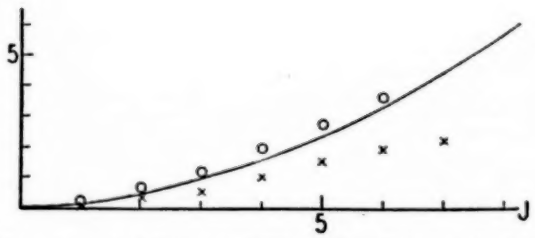

FIG. 2. Λ-doubling for $3p^3\Pi$ of D_2. Curve: calculated regular Λ-doubling for $V=0$. x Observed values for $V=0$, o for $V=2$.

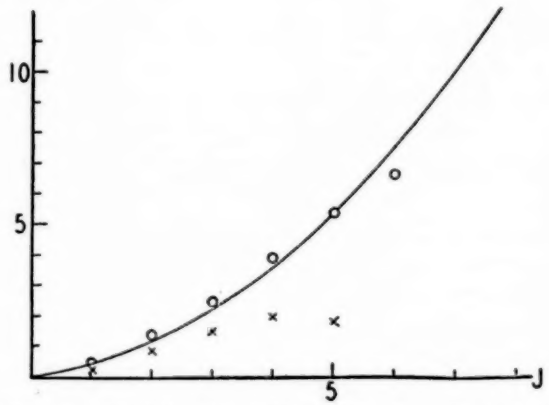

FIG. 3. Λ-doubling for $3p^3\Pi$ of HD. Curve: calculated regular Λ-doubling for $V=0$. x Observed values for $V=2$, o for $V=1$.

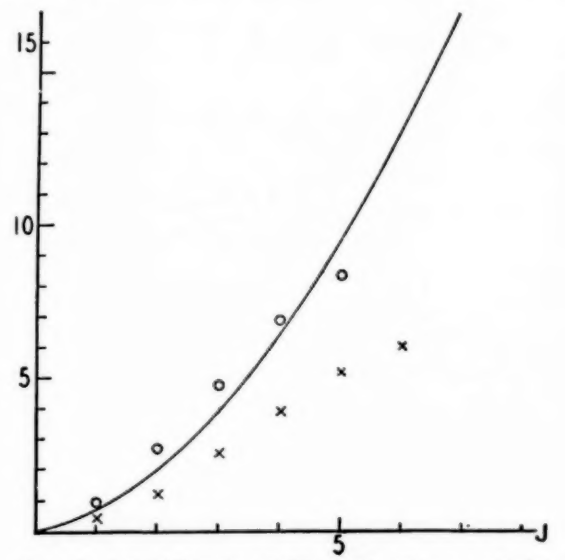

FIG. 4. Λ-doubling for $3p^3\Pi$ of H_2. Curve: calculated regular Λ-doubling for $V=0$. x Observed values for $V=0$, o for $V=2$.

It may even occur that the deviation is larger than the regular doubling in which case the total doubling becomes negative.

The opposite state of affairs exists if the $3p\Sigma$ level lies just *below* the neighboring $3p\Pi$ level as is the case for $V=2$ in D_2, $V=1$ in HD, and $V=2$ in H_2. Then the Λ-doubling should be larger than the regular doubling and that is found to be the case (see Figs. 2–4). In judging the agreement it must be borne in mind that the drawn out curve is the regular Λ-doubling for $V=0$, whereas the regular Λ-doubling for $V=1$ and $V=2$ is lower (about 25 percent lower for the $V=2$ level of H_2). The figures show that the deviations from the regular curve become relatively much larger for larger J when the doubling is *below* its regular value and the opposite is true when it is *above* its regular value.

The reason for this is that when the $p\Pi$ level lies below the $p\Sigma$ level the distance δ between rotational levels with the same J decreases with increasing J, as the spacing of the $p\Pi$ rotational levels is larger than the spacing of the $p\Sigma$ levels. This means that the higher levels are relatively more affected because of their closer proximity than the lower ones. If the $p\Pi$ state is above the $p\Sigma$ state just the opposite takes place. All this is in agreement with the experimental facts.

§6. True Perturbations

We come now to the cases where the $p\Sigma$ levels lie so closely above the $p\Pi$ levels that the interaction becomes considerable and we have true perturbations. Fig. 1 shows that this is the case for $V=1$ in H_2 and D_2 and $V=0$ in HD. The data are most complete for the pair $V=1$ of $3p^3\Pi$ and $V=5$ of $3p^3\Sigma$ of D_2 and therefore we shall consider this case more in detail. The two other cases mentioned are of the same kind.

The magnitude of the perturbation can be obtained with great accuracy in the following way. The total Λ-doubling is the sum of the regular Λ-doubling which can be calculated in the way indicated in §4 and the perturbation due to the $V=5$ level of $3p\Sigma$. By subtracting therefore the calculated regular Λ-doubling from the total doubling we obtain the amount of the perturbation. According to theory the perturbation of the $V=5$ state of $3p\Sigma$ is of the same magnitude but opposite sign. By subtracting resp. adding the amount of the perturbation to the pair of the perturbed levels we obtain the unperturbed states.[12] The difference between pairs of such

[12] Strictly speaking the interactions of the $3p\Pi$ $V=1$ level with the $3p\Sigma$ $V=1$ and the $3p\Sigma$ $V=5$ levels are not inde-

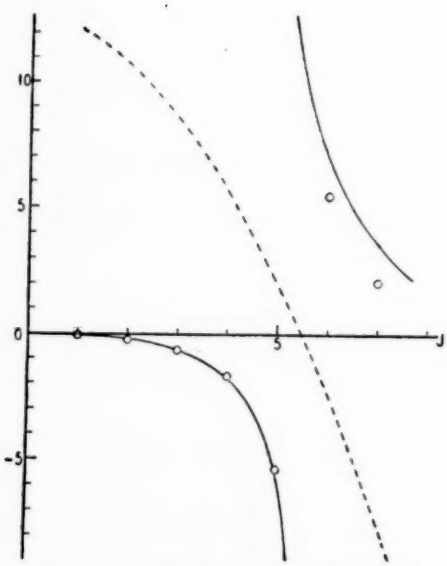

FIG. 5. The solid curve represents the calculated perturbations for the $3p^3\Pi$, $V=1$ level of D_2. o are the observed perturbations. The dotted curve gives the distance between corresponding rotational levels of $3p^3\Sigma$, $V=5$ and $3p^3\Pi$, $V=1$. (The scale for this curve is ten times smaller than that indicated by the figures on the left.)

levels with the same J is represented by the dotted curve in Fig. 5. The o mark the observed perturbations (on a tenfold magnified scale). It is seen that the perturbations become rapidly larger as the distance between the levels decreases and that they change their sign when the two levels cross over. The solid curve represents the perturbations calculated according to (13) and (18) of the theoretical part, the constant α being chosen in such a way as to give the best agreement for small values of J. It is seen that the agreement is very good for small J but that after the break there are discrepancies much larger than the errors of measurement. They are due to the approximate character of our calculations and undoubtedly the agreement could be made much better by going to higher approximations.

The value of the constant α is 4.9 from which it follows according to (17) that $B_{15}=1.5$. That is the same order of magnitude as was found for B_{04} in §5.

In all cases the perturbations of the $3p\Sigma$ state are of the same magnitude and opposite sign as those for the $3p\Pi$ state with which they interact. Only they cannot be ascertained with the same precision as those of the $p\Pi$ states as the unperturbed states are unknown whereas for the $p\Pi$ levels they are exactly given by the unaffected $p\Pi^-$ states.

There is a perturbation of smaller magnitude than those mentioned above in the $3p\Sigma\, V=7$ level of D_2. As Fig. 1 shows, this perturbation cannot be due to the interaction with a $3p\Pi$ state. It is probable that it is caused by the interaction with the $4p^3\Sigma$ level which, however, has not yet been established empirically with sufficient certainty to verify this unambiguously.

§7. PREDISSOCIATION

The vibrational levels of the $3p\Sigma$ state are discreet only up to a certain limit. Beyond this limit which is indicated in Fig. 1 the molecule is dissociated into a normal and an excited atom in the second quantum state, and the energy levels are continuous. The nature of the wave functions is not changed in such a way as to affect materially the interaction with the $3p\Pi$ state. This means that the continuous levels interact with the neighboring $3p\Pi$ levels in essentially the same way as the discreet levels. A characteristic feature of such interaction is that the molecule oscillates back and forth between the two interacting states. As the $3p\Sigma$ state is dissociated the $3p\Pi$ state will also be dissociated by the interaction (predissociated) i.e., the $3p\Pi^+$ levels above the dissociation limit of the $3p\Sigma$ state will be destroyed as discreet levels. The bands originating from these levels will therefore be absent.[13] The Fig. 1 shows that this must be the case for $V>3$ in H_2 and HD and for $V>4$ in D_2, and this agrees exactly with the experimental observations (point 5 of §2).

All this applies only to the $3p\Pi^+$ level which gives the P and R branches, as the $3p\Pi^-$ level which gives the Q branches is not affected at all by the interaction. This explains why only the P and R branches are absent, whereas the Q branches show no changes.

In a previous paper[2] this phenomenon was used to determine the heat of dissociation of H_2.

pendent as they are caused by the same interaction force. It can be easily shown, however, that they can be treated as if they represented separate interactions, if first the regular Λ-doubling is taken into account and the new levels, shifted from their original position by the amount of the regular Λ-doubling are taken as the unperturbed states for the interaction between the close pairs.

[13] The continuous spectrum which should come in its place, is too weak to be noticed.

The Magnetic Anisotropy of Crystals of Sn, and of Sn with Added Sb, Cd, or Ga*

HAROLD J. HOGE, *Sloane Physics Laboratory, Yale University*

(Received June 27, 1935)

The principal magnetic susceptibilities of single crystals of white (tetragonal) tin have been determined. Crystals were grown by the traveling furnace method. Perpendicular to the tetragonal axis the susceptibility (per unit volume) is $\kappa_\perp = 0.197 \times 10^{-6}$; parallel to the axis it is $\kappa_{\parallel} = 0.176 \times 10^{-6}$. The ratio $\kappa_\perp/\kappa_{\parallel}$ is strongly influenced by the addition of small amounts of certain elements. For tin containing no added element this ratio is 1.120. Adding 0.60 percent Sb the ratio is 1.200; 0.76 percent Cd, 0.923; 0.89 percent Ga, 0.897. The relation between the change in this ratio and the number of valence electrons of the added element is compared with available data for bismuth.

THAT the crystal structure of tin controls its magnetic properties is evident from the fact that white tin is paramagnetic, grey tin diamagnetic. It therefore seemed important to investigate the magnetic anisotropy of the non-cubic form (white tin) and to modify this anisotropy in any feasible way. The method recently developed by Goetz and Focke[1] and applied by them to bismuth (diamagnetic) were obviously suitable with such minor changes as were made necessary by the lower absolute values of the principal susceptibilities of tin. The investigators just referred to grew single crystals suitable for magnetic measurements by the Gouy method and found how the two principal susceptibilities were affected by impurities.

Impurities which can be entrapped in crystals are of greater interest than those which cannot. Whether there is true solution in all such cases is not yet clear, but it appeared reasonable to try first impurities known to dissolve in tin. Of these it has been possible to study only antimony and cadmium. Gallium was added to the list because of its low melting point, peculiar crystal structure, and favorable position in the periodic table.

Experimental Procedure

The tin selected for definitive experiments was a particular lot of Baker's "C. P. Analyzed" containing As 0.0000 percent; Pb 0.003 percent; Fe 0.002 percent; Zn 0.000 percent; Cu 0.000 percent. Since not over one percent of Sb, Cd, or Ga was added, ordinary commercial grades of these elements could be used. Alloys were prepared by weighing and were melted under hydrogen in Pyrex. The low range of solid solubilities made it inconvenient to obtain a series of the desired concentrations by diluting a richer alloy. After thorough mixing a stick 7 inches (18 cm) long and 0.1 inch (0.254 cm) square was cast in a two-piece slate mold.

This polycrystalline casting was placed in a snugly fitting graphite box (Fig. 1). One end of

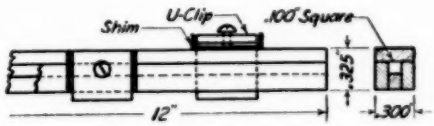

FIG. 1. Graphite box in which crystals were grown.

the box was closed by a steel plug. At the other end a seed crystal could be brought into contact with the casting.

This assembly was then placed in a horizontal position inside a crystal growing apparatus similar to that described by Hasler.[2] The tubular furnace which traverses the casting was made quite short (4 cm) and the temperature gradient on the exit side was made steeper by directing air jets against the glass wall of the tube containing the graphite box. Cooling of the furnace by this jet system was prevented by an asbestos screen. Preliminary tests showed that a steep temperature gradient is essential to success, and that 2 millimeters per minute is a suitable furnace speed. The use of a short furnace ensures against too much change in concentration of soluble impurities. Hydrogen was used to prevent oxidation. The temperature gradient was further increased by causing the hydrogen to flow past the crystal in the direction in which the furnace moved. That the temperature gradient requires

* Part of a dissertation presented for the degree of Doctor of Philosophy in Yale University.

[1] A. Goetz and A. B. Focke, Phys. Rev. **45**, 170 (1934), and preceding papers.

[2] M. F. Hasler, Rev. Sci. Inst. **4**, 656 (1933).

special control was shown by the fact that it was possible to initiate the growth of crystals with the tetragonal axis at a large angle to the axis of the casting by the use of a steel plug with its end beveled at a sharp angle. This procedure was suggested by the experimental results of Palibin and Froiman,[3] and was a convenient way to get seed crystals of the desired orientation, which is with the tetragonal axis perpendicular to the axis of the specimen.

The castings thus prepared were etched in hydrochloric acid solutions properly modified to prevent a too rapid attack. The etching showed at a glance whether a single crystal had been obtained, and if so, permitted its orientation to be determined by optical means. The most important etch planes were found to be $\{101\}$ and $\{301\}$,[4] these indices referring to the smaller of the two commonly chosen unit cells.

Susceptibilities were measured by the Gouy method, in which the force on a long specimen of uniform cross section is given by $F=\frac{1}{2}(\kappa-\kappa_0)A(H^2-H_0^2)$. Here κ and κ_0 are the susceptibilities (per unit volume) of the specimen and of the surrounding medium (air), H and H_0 are the field strengths at the two ends of the specimen, and A is its cross section. Since κ_0 is known and H_0^2 is negligible for such long specimens, the quantities to be measured are F, A, and H.

The force F was measured by counterpoising the specimen on a sensitive microbalance, and increasing the counterpoise as necessary when the field was applied. Readings were taken to the nearest 0.01 milligram. High sensitivity was required because of the small magnitude of F, which was of the order of 3 milligrams.

The fields H and H_0 were measured with a search coil attached to a pendulum and connected to a low resistance (16 ohms) Leeds and Northrup type HS-2285e galvanometer which was calibrated with a standard mutual inductance. Field strengths H of about 24,000 gauss were employed, in which case H_0 was of the order of 650 gauss.

The cross section of the specimen was found by lowering it a known distance into a tube of ethyl alcohol and measuring the rise in the liquid level with a traveling microscope. This rise was most easily measured in a connecting side tube of small diameter. The apparatus was calibrated by immersing pieces of drill rod of known cross section.

Sections 3.5 inches (9 cm) long were cut from the good crystals, selected to give the most uniform cross section in the non-homogeneous part of the field. The bar to be cut was laid in the jaws of a pair of tin snips and allowed to fall into the hand when cut, so that all strains would be localized at the ends of the specimen.

The crystal hanger contained a device which, when the balance was arrested, allowed the crystal to be lifted, rotated about its axis, and reseated without lateral displacement. A crystal of the proper orientation could thus be set with its tetragonal axis either parallel to or perpendicular to the field. Since all directions perpendicular to the tetragonal axis are equivalent, the susceptibility in any arbitrary direction in a tetragonal crystal is given by $\kappa=\kappa_{\parallel}\cos^2\alpha+\kappa_{\perp}\sin^2\alpha$, where α is the angle between the applied field and the tetragonal axis. Measurement of $\kappa_{\parallel}$ and $\kappa_{\perp}$ therefore gives complete information about the magnetic properties of any crystal. Since the polycrystalline susceptibility of tin is temperature independent[5] it seemed unlikely that small temperature fluctuations would introduce any error, and all measurements were made at room temperature.

Results

For pure tin: $\kappa_{\perp}=0.197\times10^{-6}$, $\kappa_{\parallel}=0.176\times10^{-6}$, $\kappa_{\perp}/\kappa_{\parallel}=1.120$. Taking the density of tin as 7.3 the mass susceptibilities are: $\chi_{\perp}=0.0270\times10^{-6}$, $\chi_{\parallel}=0.0241\times10^{-6}$. The Voigt-Thomson[6] relation gives for an ideal polycrystalline aggregate: $\chi=\frac{1}{3}(2\chi_{\perp}+\chi_{\parallel})=0.0259\times10^{-6}$, which is in good agreement with previously published results.[7]

The experimental data are given in Table I. Figs. 2 to 4 show the variation of the two principal susceptibilities for each impurity as a function of its concentration. Fig. 5 shows the ratio of these susceptibilities ($\kappa_{\perp}/\kappa_{\parallel}$) for each impurity as a function of its concentration. The effect of Sb is to decrease both $\kappa_{\perp}$ and $\kappa_{\parallel}$, $\kappa_{\perp}/\kappa_{\parallel}$ increasing.

[3] P. A. Palibin and A. I. Froiman, Zeits. f. Krist. **85**, 322 (1933).
[4] Details of the optical apparatus used and of the identification of the etch planes will be given elsewhere.
[5] H. Endô, Sci. Rep. Tohoku Imp. Univ. **16**, 201 (1927).
[6] W. Voigt, *Lehrbuch der Kristallphysik* (1928), p. 960.
[7] *International Critical Tables*, Vol. 6, p. 355.

TABLE I. *Susceptibility data on alloys if single crystals of tin.*

CRYSTAL NO.	ALLOY WT. %	ORIENTATION	CROSS SECTION	FORCE⊥*	FORCE∥*	FIELD (gauss)	$H^2-H_0^2$ $\times 10^{-8}$	$\kappa_\perp$‡ $\times 10^{-6}$	$\kappa_\parallel$‡ $\times 10^{-6}$	$\kappa_\perp/\kappa_\parallel$
19	0.09 Sb	89.9°	0.06493 cm²	3.371 mg	2.920 mg	24,700	6.0967	0.1959	0.1736	1.127
				3.375	2.925	24,700	6.0967	.1961	.1738	1.128
20	.26 Sb	86°	.06278	3.135	2.660	24,400	5.9494	.1935	.1686	1.148
				3.138	2.663	24,400	5.9494	.1937	.1687	1.148
18	.09 Sb	89.9°	.06278	3.143	2.705	24,304	5.9026	.1952	.1721	1.134
				3.130	2.703	24,378	5.9386	.1935	.1711	1.131
17	Stock B	90°	.06329	3.198	2.795	24,353	5.9265	.1961	.1751	1.120
				3.193	2.788	24,304	5.9026	.1965	.1753	1.121
13#	Stock B	89.9°	.06046	3.265	2.865	24,304	5.9026	.2083	.1864	1.117
8	Stock B	87°	.06193	3.103	2.745	24,378	5.9386	.1944	.1753	1.109
21	0.76 Cd	85.5°	.06244	2.823	3.105	24,378	5.9386	.1782	.1931	.9228
				2.830	3.108	24,378	5.9386	.1786	.1933	.9240
23	.50 Cd	87°	.06391	3.033	3.104	24,333†	5.9167	.1862	.1899	.9805
16	Stock B	89°	.06123	3.130	2.725	24,324†	5.9123	.1985	.1765	1.125
				3.135	2.733	24,324†	5.9123	.1987	.1770	1.123
27	0.25 Cd	89°	.05631	2.775	2.683	24,324	5.9123	.1924	.1870	1.029
				2.775	2.675	24,294	5.8978	.1928	.1869	1.032
28	.12 Cd	88°	.06391	3.153	2.888	24,294†	5.8978	.1930	.1792	1.077
				3.143	2.863	24,294	5.8978	.1924	.1779	1.082
31	.60 Sb	88°	.06262	2.963	2.383	24,259	5.8808	.1867	.1558	1.198
				2.945	2.360	24,259†	5.8808	.1857	.1546	1.201
32	.42 Ga	87°	.06193	3.075	3.035	24,288	5.8948	.1941	.1919	1.011
				3.058	3.020	24,288†	5.8948	.1932	.1911	1.011
33	.89 Ga	88°	.06262	3.133	3.555	24,298	5.8997	.1952	.2176	.8971
				3.128	3.553	24,298†	5.8997	.1949	.2175	.8961

* After subtracting suspension correction of 0.1 mg.
‡ After adding air correction of 0.029×10^{-6}.
† Fluxmeter calibrated at time of taking this reading.
# Not averaged.

When Cd is added $\kappa_\perp$ decreases and $\kappa_\parallel$ increases; $\kappa_\perp/\kappa_\parallel$ therefore decreases. At 0.4 percent cadmium $\kappa_\perp = \kappa_\parallel$ and the crystal is magnetically isotropic. When Ga is added $\kappa_\perp$ changes very little while $\kappa_\parallel$ increases rapidly; $\kappa_\perp/\kappa_\parallel$ decreases as it does when Cd is added.

It may be seen that Cd and Ga, the two elements having fewer valence electrons than tin, cause a decrease in $\kappa_\perp/\kappa_\parallel$. On the other hand Sb, which has one more valence electron than tin, causes an increase in this ratio. The significance of this finding is increased by the fact that $\kappa_\perp/\kappa_\parallel$

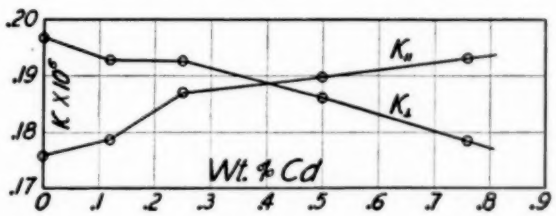

FIG. 3. Susceptibilities of tin containing cadmium.

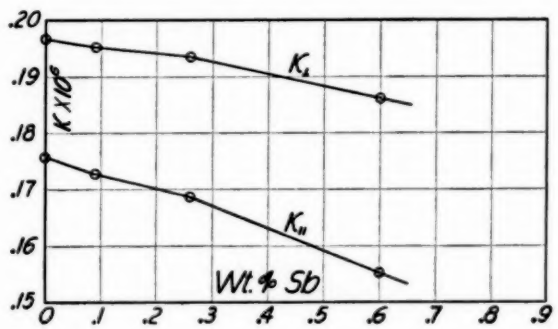

FIG. 2. Susceptibilities of tin containing antimony.

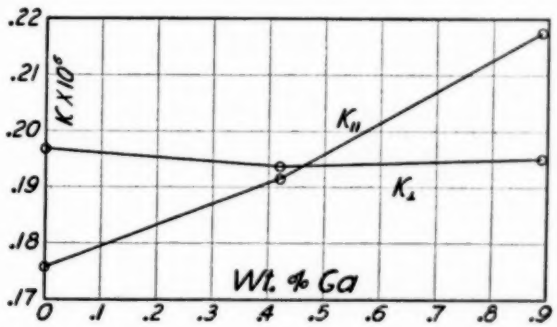

FIG. 4. Susceptibilities of tin containing gallium.

is not subject to errors made in measuring either field strength or crystal cross section, since these variables cancel out. Therefore, although the probable error in κ may be as high as 2 percent, the probable error in $\kappa_\perp/\kappa_{||}$ is considerably less. The precision in measurement of κ was checked by determining the mass susceptibilities of distilled water and fused quartz. Results were, for water, $\chi=-0.738\times10^{-6}$ compared with the accepted value of -0.720×10^{-6}; and for fused quartz $\chi=-0.420\times10^{-6}$ compared with a value of -0.42×10^{-6} obtained by Dr. C. T. Lane in these laboratories but with other apparatus.

Discussion

It is interesting to compare Fig. 5 with the corresponding data given by Goetz and Focke for bismuth. With tin, elements toward the alkali side of the periodic table decrease $\kappa_\perp/\kappa_{||}$, while those toward the halogen side increase this ratio. The exact opposite was found for bismuth. However, when account is taken of the fact that the susceptibilities of tin are both positive, while those of bismuth are both negative, this difference is perhaps to be expected. Assume for definiteness that an added impurity contributes diamagnetism parallel to the principal axis and nothing at all perpendicular to it. Then in the case of tin we are adding a negative quantity to the smaller of two positive quantities, while in the case of bismuth we are adding it to the smaller of two negative quantities. The ratio for tin will be increased and for bismuth will be decreased. Something more complicated than this actually occurs, for the magnitudes of $\kappa_\perp$ and $\kappa_{||}$ both change.

Goetz and Focke explained their results with the aid of the Ehrenfest-Raman[8, 9, 10, 11] large electron orbit hypothesis, which had previously proved useful in explaining the abnormally high diamagnetism of bismuth, antimony, and graphite crystals, and the diminution in these values when the crystals were made submicroscopic or melted. Assuming the impurity to collect in certain crystallographic planes, Goetz and Focke pointed out that these planes might act as reflecting walls to electrons moving in large orbits. A reorientation of these orbits would result, and since they are presumably large enough to surround many atomic nuclei, the diamagnetic susceptibility in certain crystallographic directions would be considerably increased at the expense of that in other directions.

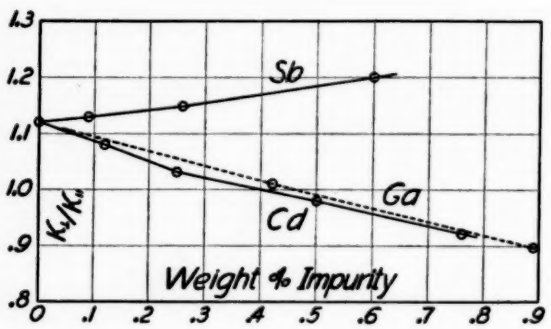

Fig. 5. $\kappa_\perp/\kappa_{||}$ ratios for tin containing impurities.

Processes of this kind are adequate to explain some of the effects of impurities on tin. The five planes having the greatest atom densities are, in order: {100} {110} {112} {101} {210}. By assuming impurities to be concentrated in {110} planes, the changes in $\kappa_\perp/\kappa_{||}$ may be explained. Planes of the form {110} are suggested as more probable than {100} by the fact that several of the crystals were covered after etching by fine lines which corresponded to traces of {110} planes. These traces were most regular and conspicuous on the lateral faces of the crystal, and were best developed in the direction most nearly parallel to the sloping isothermal surfaces in the freezing melt. That is, one of the planes (110), $(1\bar{1}0)$ was conspicuous; the other was not. It is difficult to explain these lines without attributing them to impurities, particularly since they were most pronounced in crystals containing the largest amounts of impurities. Although the lines were so widely spaced as to be visible without magnification, they certainly do not make less plausible the existence of planes of impurity spaced more or less uniformly at much smaller intervals throughout the crystal. A considerable amount of work indicates the presence of some sort of secondary structure in metals, so that there is no longer much question of its existence. We are now more interested in the sizes, causes, and regularity of these secondary patterns.

[8] P. Ehrenfest, Physica **5**, 388 (1925).
[9] P. Ehrenfest, Zeits. f. Physik **58**, 719 (1929).
[10] C. V. Raman, Nature **123**, 945 (1929).
[11] C. V. Raman, Nature **124**, 412 (1929).

In the present work the magnitude of the observed changes (20 percent in $\kappa_\perp/\kappa_{||}$ for less than 1 percent added impurity) makes it possible to associate the changes not with the mere presence of the impurity but with the effect of its presence on the rest of the crystal. Goetz and Focke point out that a distribution of impurity in widely separated planes could be expected to produce a larger effect than a uniform volume distribution. Furthermore, a distribution in planes accounts much more readily for anisotropic changes in susceptibility.

To explain why an element having more valence electrons than tin should have an opposite effect to one having less, we may assume either that different impurities go into different planes, or that they go into the same planes but affect the crystal differently.

One limitation of the large orbit hypothesis should be pointed out. A mere rearrangement of existing orbits cannot affect the calculated ideal polycrystalline susceptibility, for any increase in $\kappa_\perp$ would result in a corresponding decrease in $\kappa_{||}$, and *vice versa*. As can be seen from Figs. 2 to 4, the corresponding polycrystalline susceptibility (which would be given by a line 1/3 the distance from $\kappa_\perp$ to $\kappa_{||}$) does not remain constant.

If all added impurities form reflecting walls, then to explain changes in $\kappa_\perp/\kappa_{||}$ we must assume that Cd or Ga collects in planes parallel to the axis while Sb collects in planes perpendicular to it. For example, the addition of Cd decreases $\kappa_\perp/\kappa_{||}$. If Cd collects in any set of planes parallel to the tetragonal axis, we would expect an increase in the area of large orbits projected on these planes, and an increased diamagnetism perpendicular to the axis. The net positive value of $\kappa_\perp$ would therefore be lowered relative to $\kappa_{||}$, and $\kappa_\perp/\kappa_{||}$ would decrease, as is actually observed.

One limitation of the large orbit hypothesis has already been mentioned. Another appears when we assume that impurity collects in planes parallel to the tetragonal axis, for unless conditions of growth favor one plane more than another there is no reason to expect impurity to collect in, say, (110) and not to collect in $(1\bar{1}0)$. If it collects in both the planes of form {110} the crystal is divided by walls of impurities into narrow rectangular prisms, and no large orbits can exist at all. We may avoid this situation only by assuming that all impurities collect in (001) planes, which divide the crystal not into prisms but into layers. But if we do so there is still the difficulty of explaining the opposite effects of different impurities.

Honda and Shimizu[12] have suggested that increase in lattice constants may produce diamagnetism. In this connection the results of Bowen and Morris Jones[13] have some bearing on the present work. By x-ray investigation they found that when Sb is added to tin there is a gradual expansion of the tin lattice up to the limit of solid solubility, with no change, however, in the ratio of the lattice parameters. Fig. 2 shows a decrease in paramagnetism, as this line of argument would predict. It would be interesting to see if Ga, which increases the paramagnetism of tin, simultaneously decreases its lattice constants.

In comparing the effects of impurities on tin with the effects on bismuth it should be pointed out that there is little evidence in the present work for a critical concentration of impurity corresponding to the complete filling of a set of uniformly spaced planes with a one- or two-atom layer of impurity. The nearest thing to such evidence is the dip in the Cd curves (Fig. 3) near the origin. Since all the critical concentrations reported by Goetz and Focke lay below 0.1 percent, it is not impossible that minima in these curves occur at lower concentrations than any yet used. The stock tin was not, however, pure enough to warrant studies at such low concentrations. It will be observed that the changes in $\kappa_\perp/\kappa_{||}$ for tin are much smaller and much more nearly linear than those for bismuth over the same range in concentration. The approximate linearity may be due merely to the smaller range of $\kappa_\perp$, $\kappa_{||}$, and of their ratio, in the present case.

In conclusion the author wishes to express his appreciation to Professor L. W. McKeehan, director of the research, for his ready advice and suggestions. He is also indebted to Dr. C. T. Lane and Dr. A. B. Focke for much valuable aid.

[12] K. Honda and Y. Shimizu, Nature **135**, 108 (1935).
[13] E. G. Bowen and W. Morris Jones, Phil. Mag. **12**, 441 (1931).

The Principal Expansion Coefficients of Single Crystals of Mercury

DONALD M. HILL, *Rutgers University*

(Received June 17, 1935)

The expansion coefficients were measured at 5° intervals from −115°C to −160°C and mean values found from −160°C to −190°C. The upper temperature limit was set by a recrystallization process which set in between −115°C and −110°C. $\alpha_{\parallel}$ was found to be larger and to increase more rapidly with the temperature than $\alpha_{\perp}$. The volume coefficient plotted in conjunction with Carpenter and Oakley's measurements give values of the volume coefficient from the melting point to −160°C where the coefficient apparently begins to decrease rapidly with the temperature.

INTRODUCTION

THE properties of single crystals and the variation of those properties with the temperature are of considerable importance in theoretical work on the solid state. The only previous measurements of the principal expansion coefficients of mercury are those of Grüneisen and Sckell[1] who measured only the mean values of the expansion coefficients over the large temperature interval from −190°C to −78°C and were unable to find how the coefficients vary with the temperature. Even the volume coefficient has not been satisfactorily measured. Dewar[2] found the value 8.87×10^{-5} from −188.7°C to the melting point; Grunmach,[3] 12.3×10^{-5} from −80°C to the melting point; and Bridgman[4] obtained the values 12.5×10^{-5} and 16.5×10^{-5} just below the melting point quite incidentally in the course of an investigation on the change of volume on freezing. Carpenter and Oakley[5] measured the volume expansion coefficient over the range −90°C to the melting point, but their measurements were not accurate or extended enough to show other than a linear variation with the temperature.

The present research was begun in 1932 in an attempt to find how the volume coefficient varies with the temperature by measuring the linear expansion coefficients of polycrystalline rods. However, the results were so erratic that it became evident that it would be necessary to use single crystals and measure the principal expansion coefficients.

CRYSTAL STRUCTURE

Mercury crystallizes in the trigonal system[6] so that it is necessary to measure only the coefficients parallel and perpendicular to the trigonal axis.[7] The coefficient in a direction making an angle θ with the trigonal axis is given by the relation:

$$\alpha_\theta=\alpha_{\parallel}\cos^2\theta+\alpha_{\perp}\sin^2\theta$$
$$=\alpha_{\parallel}+(\alpha_{\perp}-\alpha_{\parallel})\sin^2\theta, \quad (1)$$

so that α_θ is linear with $\sin^2\theta$. The angle θ which the trigonal axis makes with the axis of the single crystal rod will hereafter be called the orientation. If the coefficients of a number of crystals with different known orientations are measured and plotted against $\sin^2\theta$, the intercepts of the straight line through them at $\sin^2\theta=0$ and $\sin^2\theta=1$ will be $\alpha_{\parallel}$ and $\alpha_{\perp}$, respectively.

The specific resistance in a direction making an angle θ with the trigonal axis is given by the relation:[8]

$$\rho_\theta=\rho_{\parallel}\cos^2\theta+\rho_{\perp}\sin^2\theta$$
$$\sin^2\theta=(\rho_\theta-\rho_{\parallel})/(\rho_{\perp}-\rho_{\parallel}). \quad (2)$$

This offers a means of determining $\sin^2\theta$ since Sckell[9] has measured $\rho_{\parallel}$ and $\rho_{\perp}$ at certain known temperatures, the values being later corrected by Grüneisen and Sckell.[10] Sckell's curves show that

[1] E. Grüneisen and O. Sckell, Ann. d. Physik **19**, 387 (1934).
[2] J. Dewar, Proc. Roy. Soc. **A70**, 237 (1902).
[3] L. Grunmach, Physik. Zeits. **3**, 134 (1902).
[4] P. W. Bridgman, Proc. Am. Acad. **47**, 343 (1911).
[5] L. G. Carpenter and F. H. Oakley, Phil. Mag. **12**, 511 (1931).
[6] M. C. Neuburger, Zeits. f. anorg. allgem. Chemie **212**, 40 (1933).
[7] W. Voigt, *Lehrbuch der Kristallphysik*, p. 290.
[8] W. Voigt, *Lehrbuch der Kristallphysik*, p. 344.
[9] O. Sckell, Ann. d. Physik **6**, 932 (1930).
[10] E. Grüneisen and O. Sckell, Ann. d. Physik **19**, 387 (1934).

$\rho_{\parallel}$ and $\rho_{\perp}$ are sufficiently linear in the liquid air region to allow interpolation from the two temperatures at which he made measurements in that region to any other temperatures in the region. Thus, measurements of ρ_{θ} and the temperature allow $\sin^2\theta$ to be calculated from Eq. (2).

Sckell found that $\rho_{\parallel}$ was smaller than $\rho_{\perp}$ and Eq. (2) shows that $\rho_{\parallel}$ should therefore be the smallest possible value of ρ. In the present work three crystals were found which had smaller values of ρ than that given by Grüneisen and Sckell by 0.2, 0.3 and 0.5 percent. Although only the last is outside the limit of experimental error it appears quite probable that the value of $\rho_{\parallel}$ given by Grüneisen and Sckell is still high, especially since their crystal No. 13 was also lower by 0.4 percent than the value they gave as most probable.

Experimental

Preliminary work with single crystals showed that they frequently recrystallized so that it was necessary to use a method whereby the specific resistance and hence the orientation could be determined both before and after the expansion measurement. This could be done if the crystals were grown in the form of cylindrical rods of uniform cross section. A method was adopted which was quite similar to that employed by Grüneisen and Sckell.

Plaster molds, 30 cm long by 0.8 cm inside diameter, were made by clamping a thinly paraffined drill rod on the axis of a glass tube which was thickly paraffined on the inside. Patching plaster was poured between the tube and the rod and the air bubbles pumped out with an aspirator. After the plaster set, the mold was removed from the glass tube by melting the paraffin and the rod removed from the center of the mold in the same manner. A mold made in this way was straight, circular, of uniform diameter, and the inside had an almost polished appearance. Deep grooves were made lengthwise of the mold so that it could be broken free from the crystal. Pyrex tubes ending in various types of tips were waxed into the bottoms of the molds. In some the tubes were drawn down to straight capillaries 0.75 mm inside diameter and 4 cm long, in others the tubes were melted down to thick-walled capillaries 0.5 mm to 1.5 mm inside diameter below which bulbs of from 2 to 4 cc capacity were blown. The third type was similar to the second but had one or two tungsten wires sealed into the bottom of the bulb and extending up to about the center of the bulb. The type of tip seemed to have very little influence on the percentage of single crystals obtained or on the orientation. The orientations were apparently random.

The molds were filled in a vacuum by placing a glass reservoir containing the mercury at the top end of the mold and sealing both mold and reservoir in a larger glass tube which was then evacuated to fluorescence for several hours, the mercury being heated in the mean time to drive out water vapor and gases. The mercury was then poured into the mold by tipping the apparatus.

The crystals were grown either by lowering the molds at the rate of about 0.2 cm/min. into a liquid-air bath by means of a set of reduction gears or by suspending the molds in a large Dewar flask so that the tips were about 1/3 immersed in liquid air in the bottom of the flask. In the second method the process was hastened by lowering the molds from time to time, care being taken that the crystallization was always well above the liquid-air level. This method required about $2\frac{3}{4}$ hours to freeze the 28 cm by 0.8 cm crystals and was employed for most of the crystals.

The mercury was cleaned with dilute potassium hydroxide, dilute nitric acid, and then distilled once in a vacuum and twice in an air stream of 2.5 cm pressure by Hulett's method.[11]

The mold containing the crystal was removed from liquid air and the ends sawed off with a band saw to the desired length of 25.5 cm. The mold was broken free from the crystal along the previously made grooves and the crystal fastened to a grooved wooden block to prevent deformation in handling. The block containing the crystal was then clamped in a previously cooled wooden measuring bench which consisted essentially of a rod of seasoned hard wood containing three steel needle points spaced 10 cm apart and used

[11] G. A. Hulett, Phys. Rev. **33**, 307 (1911).

as potential probes. Current leads were clamped on the ends of the crystal and the whole lowered into a Dewar flask. The distance between the needle points was determined in liquid air by immersing the wooden rod so that the needles protruded above the air. The cross-sectional area was calculated from the length, mass and the density measurements of Dönitz.[12]

A Leeds and Northrup type K potentiometer was adapted to measuring the resistance by adding a second shunt to extend the range by a factor of 10. The individual and combined resistances of the two 10 cm sections of the crystal were determined separately, a necessary condition that the crystal be single being that the two sections have equal resistances. Errors from thermoelectric effects were eliminated by reversing the current through the crystal and through the potentiometer and repeating the measurements. Readings of 10^{-4} volt could be duplicated to 10^{-7} volt. The resistance of a 10-cm length of a crystal was of the order of 10^{-4} ohm and the measured resistance of the two sections always agreed with the sum of their separate resistances to about 0.1 percent.

The expansion apparatus consisted of a quartz tube, 50 cm long and 0.8 cm inside diameter, suspended from a rigid support and hanging in a cylindrical copper vessel, 40 cm deep and 7.5 cm in diameter, containing isopentane. The copper cylinder was supported in a large Dewar flask 48 cm deep and 10 cm in diameter. The crystal was placed in the quartz tube and a smaller quartz tube, about 26 cm long, set on the crystal so that the top of the smaller tube extended out of the larger one. On the top end of the smaller tube a piece of plane glass was cemented and served as a support for the back leg of an optical lever, the front legs of which rested on the same support used for the larger quartz tube. The optical lever served to measure the relative expansion of the crystal and an equal length of quartz.

Isopentane (boiling point 20°C to 30°C) served admirably for a bath down to about −165°C. It became quite viscous near −165°C and froze a little below −167°C when stirred. To aid in the proper stirring of the bath, a baffle plate was soldered across one side of the copper cylinder and extending from 1 cm from the bottom to 4 cm from the top. The bath was stirred by passing compressed air down a tube behind the baffle almost to the bottom of the cylinder, as the bubbles rose they kept the liquid circulating.

In order to be sure that the temperature of the crystal was the same as that of the bath, the quartz tube containing the crystal was ground completely open in slits on opposite sides of the tube beginning 1 cm from the bottom and extending upward 22 cm so that the crystal was in contact with the bath.

The temperature of the bath was measured with a platinum resistance thermometer calibrated at the boiling point of oxygen, the sublimation point of carbon dioxide, the freezing point of mercury and the freezing point of water.

The bath was cooled to −165°C by pouring liquid air between the cylinder and the Dewar flask, the crystal was removed from liquid air and suspended in the bath and then the bath was allowed to warm slowly by radiation and conduction. The rate of temperature rise varied from about 10°/hr. at −160°C to 8°/hr. at −100°C. Readings of the expansion and temperature were made every 5 to 12 minutes.

The length of the crystal at −160°C was found from cathetometer measurements between fiducial marks on the quartz tube in which it was contained, and on the tube set on the crystal, and from the known depth and length of those two tubes.

The change in length of the crystal was plotted against the temperature on a large scale graph. The slope of this curve was measured with a straight-edge at 5° intervals and the expansion coefficient calculated from the equation:

$$(\alpha_\theta)_T = (1/L_T)(\Delta L/\Delta T)_T.$$

Since the bath could not be used below −165°C the mean expansion coefficient from −190°C to −160°C was found. The crystal was suspended in a liquid air bath and the necessary readings taken, then the liquid air bath was quickly replaced with the pentane bath which had been previously cooled to −165°C and readings taken as the bath warmed.

[12] E. Grüneisen and O. Sckell, Ann. d. Physik **19**, 389 (1934).

A correction for the expansion of quartz was made from the equations of Souder and Hidnert.[13] It amounted to less than one percent.

Recrystallization

In the preliminary work on polycrystalline rods it was found that either plastic deformation, due to the weight of the crystal, or crystal growth set in at a temperature of about −90°C for, when the crystal was cooled a few degrees and then allowed to warm up again, the expansion curve fell below the original curve. At higher temperatures this effect increased but at lower temperatures it was not noticeable.

In single crystals a recrystallization or a breaking up of the single crystals into smaller crystals seemed to take place as they were warmed. This was probably caused by deformation of the extremely soft crystals since Sckell[14] and Reddemann[15] who did not remove their crystals from the glass molds in which they were grown were not bothered by the effect. Three crystals which were kept in liquid air for three days showed no change in orientation during that time but Table I shows that (except for No. 23 which was badly bent) the three crystals which were warmed to the highest temperatures experienced the greatest changes in $\sin^2\theta$. Moreover, the expansion curves of these three crystals showed corresponding changes in slope and curvature at a temperature between −110°C and −115°C. For this reason the expansion measurements were carried to only −115°C.

Table I. *Changes in resistance of sections and in orientation during the expansion measurements.*

Crystal No.	% Diff. Between Sections		$\sin^2\theta$		$\Delta \sin^2\theta$	Warmed to
	before*	after*	before*	after*		
23**	0.2%	1.3%	0.654	0.432	0.222	−112°C
6	.1	9.0	.991	.824	.167	−78
20	.1	10.0	.077	.238	.161	−93
19	.3	7.5	.285	.403	.118	−93
18	.3	3.2	.787	.688	.099	−112
32	2.0	2.0	.540	.564	.024	−112
14	0.5	2.4	.850	.827	.023	−111
26	.3	0.6	.975	.994	.019	−112
27	.1	.5	.907	.920	.013	−113
35	.3	.2	.150	.143	.007	−112
12	.0	.3	.046	.053	.007	−111
21	.0	.6	.000	.000	.000	−112
30	.4	.1	.000	.000	.000	−113
37	.0	—	.000	—	—	−143
36	.7	—	.072	—	—	−143
34	1.0	—	.098	—	—	−143
33	0.2	—	.922	—	—	−143

* Before and after the expansion measurement.
** No. 23 was badly bent before the second measurement.
— The dashes indicate that no measurement was made.

Frequently only one section of a crystal would change its orientation. The change was usually toward a mean value of $\sin^2\theta$. This behavior can also be noted in Fig. 2 of Grüneisen and Sckell.

Results

The measurements of α_θ are plotted in Figs. 1, 2 and 3. Figs. 1 and 2 show α_θ plotted against $\sin^2\theta$ for all the crystals at the indicated temperatures. In Fig. 3 the mean expansion coefficients from −190°C to −160°C for the six crystals measured in that interval are plotted against $\sin^2\theta$.

Table II contains the values of $\alpha_{||}$ and $\alpha_\perp$ read from Figs. 1, 2 and 3, and also the volume coefficient, $\alpha_{||}+2\alpha_\perp$. In Fig. 4, $\alpha_{||}$ and $\alpha_\perp$ are plotted as functions of the temperature. The mean values from −190°C to −160°C are not plotted since the other measurements are at definite temperatures, but the mean values indicate that the coefficient may begin to decrease rapidly just below −160°C. The temperature range is not sufficient to warrant drawing the curves. $\alpha_{||}$ decreases more rapidly with the temperature than $\alpha_\perp$ as Grüneisen predicted from the elastic constants, the mean expansion coefficients from −78°C to −190°C, and the known behavior of the thermal pressure coefficients.[16]

Table II. *Values of the coefficient of expansion parallel and perpendicular to the trigonal axis.*

T°C	$\alpha_{||}\times10^5$	$\alpha_\perp\times10^5$	$(\alpha_{||}+2\alpha_\perp)\times10^5$
−115	4.98	3.77	12.52
−120	4.96	3.75	12.46
−125	4.88	3.72	12.32
−130	4.80	3.69	12.18
−135	4.75	3.68	12.11
−140	4.66	3.60	11.86
−145	4.64	3.56	11.76
−150	4.60	3.55	11.70
−155	4.55	3.54	11.63
−160	4.49	3.52	11.53
−190/−160	4.26	3.34	10.94

[13] W. Souder and P. Hidnert, Bur. Stand. Sci. Pap. No. 524 (1926).
[14] O. Sckell, Ann. d. Physik **6**, 932 (1930).
[15] H. Reddemann, Ann. d. Physik **14**, 139 (1932).
[16] E. Grüneisen and O. Sckell, Ann d. Physik **19**, 407 (1934).

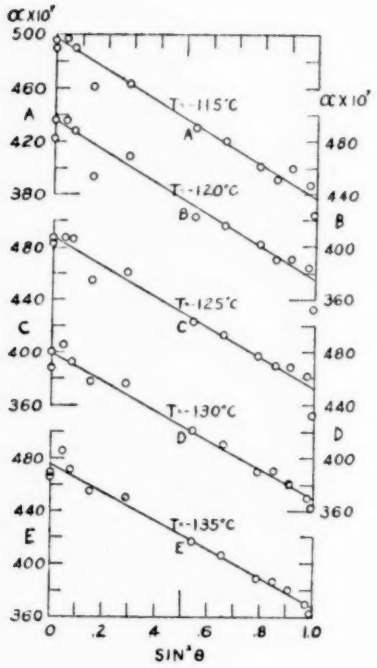

FIG. 1

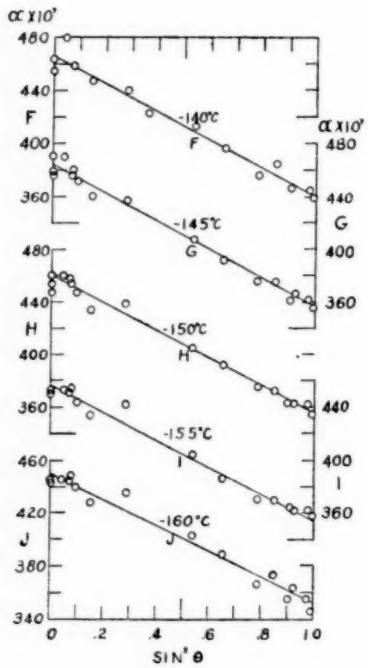

FIG. 2

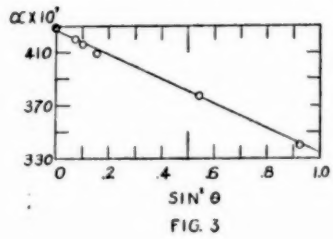

FIG. 3

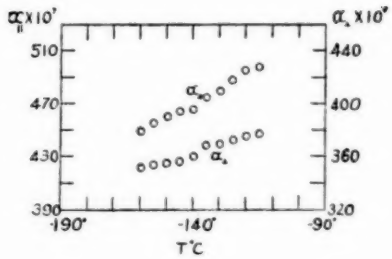

FIG. 4

FIG. 1. α_θ as a function of $\sin^2\theta$ at the indicated temperatures. The letters connect the curves with the corresponding scales.

FIG. 2. α_θ as a function of $\sin^2\theta$ at the indicated temperatures. The letters connect the curves with the corresponding scales.

FIG. 3. The mean expansion coefficient from $-190°C$ to $-160°C$ as a function of $\sin^2\theta$.

FIG. 4. $\alpha_\parallel$ and $\alpha_\perp$ plotted as functions of the temperature.

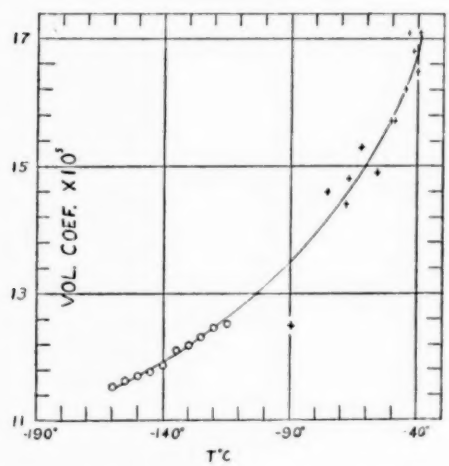

FIG. 5. The volume coefficient as a function of the temperature. The circles are the present measurements, the + signs are the measurements of Carpenter and Oakley.

The volume coefficients as functions of the temperature are plotted in Fig. 5. The circles represent the values found in the present research, the + signs are the measurements by Carpenter and Oakley.[17] These authors represented their measurements with a straight line, but when they are compared with the present measurements it is evident that except for the point at $-89.7°C$ their data are better represented by the smooth curve drawn in Fig. 5. The mean value of the volume coefficient from $-78°C$ to $-190°C$, found by extending the smooth curve to $-190°C$, is 12.23×10^{-5}. This agrees well with the value 12.2×10^{-5} found by Grüneisen and Sckell. If the lower end of the curve should bend down, as the mean value from $-160°C$ to $-190°C$ indicates that it does, the agreement would not be much affected. The data are insufficient to give the form of the curve below $-160°C$.

The writer wishes to express his appreciation to Professor George Winchester for suggesting the problem, for his many helpful suggestions, and for his constant interest throughout the course of the work.

[17] L. G. Carpenter and F. H. Oakley, Phil. Mag. **12**, 518 (1931).

Quenching of Cadmium Resonance Radiation by Foreign Gases

HARRY C. LIPSON AND ALLAN C. G. MITCHELL, *Department of Physics, New York University, University Heights*

(Received July 13, 1935)

Measurements have been made on the quenching of the cadmium resonance line 3261 by H_2, D_2, CO, NH_3, N_2 and CH_4. The experiment was carried out by comparing the intensity of 3261 emitted from a cell containing Cd vapor and foreign gas with that from a cell containing Cd vapor only. The cells were illuminated simultaneously and the results obtained by the method of photographic photometry. The experiments were performed under conditions (low vapor pressure, short light path through the vapor and small foreign gas pressure) which warrant the application of the Stern-Volmer formula. The quenching cross sections obtained therefrom are: H_2, 0.67; D_2, 0.19; CO, 0.14; NH_3, 0.041; N_2, 0.021; CH_4, 0.012×10^{-16} cm^2.

INTRODUCTION

THE term quenching implies a reduction in the intensity of resonance radiation due to the presence of a foreign gas. Collisions of the second kind between foreign gas molecules and excited atoms lead to a removal of the latter from the excited state before they have time to radiate, thus causing a diminution in the intensity of the emitted radiation. Under certain conditions a quenching collision cross section, σ_Q^2, can be determined, which in turn may be correlated with the particular process taking place, if the energy levels of the foreign gas molecule are known.

After Wood's first discovery[1] of the quenching of resonance radiation, a great deal of work was done on Hg and Na in which the cross sections for various gases were fairly well established, especially in the case of mercury. The first quantitative work in this field was done by Stuart on mercury[2] whose work was repeated and extended by Zemansky[3] and Bates.[4] With apparatus similar to that of Stuart, Mannkopf[5] measured the quenching of sodium resonance radiation. The work of Bates[6] and Bender[7] on the quenching of Cd resonance radiation was purely of a qualitative nature and no attempt was made to determine collision cross sections. Cadmium exhibits a spectrum of the same type as that of mercury, the main difference, as far as this experiment is concerned, is that the energy difference between the normal state and the ^3P levels is less in the case of cadmium (see Fig. 1) than in the case of mercury ($6^3P_2-6^3P_1=0.57$ v, $6^3P_1-6^3P_0=0.20$ v, $6^3P_1-6^1S_0=4.86$ v).

[1] R. W. Wood, Physik. Zeits. **13**, 353 (1912); Phil. Mag. **27**, 1018 (1914).
[2] H. Stuart, Zeits. f. Physik **32**, 262 (1925).
[3] M. W. Zemansky, Zeits. f. Physik **36**, 919 (1930).
[4] J. R. Bates, J. Am. Chem. Soc. **52**, 3825 (1930); **54**, 569 (1932).
[5] R. Mannkopf, Zeits. f. Physik **36**, 315 (1926).
[6] J. R. Bates, Proc. Nat. Acad. Sci. **14**, 849 (1928).
[7] P. Bender, Phys. Rev. **36**, 1535 (1930).

EXPERIMENTAL PROCEDURE

The top view of the full experimental arrangement is represented in Fig. 2. Light from a quartz discharge tube, S, containing cadmium vapor, and through which hydrogen was circulated to carry the discharge, was focused by means of a quartz lens, L, on two resonance cells placed one above the other. In one arm of each

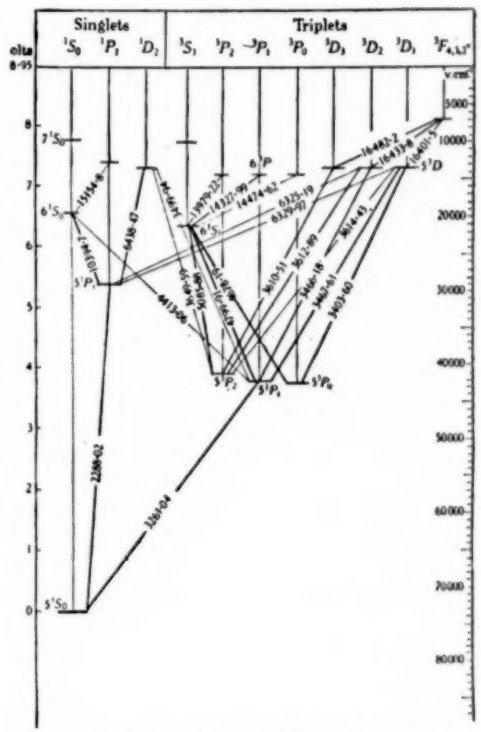

FIG. 1. Energy level diagram of cadmium.

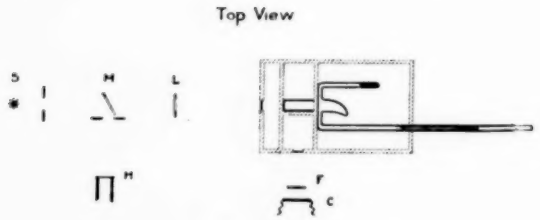

FIG. 2. Diagram of apparatus.

cell pure cadmium was distilled; the other arm was connected to the pumping system and to the source of a foreign gas. The cells could be isolated from the rest of the system by stopcocks and magnetic cut-offs to prevent cadmium from condensing outside the furnace. The vapor pressure of cadmium was determined by the temperature of the side arms which was maintained at 210°C throughout the experiment. A separate electric heating circuit maintained a considerably higher temperature in the front part of the furnace to prevent cadmium from condensing on the windows of the cells. The resonance radiation was taken out at right angles, passed through a filter to cut off the 2288 line, and 3261 was photographed by means of a camera fitted with a quartz lens.

On the photograph there appeared two images, one from each resonance cell. The lower cell usually contained cadmium vapor plus foreign gas while the upper cell contained cadmium vapor alone and served as a standard of comparison. In this manner any fluctuations in the light source were compensated.

Reasonable care was taken to insure purity of the gases used. Hydrogen was admitted to the system by diffusion through a heated palladium tube. Nitrogen was generated by heating sodium azide and was stored over metallic sodium. Carbon monoxide was generated by the action of sulphuric acid on sodium formate, while methane was prepared by heating sodium acetate and sodium hydroxide. Anhydrous ammonia, obtained from a tank, was stored over potassium hydroxide and was further purified by condensing in liquid air and pumping off the residual noncondensible gases. Deuterium (100 percent pure) was obtained through the courtesy of the Frick Chemical Laboratory, Princeton University.

The procedure adopted was first to reflect the light from the arc by a mirror, M, into a Hilger quartz spectograph, H (see Fig. 2) and place intensity-time calibration marks on a photographic plate; then to remove the mirror, allow the light to fall on the two resonance cells and photograph on the same plate the resonance radiation from the two cells, first in the absence of the foreign gas and then in the presence of the varying amounts of the gas in the lower cell. Each pressure change was made slowly and the cadmium vapor was allowed to reach equilibrium before a photographic exposure was made.

The plate blackenings were traced on a microphotometer and then translated into light intensities by means of the calibration marks mentioned above. The quenching, Q, was determined by dividing the intensity of the resonance radiation from the cell containing the foreign gas by the radiation intensity from the cell containing cadmium vapor only and the reciprocal of this quenching was plotted against the foreign gas pressure in mm.

EXPERIMENTAL RESULTS

The experimental results are given in Figs. 3, 4, 5 and 6 and Table I. As is seen in Fig. 3, hydrogen quenches very efficiently, the effect being first noticeable at pressures as low as 0.01 mm and the

TABLE I. *Quenching slopes and collison cross sections for the quenching of Cd resonance radiation by foreign gases.*

Gas	H_2	D_2	CO	NH_3	N_2	CH_4
Slope (mm^{-1})	2.45	0.50	0.15	0.063	0.022	0.016
$\sigma_Q^2(\times 10^{16}\ cm^2)$	0.67	0.19	0.14	0.041	0.021	0.012

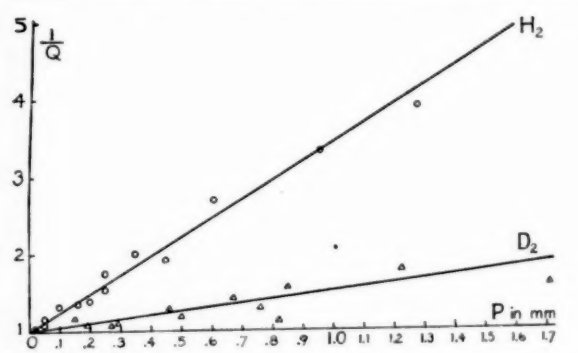

FIG. 3. Quenching of Cd resonance radiation (3261) by H_2 and D_2.

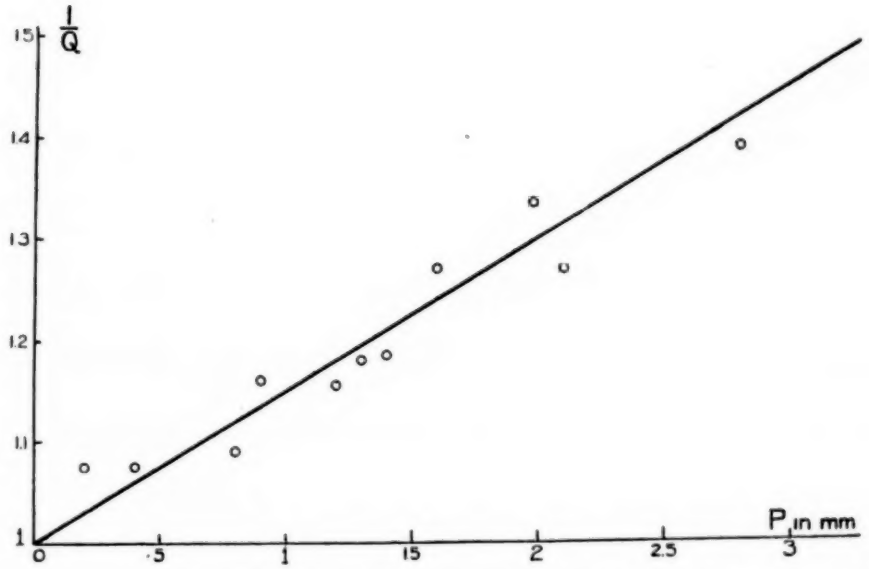

FIG. 4. Quenching of Cd resonance radiation (3261) by CO.

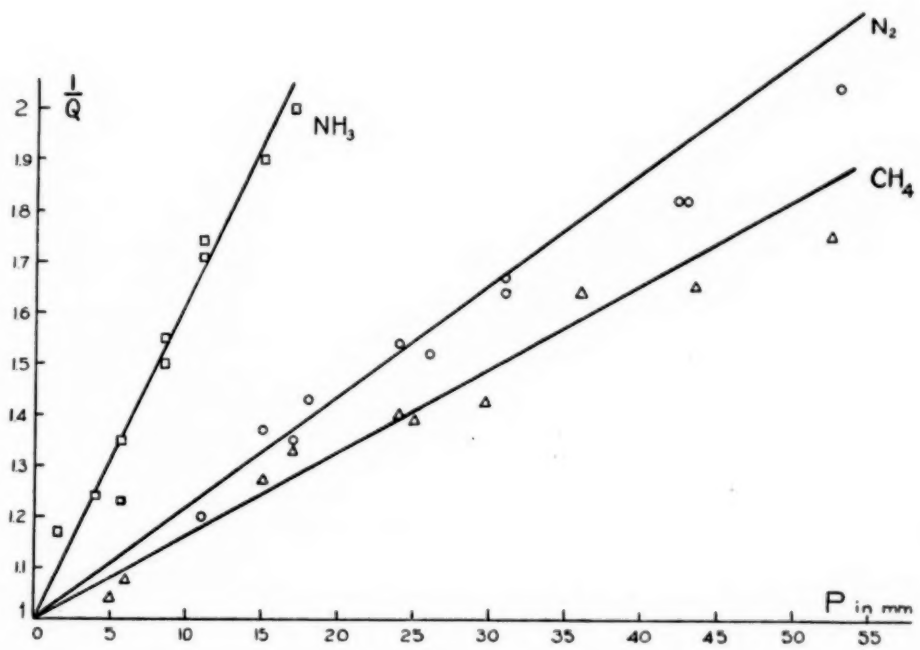

FIG. 5. Quenching of Cd resonance radiation (3261) by N_2, CH_4 and NH_3

intensity of the resonance radiation being reduced to half of its original value at about 0.4 mm of H_2. The quenching by deuterium is of the same order of magnitude as that of hydrogen although the "half-value" occurs at 1.5 mm. Carbon monoxide, Fig. 4, is less efficient than hydrogen, 0.4 mm decreasing the resonance radiation intensity to only about 95 percent of its maximum. Ammonia, Fig. 5, quenches moderately, the curve lying between those of nitrogen and carbon monoxide. Nitrogen and methane are very ineffective as quenching agents, the phenomenon not being observed until a pressure of a few millimeters was reached and the intensity

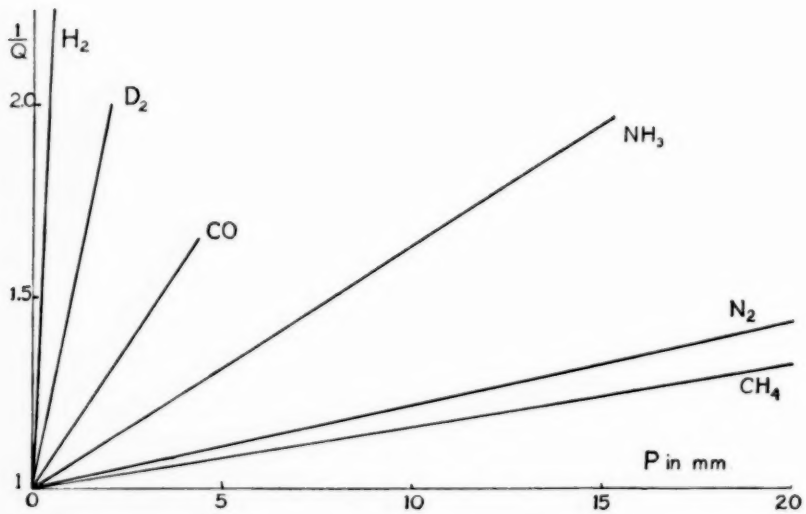

FIG. 6. Quenching of Cd resonance radiation (3261) by foreign gases.

dropping to approximately half-value at 45 mm in the case of N_2 and 60 mm in the case of CH_4. The relative quenching efficiency of all the gases is shown in form of slopes in Fig. 6.

DISCUSSION AND INTERPRETATION OF RESULTS

The correct interpretation of quenching experiments is affected mainly by two factors:

1. The diffusion of imprisoned resonance radiation, i.e., reabsorption of the emitted resonance radiation on its way out through the gas to the exit window, giving rise to secondary radiation, which absorbed again will produce tertiary radiation, and so on.

2. The alteration of the width and the position of the absorption line relative to the exciting line, which is due to the collisions of atoms with foreign gas molecules (Lorentz broadening).

Unless the above difficulties are overcome, a quenching curve can give no information leading to the computation of collision cross sections and in some cases[3, 5] it is not even evidence that quenching takes place at all.

The present work was performed under conditions in which these two effects were largely eliminated. Thus, Lorentz broadening was reduced by operating with pressures of foreign gas as low as was compatible with the quenching process. As to diffusion of the imprisoned resonance radiation this was eliminated, first by keeping the cadmium vapor pressure low (5.6×10^{-4} mm corresponding to 210°C at which the absorption coefficient at the center of the 3261 line is about 0.4) and second, by placing both the entrance and the exit window of the resonance cell near a common edge, so that only a small portion of the Cd vapor was exposed to the incident radiation, thus permitting only the primary resonance radiation to be re-emitted.

The fulfilment of the above conditions warrants an application of the Stern-Volmer formula:[8]

$$Q = 1/(1+\tau Z_Q) \qquad (1)$$

where Q = quenching of the resonance radiation, τ = the lifetime of the excited atom, and Z_Q = the number of quenching collisions per sec., per cc, per excited atom.

Since Z_Q varies linearly with the foreign gas pressure, p, a plot of the reciprocal of Q against p should result in a straight line. This was found to be true in the present investigation, as attested by the above graphs. Above a certain pressure, the deviation from straight lines can probably be accounted for by Lorentz broadening.[9]

The quenching collision cross sections, σ_Q^2, were determined as follows:

The Stern-Volmer formula, (1), gives a relation between the quenching Q and the total number of quenching collisions Z_Q. The latter can be calculated on the basis of the Maxwellian distri-

[8] O. Stern and M. Volmer, Physik. Zeits. **20**, 183 (1919).
[9] Mitchell and Zemansky, *Resonance Radiation and Excited Atoms* (The Macmillan Co., 1934), p. 224.

bution of velocities, resulting in the equation

$$Z_Q = 2Nn\sigma_Q^2[2\pi kT(1/M_1+1/M_2)]^{\frac{1}{2}} \quad (2)$$

where M_1 and M_2 = molecular weights of the colliding particles, N and n = their molecular concentrations, and k = universal gas constant or expressed in terms of the pressure in mm of Hg

$$Z_Q = 2666.6\sigma_Q^2[2\pi N/kT(1/M_1+1/M_2)]^{\frac{1}{2}}\cdot p. \quad (3)$$

From (1) and (3) it follows that the collision cross section is given by

$$\sigma_Q^2 = \frac{1/(Q\cdot p)}{\tau 2666.6[2\pi N/kT(1/M_1+1/M_2)]^{\frac{1}{2}}}. \quad (4)$$

The values $1/(Q\cdot p)$ are the slopes of the quenching curves and could be read for each gas from Figs. 3, 4 and 5; they are given in Table I. The temperature of the cadmium vapor was 210°C and the mean life for the 5^3P_1 state of Cd was taken as $\tau = 2.5\times10^{-6}$ sec.[10] The values of the quenching collision cross sections thus computed from (4) are given in the same table.

The high quenching efficiency of hydrogen was interpreted by Bender[7] as due to a collision of an excited Cd atom in the 5^3P_1 state with a normal H_2 molecule, resulting in a formation of an unexcited cadmium hydride molecule and an atom of hydrogen

$$\begin{array}{lll} \mathrm{Cd}\ (5^3P_1) + & \mathrm{H_2} \rightarrow \mathrm{Cd\ H} + \mathrm{H} \\ 3.78\ \mathrm{v} & 4.44\ \mathrm{v} \qquad 0.67\ \mathrm{v} \end{array}. \quad (5)$$

This process seems to be highly probable, as indicated by the energy balance of the equation, in which the energy required for the above reaction differs from the energy available by less than half of one percent. This was further substantiated in Bender's experiment by the appearance of CdH bands in the resonance cell and the formation of atomic hydrogen found as water frozen out by the liquid air trap, due, probably, to a reduction by atomic hydrogen of some oxide present in the Cd supply.

However, simple calculations made on the basis of the data given by Jevons[11] indicate that H_2 has a vibrational level of the normal electronic state at 3.73 volts, which, from purely energetic considerations makes the following process also possible: upon collision, the excited Cd atom gives up 3.78 volts to raise the H_2 molecule to a 3.73-volt vibrational level:

$$\begin{array}{lll} \mathrm{Cd}\ (5^3P_1) + \mathrm{H_2} \rightarrow & \mathrm{Cd}\ (5^1S_0) + (\mathrm{H_2})_v \\ 3.78\ \mathrm{v} & 3.73\ \mathrm{v} \end{array}. \quad (6)$$

Although in this reaction the energy discrepancy is larger (about 1.5 percent), still the above process seems to be very plausible.

Similar considerations can probably apply to deuterium (energy of dissociation of D_2 is the same as that of H_2; there is also a vibrational level at 3.72 volts) although no attempt was made to detect the existence of the CdD bands.

The quenching by CO, N_2 and CH_4 cannot be accounted for by a dissociation process, since the energies of dissociation of these molecules are far in excess of the energy available (10.0 volts for CO, 9.1 for N_2, 16.3 for CH_4). However, the carbon monoxide molecule has a vibrational level at 3.83 volts, which being near the excitational level of the 3261 Cd line makes the following reaction possible:

$$\begin{array}{lll} \mathrm{Cd}\ (5^3P_1) + \mathrm{CO} \rightarrow & \mathrm{Cd}\ (5^1S_0) + (\mathrm{CO})_v \\ 3.78\ \mathrm{v} & 3.83\ \mathrm{v} \end{array}. \quad (7)$$

In this case the energy discrepancy is 1.5 percent.

The nearest vibrational level of nitrogen is at 3.48 volts, indicating an energy discrepancy of 8 percent; concerning the CH_4 molecule there are not sufficient band spectra data known to consider the quenching by methane from above point of view. However, at the temperature used (210°C), the average kinetic energy of translation of a molecule ($\frac{3}{2}kT$) is about 0.07 volt, which corresponds to the energy difference between the excited 5^3P_1 and the metastable 5^3P_0 state of Cd. Thus, perhaps, the quenching by N_2 and CH_4 can be explained in terms of a transfer of the excited Cd atom to the metastable state, resulting in a loss of 0.07 volt to the molecules in a form of a translational kinetic energy, e.g.,

$$\begin{array}{lll} \mathrm{Cd}\ (5^3P_1) + \mathrm{N_2} \rightarrow & \mathrm{Cd}\ (5^3P_0) + (\mathrm{N_2})\ \mathrm{K.E.} \\ 3.78\ \mathrm{v} & 3.71\ \mathrm{v} \qquad 0.07\ \mathrm{v} \end{array}. \quad (8)$$

[10] Reference 9, p. 147.

[11] W. Jevons, *Report on Band-Spectra of Diatomic Molecules* (The Physical Society, London, 1932), p. 269.

Of course, the reverse process is plausible and undoubtedly takes place also, in which a collision between a metastable atom and the gas molecule results in a transfer of the Cd atom back to the 5^3P_1 state, but as has been shown by Klein and Rosseland[12] this type of a collision (collision of the first kind) is less probable than the former, since a fast molecule will remain in the neighborhood of an atom during a shorter interval of time than a slow one. This point of view seems to be confirmed by Bender's observation of an increase in the relative intensity of the 3404 line over the remainder of the spectrum in the presence of N_2 and CO but not in the presence of H_2. This line results (see Fig. 1) in the absorption of an energy quantum from the 5^3P_0 state to the 5^3D_1 state and a subsequent re-emission, and thus a heavy population of the metastable state will favor an increase in its intensity.

Because of the meager data existing about the energy levels of the ammonia molecule it is not possible to ascribe any definite process to the quenching by ammonia. No evidence was obtained for its decomposition under the influence of excited cadmium atoms, in agreement with Bates and Taylor.[13] The test is not conclusive, however, since the intensity of the source may have been too small to produce a measurable chemical effect, although it was large enough for the measurement of quenching. In view of the fact that some decomposition might have occurred and the resulting products might have had an effect on the intensity of the resonance radiation, exposures were made at the same ammonia pressure, first with a fresh sample of gas and next with a sample which has been irradiated previously for 15 minutes. There was no detectable difference in the quenching between the two cases.

Lastly, the collision between any one of the above molecules and the Cd atom cannot result in raising them either to an excited electronic level or to some rotational level, in the first case, the energies required being too high (the first excitational level of H_2 is 11.1 v, CO—4.8 v, N_2 —8.5 v) in the second case the energies being only of the order of a fraction of a volt.

In conclusion, it ought to be emphasized that it is difficult to interpret quenching in terms of one process alone, the reactions taking place within the resonance tube being of a very complicated nature. It may be that quenching by a particular gas can be explained by all the processes mentioned above, there being only a degree of effectiveness of one reaction over the other. Thus, perhaps one can venture an opinion that the process, in which the discrepancy between the energy required and the energy available is small, is more responsible for the quenching phenomenon than the one in which a corresponding discrepancy is large.

The authors wish to acknowledge their indebtedness to Dr. R. L. Garman of the Chemistry Department of the Washington Square College for making the microphotometer traces.

[12] O. Klein and S. Rosseland, Zeits. f. Physik **4**, 46 (1921).

[13] J. R. Bates and H. S. Taylor, J. Am. Chem. Soc. **50**, 771 (1928).

Intensity of Diffraction of Electrons by ZnO

H. J. YEARIAN, *Purdue University*

(Received July 18, 1935)

Electron diffraction patterns of ZnO powder have been obtained in the range from 10 to 80 kv by using two types of camera. The intensity distribution has been determined photographically and shows marked deviations from the intensity distribution of the corresponding x-ray pattern. It has been shown that these deviations are not due to impurities, difference in structure due to methods of preparation, coincidences with another form of ZnO, or due to preferred orientation. The scattering as a function of $\sin(\theta/\lambda)$ is discussed on the basis of additional surface reflection, dynamic reflection and refraction of the electrons, and it is found that also these effects cannot account for the anomalous intensity distribution. Complete agreement between experimental and calculated curves for the scattering factor is obtained by assuming a distortion of the electron cloud (M shell of the zinc and L shell of oxygen) resulting in a different parameter for the distance Zn nucleus—oxygen nucleus, and Zn electrons-oxygen electrons. The resulting structure factor has the form

$$S=Z(\mathrm{Zn})-\Sigma F_{n,\,l}(\mathrm{Zn})e^{2\pi i a_{n,\,el}}+Z(\mathrm{O})e^{2\pi i q l}-F_{n,\,l}(\mathrm{O})e^{2\pi i(q+b_{n,\,e})l}.$$

IT is known that while the scattering of x-rays is not influenced by the nucleus of the scattering atom, electron diffraction is affected by the nucleus as well as by the electronic cloud; electron diffraction is therefore able, at least in principle, to locate the position of both nucleus and electrons in a crystal lattice.

In view of these considerations experimental investigations of the intensity of diffraction of high speed electrons in a powder, using photographic recording, have been undertaken, with the object of determining the atom factor for the diffraction of electrons.[1]

The wave-mechanical theory of the electron diffraction atom factor E, has been put in an especially simple form by Mott,[2]

$$E=(Z-F)/(\sin\theta/\lambda)^2. \qquad (1)$$

θ is the half-angle of scattering, Z the atomic number of the scatterer, and F its x-ray atom factor. This expression is derived for a free atom and is based on the assumption that the atom is spherically symmetric about its nucleus, and that the plane wave of the electron beam is undistorted by the atom. The first of these assumptions, as Mott points out, may not be valid for an atom bound in a crystal lattice, but the second should be acceptable for electrons of sufficiently high velocity.

This expression has been found to agree quite well with experiments carried out on gold, silver and aluminum.[3]

EXPERIMENTAL PROCEDURE

Diffraction photographs were obtained in two cameras illustrated in Figs. 1a and b.

The first camera, Fig. 1a, consists of a brazed and soldered brass box B 25 cm long closed with a lid and rubber gasket. Electrons from a very small conical filament of tungsten, F, are accelerated to the anode by a potential of the order of 20–30 kv, and a fine beam is formed by the slits S_1 and S_2 drilled with 0.15 mm and 0.1 mm holes, respectively. S_3 is a shielding slit on which the specimen is mounted. The diffraction pattern is recorded on a plate (Eastman lantern slide) at P. A two-stage Hg diffusion pump backed by a Cenco Megavac produced a vacuum of 10^{-5} mm Hg. The potential for this camera is supplied by a 30 kv full wave filtered rectifier.

In order to obtain the multiple exposures necessary for establishment of the intensity-density characteristic of the plate, a large diaphragm E with two 30° segments cut away is placed in front of the plate. This diaphragm is rotated about an axis parallel to the beam by a weight (not shown) and stopped in five adjacent positions by a catch operated by a solenoid. The diaphragm is controlled automatically by a motor driven switch which also automatically times the five exposures in the ratio of 1 : 2 : 3 : 4 : 5 by means of a pair of small Helmholtz coils. All the necessary exposures are easily made in

[1] H. J. Yearian and K. Lark-Horovitz, Phys. Rev. **42**, 905 (1932); K. Lark-Horovitz, H. J. Yearian and E. M. Purcell, Phys. Rev. **45**, 123 (1934); K. Lark-Horovitz, H. J. Yearian and J. D. Howe, Phys. Rev. **47**, 331 (1935).

[2] N. F. Mott, Proc. Roy. Soc. **A127**, 658 (1930); G. P. Thomson, Proc. Roy. Soc. **A125**, 352 (1929); H. Mark and R. Wierl, Zeits. f. Physik **60**, 741 (1930).

[3] The apparent discrepancy in the case of Al disappears when a temperature correction is applied. The comparison with the analysis of a number of other substances will be presented in later papers.

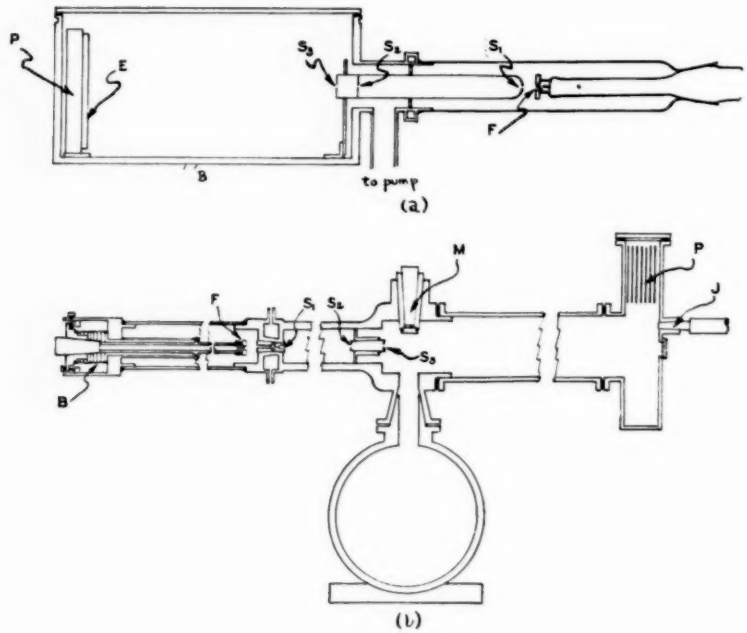

FIG. 1.

approximately one second more than the total exposure time (of the order of 20 seconds), so that current-voltage conditions are relatively easy to maintain.

The second camera, Fig. 1b, has been used up to 80 kv. It is assembled of brass parts with the removable joints sealed with sulphur free rubber gaskets. Electrons from a small filament *F*, mounted adjustably on a flexible bellows, *B*, form a narrow beam defined by the 0.15 mm hole in the anode S_1, and the 0.10 mm hole in slit S_2. The specimens are mounted either on the shielding slit S_3 or on a universal mounting operated by the double cone joints *M*. The camera is mounted directly on a Holweck molecular pump backed by a Cenco Megavac, giving a very high pumping speed. The potential is supplied by a 120 kv full wave filtered rectifier

The pattern is recorded on plates held in the magazine *P*. This magazine holds seven plates each of which may be pulled over the camera opening, exposed and returned, by means of a traveling carriage operated by a ground joint *J*. Also a screen with a rectangular opening may be brought into position over the camera so that five exposures may be made in strips on each plate in order to obtain its intensity-density characteristics. The exposures are timed by contacts on a motor-driven screw; these are adjustable to 20 sec. in steps of 1/20 sec.*

Specimens of ZnO were formed by catching the fumes from a zinc arc on the last diaphragm of the slit system. The deposited crystallites grow into the slit opening, and with a sufficiently fine deposit excellent diffraction patterns are obtained, Fig. 2.

The measurements of the rings in this pattern agree very closely with those calculated from x-ray data, as is shown in columns 1 and 2 of Table I. Columns 3 and 4 give a comparison of estimated intensities. It is evident that there are large discrepancies in the intensities which must

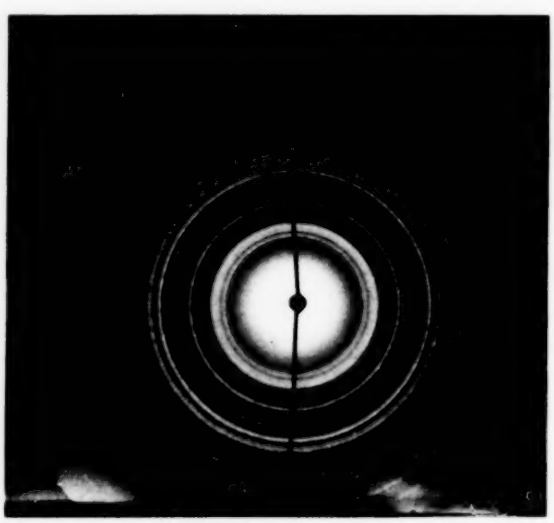

FIG. 2. Pattern of ZnO: 71.5 kv, 1.0 ma, 0.75 sec. exposure.

* This camera has recently been improved to a quite universal form. A detailed description will be published shortly.

TABLE I.

ZnO Hex. Close packing $a=3.24$Å $c/a=1.599$ $p=\frac{3}{8}$ C_{6v}^4 Zn(000), $(\frac{1}{3}\,\frac{2}{3}\,\frac{1}{2})$; O(00$p$), $(\frac{1}{3}\,\frac{2}{3}\,p+\frac{1}{2})$

hkl	sin θ/λ obs.	sin θ/λ calc.	Est. int. elec.	Est. int. x-ray	Mean rel. int.	Ave. dev.	*f*	S_2^2	S_1 Obs. mean
001		.0965						0	
100	.1783	.1782	4	4.5	1.60	.11	6	1	2.14
002	.1941	.1930	6	3.25	2.09	.17	2	4	2.64
101	.2042	.2026	5	5	3.46	.27	12	3	1.87
102	.2637	.2627	5	4	1.46	.10	12	3	4.64
003		.2895						0	
110	.3093	.3086	4	5	1.40	.15	6	4	5.21
111		.3234						0	
103	.3407	.3394	6	4.75	2.97	.32	12	3	8.19
200	.3594	.3563	2	2	.243	.014	6	1	6.74
112	.3654	.3640	4	5	1.48	.15	12	4	6.17
201	.3718	.3692	3	3.5	.528	.065	12	3	4.46
004	.3872	.3860	1	1.75	.236	.018	2	4	7.10
202	.4074	.4053	2	2.25	.266	.054	12	1	7.26
113		.4232						0	
104	.4269	.4252	3	1.25	.197	.040	12	1	7.08
203	.4614	.4592	4	4	.571	.079	12	3	8.91
120	.4752	.4715	1	2.5	.226	.053	12	1	10.5
211	.4835	.4812	2	3.5	.370	.066	24	3	5.89
005		.4826						0	
114	.4973	.4943	2	2.5	.320	.054	12	4	7.13
212	.5165	.5094	5	2.5	.216	.115	24	1	9.26
105		.5144		4	.574	.115	12	3	12.45
204	.5297	.5254	1	1.25	.065	.010	12	1	7.78
300	.5386	.5346	2	3	.271	.036	6	4	11.9
301		.5432						0	
213	.5580	.5533	4	4.75	.524	.105	24	3	10.6
302		.5682	3	3.75	.273	.023	12	4	10.2
115		.5727						0	
006	.5791	.5789	?	1	.041	.011	2	4	10.0
205	.6000	.5999	3	3.75	.277	.024	12	3	12.6
106	.6078	.6059	2		.055	.004	12	1	10.8
303		.6078						0	
214	.6082	.6093	1		.048	.002	24	1	7.39
220		.6173	1	3.5	.080	.024	6	4	10.0
221		.6248						0	
310		.6424			.066	.014	12	1	14.4
222	.6505	.6468			.155	.026	12	4	11.4
311		.6497			.131	.021	24	3	8.63
312	.6586?	.6706			.062	.004	24	1	11.2
215	.6776	.6743			.264	.033	24	3	13.5
007		.6754						0	
206		.6798			.026	.003	12	1	10.6
223		.6741							
107	.7028	.6986							
313	.7099	.7047							
224		.7280							
216	.7466	.7467							

be accounted for. The discrepancy is also apparent in the comparison of electron and x-ray microphotometer records in Fig. 3.

Inspection shows that planes for which the third index is small are relatively too weak in the electron diffraction pattern. For example, in the x-ray pattern 110 is stronger than 103, but this relation is reversed in the electron pattern. It is interesting to note that these same differences are apparent in the electron diffraction patterns of ZnO reproduced by Ponte[4] and Dauvillier[5] and by Finch and Quarrell.[6] According to formula (1) electron intensities should differ from the x-ray intensities, but only as a monotonous function of sin (θ/λ) and not irregularly from peak to peak.

[4] H. Ponte, Comptes rendus **188**, 244 (1929).
[5] M. A. Dauvillier, J. de physique **3**, 229 (1932).
[6] G. I. Finch and A. G. Quarrell, Proc. Roy. Soc. **A141**, 398 (1933).

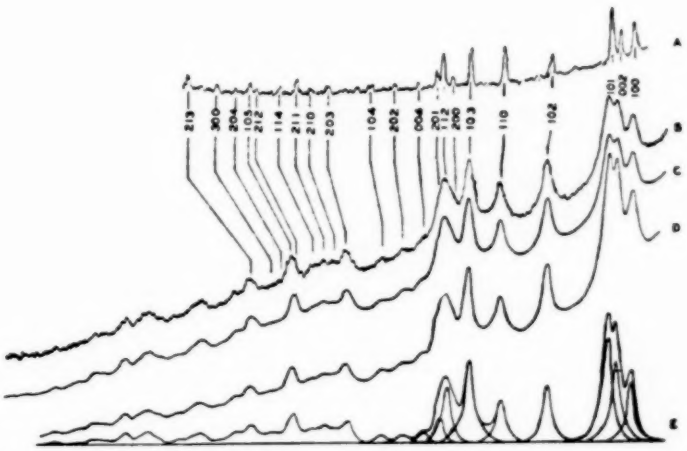

FIG. 3. Microphotometer curves of ZnO diffraction patterns. *A*, x-ray pattern; *B*, electron pattern; *C*, "most probable" trace; *D*, trace *C* converted to optical density; *E*, curve *D* reduced to flat background and partially resolved.

Discussion

Intensity anomalies of this kind might be caused by impurities, preferred orientation, method of depositing powder and influence of its support, or by an erroneous application of the kinematical theory of diffraction neglecting absorption, extinction, refraction and the possible influence of cross gratings. In the search for the possible causes of the unexpected intensity distribution, over 200 plates have been taken under different conditions at potentials ranging from 10 to 80 kv.

No difference has been found between the diffraction patterns from C.P. and spectroscopically pure† zinc. Specimens have been prepared on brass, copper, gold, platinum and molybdenum slits without change. To check the effect of the form of powder deposit, pictures have been taken with both commercial ZnO, and oxide from the arc collected on glass and pressed on the slit. There was no difference in the diffraction patterns from deposits of very large or very small particle size. Zinc oxide from a zinc arc sometimes forms long threads of crystallites. Patterns have been obtained from such single threads, from powder deposited on silk fibers and on thin films of celluloid. All these patterns are identical with the one illustrated.

There is no indication of preferred orientation, but to test for an axis of orientation parallel to the electron beam, a deposit was made on a slit which could be rotated. No change was produced when the slit was rotated in the range from 90° to 30° with respect to the beam. X-ray photographs of one of the specimens, moreover, gave the regular x-ray intensities.

All x-ray data on the structure of ZnO are in agreement with a single space group C_{6v}^4. A different surface structure, undetectable by x-rays, might affect the electron intensities. A comparison, however, with the intensities of the other possible space groups[7] shows that no combination of these can account for the observed electron intensities.

Coincidence of lines of some contamination could falsify the intensites. An actual impurity is improbable since no extra lines were observed. A comparison of the ZnO pattern with the cubic pattern reported by Bragg and Darbyshire,[8] the pseudomorphic form of the oxide reported by Finch and Quarrell,[6] and with zinc, shows several coincidences but in all cases there are equally strong or stronger lines in these patterns which do not coincide and would be observable if these substances were present.

From these considerations it would seem impossible that the anomalous intensities observed can be due to contamination or to preferred orientation. Further it appears very improbable that they can be explained by absorption or extinction effects. In primary extinction one might expect that intense reflections should be weakened more than weaker ones, but there is no apparent connection between the deviations in the intensities and the expected strength of reflection.

As will be shown in more detail later, the nearer a plane is to being perpendicular to the c axis, the more its intensity deviates from normal. To account for this by extinction would require a corresponding regularly increasing degree of imperfection of the crystal for such planes. This seems very artificial. The dynamical theory of electron diffraction developed by Bethe[9] in considering the effects of extinction and interaction of diffracted beam with the incident beam, predicts the appearance of reflections not possible in the usual kinematical theories. Faint "inner rings," discussed below, are sometimes found in the ZnO pattern which might be attributed to such dynamical effects. Their intensities, however, are less than one percent of the stronger regular reflections, and would indicate that the deviations of fifty percent or more observed in the regular pattern are not explainable by dynamical considerations of extinction, etc.

One could possibly explain the dependence of the intensity deviation on the direction of the diffracted rays in the crystal, as being due to absorption. The absorption in crystallites much longer parallel to the c axis than perpendicular

† The pure zinc was obtained from Adam Hilger, London, England.

[7] Wycoff, *The Structure of Crystals*, first edition, p. 275.

[8] W. A. Bragg and J. A. Darbyshire, Trans. Faraday Soc. **28**, 522 (1932).

[9] H. Bethe, Ann. d. Physik **87**, 55 (1928).

to it would weaken reflections from planes parallel to the axis more than it would reflections from planes perpendicular to the axis. Kirchner[10] has found that the total absorption coefficient (scattering plus true absorption) varies, in mica, approximately inversely as the electron velocity. Such a rapid variation of absorption should produce considerably different intensity deviations at different velocities. No noticeable difference in the intensity patterns has, however, been obtained over the whole range from 7 kv to 80 kv, and one must conclude that absorption does not account for the anomalities observed.

There is still the possibility that refraction produces the effect. On a few plates one or more very faint but sharp rings smaller than the first permissible reflection ("fractional orders") have been noted; these usually occurred when the specimen contained large crystallites. These have been explained by K. Lark-Horovitz[11] as a refraction effect since he has shown that although the refraction is negligible when high velocity electrons are incident normally on a diffracting layer and are diffracted from an inner plane, when the diffraction occurs from an exposed surface, refraction is not negligible. Indeed a lattice potential of the order of only 4 volts is necessary to produce a "half order" diffraction from 002 of ZnO.* This effect, however, can hardly be the cause of the anomalous intensity distribution since calculations have shown that the refraction is appreciable only when the incident or diffracted beam, or both, makes a very small angle with the crystal surface, and can practically enter, therefore, only in the case of planes which are developed faces of the crystallites. This necessity of very small angles also requires that the surface be exceedingly flat, "electron optically smooth," and of considerable extent, of the order of 10^3A. From these considerations it is obvious that the whole pattern could hardly be affected by refraction in the way observed. For example, the 100 and 110 intensities are reduced to approximately half as compared with reflections from 001. This would require that at least half the crystallites have these planes developed as large electron optically smooth faces and at the same time have no 001 faces so developed. But in a pseudolayer-lattice like ZnO one would expect the latter type of development to be at least as frequent as the former, and probably much more frequent.** Furthermore, the products of the many necessary refractions should appear either as visible "inner" rings, or as a broadening of the abnormally weak rings on the inner side;† this does not occur. Any broadening observed affects all rings alike without influencing their relative intensities.

The intensities would also be influenced by the diffraction from two-dimensional lattices superimposed upon that from the space grating. The occurrence of cross lattice diffraction has been frequently observed, [12] and has been theoretically treated by v. Laue.[13] Transmission through two-dimensional networks distributed at random results in a ring pattern. This has the appearance of the usual space lattice pattern but because of the variable angles of incidence on the various crystals, these rings, although sharp on their inner boundaries, fall off less rapidly on their outer edges. In this type of diffraction from the hexagonal basal planes of ZnO, the rings formed coincide with the space grating reflections of the type *hk*0, which were shown above to be too weak. Although cross grating reflections from prism planes coincide with some of the observed reflections which are too strong, it is almost certain that the basal plane effect should predominate, so that the observed intensities cannot be explained by cross grating effects. Furthermore, the asymmetry of the lines associated with this type of diffraction is not observed in the pattern.

[10] F. Kirchner, Ann. d. Physik **13**, 45 (1932).

[11] K. Lark-Horovitz and H. J. Yearian, Phys. Rev. **43**, 276 (1933).

* This explanation of "fractional orders" does not require that they be rational fractions of some plane; they can be any fraction depending upon the lattice potential and the plane spacing. Recently also G. P. Thomson has advanced this explanation (G. P. Thomson, Phil. Mag. **18**, 640 (1934)).

** See for instance the development of zinc crystals, *Handbuch der Physik* (1934), Vol. 24, No. 2, pp. 811–821.

† An effect similar to the one observed by L. H. Germer in another connection. Phys. Rev. **44**, 1012 (1933).

[12] Kikuchi, Jap. J. Phys. **5**, 83 (1928); W. L. Bragg, and F. Kirchner, Nature **127**, 138 (1931); Raether, Zeits. f. Physik **78**, 527 (1932); Steinheil, Zeits. f. Physik **89**, 50 (1934).

[13] v. Laue, Zeits. f. Krist. **82**, 127 (1932).

Atom Factor and Deviation from Spherical Symmetry

Since none of the possibilities discussed above seemed to explain the observed intensity distribution, an atom factor calculation has been made in order to investigate the atomic scattering in the crystal lattice.

The intensity calculations were made in the following way. Each of the five exposures on a plate was microphotometered on a recording instrument and the optical density of several peaks was computed and plotted against exposure. The resulting density-intensity curves were found to be linear below densities of 0.9 to 1.0. An exposure which nowhere exceeded this limit was then photometered two or three times at different positions. The superposition of these traces gave a "most probable" trace practically free of uncertainties due to grain of the plate. This trace was then converted to optical density by means of an improved design of the "logarithmic protractor" described previously.[14]

After drawing in a background curve, the converted trace was reduced to a flat background and the positions of all peaks marked. The overlapping peaks were then resolved under the condition of consistent summation of ordinates and areas, and their areas taken as a measure of the corresponding intensities. The various steps are indicated in Fig. 3.

ZnO is a hexagonal close packed lattice Zn (000, 1/3 2/3 1/2) and O (00p, 1/3 2/3 1/2+p); $p=0.375$ and $c/a=1.599$.[15] This gives a structure factor which may be written

$$S=[E_Z+E_0e^{2\pi ipl}][1+e^{2\pi i(1/3h+2/3k+1/2l)}]$$
$$=S_1'\times S_2.$$

S_1' is the structure factor of the molecule and S_2 takes into account the two molecules in the basis. By (1), (on the assumption of spherical atom symmetry, etc.)

$$E=\frac{Z-F}{\sin^2\theta/\lambda^2}$$

so that we may define

$$S_1=S_1'\times\sin^2\theta/\lambda^2=(Z_Z-F_Z)+(Z_0-F_0)e^{2\pi ipl}.$$

In terms of the observed intensities

$$I=c\frac{f|S|^2}{\sin^2\theta},$$

where f is the frequency factor, and S_1 can be calculated

$$S_1=C\sin^3\theta\sqrt{I/f}|S_2|^2,$$

since S_2 is a purely geometrical term.

The mean intensities of fourteen of the best ZnO plates in the range 18–20 kv are shown in column 6 of Table I.* The mean deviations given indicate a quite high reliability, particularly for the stronger peaks. The experimental values of S_1 deduced from these mean values are shown in column 10 and are plotted against $\sin(\theta/\lambda)$ in Fig. 4. In Fig. 5 theoretical F factors for Zn and O are shown and the theoretical values of the scattering functions S_1 calculated from them. Because of the falling-off of the F curves with angle, each $Z-F$ term in S_1 rises with angle and the exponential term produces a separate curve for each value of index l. It is at once obvious how greatly the experimental

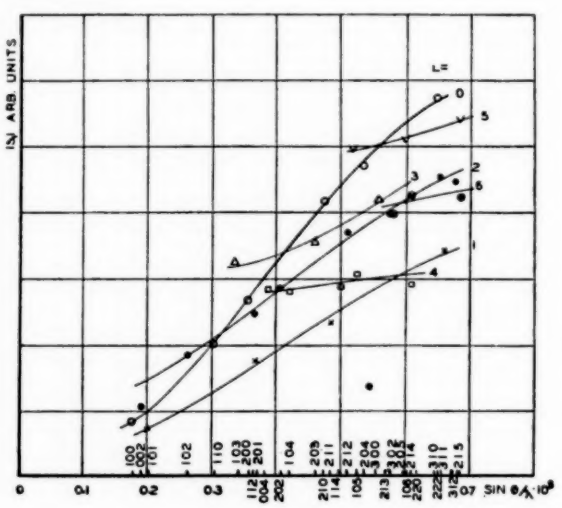

FIG. 4. Observed scattering curves.

[14] H. J. Yearian, Rev. Sci. Inst. **4**, 407 (1933).
[15] Structureberichte, 1913–1918, P. P. Ewald and C. Herman, page 79.

* Calculations have also been carried out for electron velocities up to 80 kv and for temperatures as low as −183 without appreciably different results.

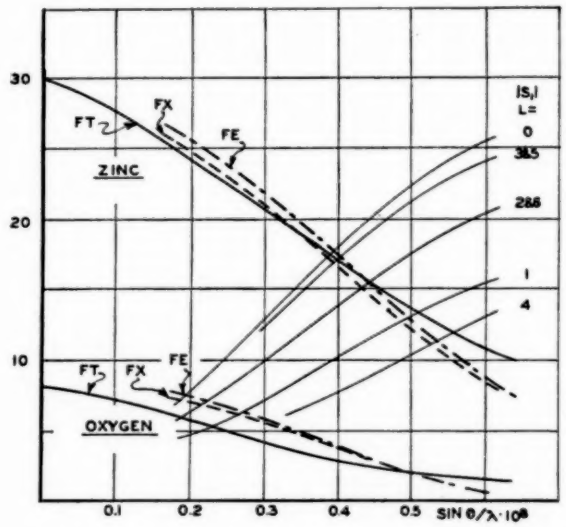

FIG. 5. F curves for zinc and oxygen. FT, theoretical (Pauling and Sherman); FX, experimental x-ray; FE, experimental electron. S_l, ideal scattering curves derived from FT.

intensities differ from the theoretical. Most of the experimental scattering curves at small angles are much too high; the displacement above the expected position is in general greater the smaller the angle and the larger the value of l.

This behavior gives a hint of possible explanation, for if φ is the angle between a reflecting plane and the c axis, then

$$\sin\varphi=(\lambda/\sin\theta)(l/2c)$$

so that the larger l or the smaller $\sin(\theta/\lambda)$ the more nearly is the plane perpendicular to the c axis, and according to the experimental curves, the higher is its reflecting power above normal. This could be accounted for if the x-ray F curves should be decreased below their normal values at the larger values of φ. This would correspond to atomic electron clouds drawn out from a spherical symmetry into an ellipsoidal form with the major axis in the c direction.

X-ray Debye Sherrer photographs of ZnO analyzed in the same way as the electron diffraction photographs, but using the appropriate x-ray intensity formula, gave scattering curves too consistent among themselves to justify the large deviations in F necessary to fit the observed electron curves under the assumption mentioned above. From these x-ray data the F curves (FX) for Zn and O were found. (The parameter p was evaluated to be $p=0.378\pm0.003$.)† The greater slope of these curves, as compared with the theoretical, (FT), may be caused by anomalous dispersion, since Cu K radiation was used. An absorption correction after the method of Rusterholz[16] or Blake[17] would result in still steeper curves. These differences in slope are quite consistent with a temperature correction of the form $e^{-B\sin^2\theta/\lambda^2}$. If the Debye-Waller exponent is used as a rough approximation for the correction in a composite hexagonal crystal, the data are satisfied by a characteristic temperature of $\theta=355°$.

Another explanation of the rise of the observed electron scattering curves with increasing angle φ between c axis and reflecting plane, is suggested by the fact that the electron and nuclear scattering is out of phase. If the center of the electron clouds is not quite coincident with the nucleus but is displaced slightly along the c axis, then an additional phase shift will enter in the structure factor and this will increase the resultant amplitude. This increase would be greatest for large values of l and for F values comparable with Z, i.e., at small values of $\sin(\theta/\lambda)$. This possibility seems reasonable also from considerations of the ZnO structure. In an ideal hexagonal close packed lattice with axial ratio $c/a=1.633$ and parameter $p=3/8=0.375$, each atom is at the center of gravity of a tetrahedron formed by atoms of the opposite kind. In the actual ZnO lattice these relations are disturbed. The axial ratio is $c/a=1.599$ and $p=0.375$. With these values the Zn$-$O distance along c and the altitudes of the tetrahedrons in this direction are decreased about two percent. The distance from a Zn atom to O atom along c is 1.94A, but to its three other O neighbors the distance is 2.041A, a difference of 5 percent. The angles between Zn$-$O bonds are also considerably affected. To maintain equilibrium with these changes, a slight shift of the electron center away from the nucleus might very well arise.

A first approximation to the effect of such a shift was obtained in the following way. Since

† Precision measurements are now being carried out by K. Lark-Horovitz and collaborators.

[16] Rusterholz, Helv. Phys. Acta. **4**, 68 (1931).

[17] F. C. Blake, Rev. Mod. Phys. **5**, 169 (1933).

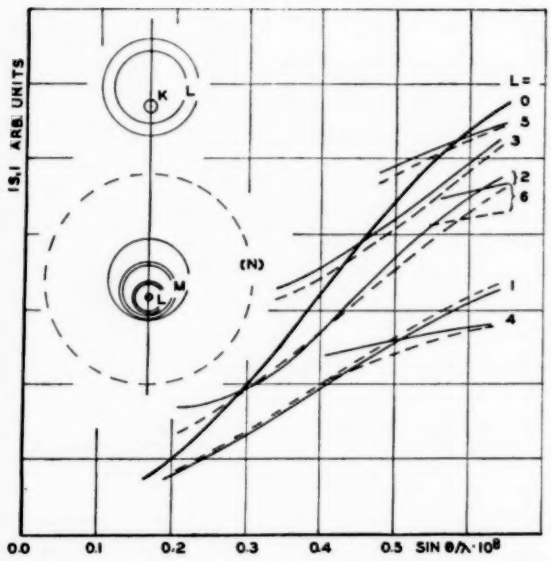

FIG. 6. Calculated scattering curves. Model of ZnO molecule with electron shells displaced to produce dotted curves; (scattering effect of zinc N shell negligible).

the scattering curves for $l=0$ and $l=1$ would be least affected by any dissymmetry along the c axis, these two experimental curves of Fig. 4 were used to calculate the experimental F curves (FE) shown in Fig. 5. Assuming the parameter p for the distance between zinc and oxygen electron centers, q for that between zinc and oxygen nuclei, and a for that between the zinc nucleus and electron center, the structure factor S_l becomes

$$S_l = Z_{Zn} - F_{Zn}e^{2\pi i a l} + Z_O e^{2\pi i q l} - F_O e^{2\pi i (p+a) l}.$$

With the experimental F values and assumed values of p, q and a, this complex summation was carried out. All combinations within the range $0.37<p<0.39$; $0.36<q<0.43$; $-0.05<a<+0.05$ were tried. The only combination which gave curves approaching the experimental ones was with $p=0.38$, $q=0.37$, and $a=-0.015$.

In these trials it was soon found that a very satisfactory set of curves could be constructed if it were allowed to let parameter a increase with angle φ. This would correspond to saying that the effective electron diffracting center of the atom, as approximated by a spherical distribution, moves farther from the nucleus for planes approaching perpendicularity with the c axis. This would seem to be at least possible for an electron distribution somewhat pear shaped in form. The best set of curves obtained under this assumption, with $p=q=0.38$, $a=+0.01$, for $\varphi<55°$ and $a=+0.02$ for φ greater than 55°, is shown as full lines, in Fig. 6. Comparison with the observed curves, Fig. 4, shows a rather remarkable agreement.

The satisfactory nature of this agreement was thought to warrant an attempt to justify the rather arbitrary assumption made of a variable nucleus-electron parameter. Since there is at present no theoretical basis for a rigorous calculation of F factor for a nonspherical electron distribution, an approximation was made by assuming each electron shell displaced a slight but fixed distance along the c axis, each shell remaining spherical.

Using F factors of the various shells from the data of Pauling and Sherman,[18] computations show that satisfactory scattering curves are obtainable with only the M shells displaced. From Bohr-Coster diagrams and the size-screening constants of Pauling and Sherman, the energies and average radii of the 3,0; 3,1 and 3,2 sub-shells of zinc are approximately: $E=136$, 90 and 12 volts per electron; and $R=0.25$, 0.28 and 0.39A, respectively. Keeping the relative displacements of the shells in rough conformation with these data, curves were constructed for various displacements. Denoting the displacements of the electron shells of zinc and oxygen by a_{nl} and b_{nl}, respectively; the set of values, $a_1=a_2=b_1=0$; $a_{3,0}=a_{3,1}=0.01$; $a_{3,2}=0.04=b_2$ corresponding to the model shown gave the dotted curves in Fig. 6. Thus distortion of the M shells alone,* if sufficiently great, may account for the observed intensities.

The rather large changes produced by these displacements are, of course, due to the 180° phase difference which exists between the nuclear and electronic scattering. At small angles where F approaches Z, an additional small phase shift in the summation has a large effect in the sum. These electronic displacements have little effect on the x-ray intensities. X-ray scattering curves computed with the same parameter values do not deviate by more than 5 percent from those calculated without displacements.

[18] L. Pauling and J. Sherman, Zeits. f. Krist. **81**, 1 (1932).

* We are indebted to Dr. Guido Beck for a valuable discussion of this point.

It has been suggested that calculation of the scattering produced by atoms slightly extended from the spherical form along the tetrahedral bond direction, as would be consistent with the peculiar tetrahedral binding in ZnO, might lead to curves in agreement with the experiments.* Rough calculations of the effect of displacing part of the zinc and oxygen scattering power along the four bond directions, instead of along only the c axis as formerly, have been made by the writer. Although such considerations are probably poor approximations of the actual tetrahedral effect, it seems quite conclusive that as long as the scattering centers are equivalent and displaced equally, the general features of the observed curves cannot be reproduced. A dissymmetry among the four directions approximately equivalent to those found in the earlier trials seems to be essential.

Considerations of the possible explanations of the anomalous intensities present in all electron diffraction photographs of zinc oxide, lead to the conclusion that distortions of the atomic electron clouds, which are plausible in principle, must be assumed. The degree of distortion necessary for explanation of the experiments is greater** than would be expected, unless the detailed quantum-mechanical investigation of electron distribution gives an unexpectedly large dissymmetry.

Effects similar to those observed in ZnO are apparently present in the diffraction from BeO, which is of the same crystal type, although sufficiently good photographs for a trustworthy analysis have not yet been obtained. Indications of the effect have been found in diffraction from ZnS and probably also exists in the case of MoS_2 as noted by K. Lark-Horovitz.

My thanks are due Professor K. Lark-Horovitz for the suggestion of this problem, and for his constant aid throughout its course. My thanks are also due Mr. A. I. May and Mr. W. C. Holden, of the Physics Shop, for the great care with which they have carried out the design of the apparatus used in the investigation.

* We are indebted to Dr. H. A. Bethe for a discussion of this possibility. Theoretical calculation of the electron distribution in tetrahedral binding is now in progress in these laboratories under the direction of Dr. L. Nordheim.

** This has been pointed out to us in discussion by Dr. G. Beck.

LETTERS TO THE EDITOR

Prompt publication of brief reports of important discoveries in physics may be secured by addressing them to this department. Closing dates for this department are, for the first issue of the month, the twentieth of the preceding month; for the second issue, the fifth of the month. The Board of Editors does not hold itself responsible for the opinions expressed by the correspondents.

Further Evidence for the Existence of K^{40}

Recently Nier[1] has obtained a peak at the 40 position in the mass-spectrographic analyses of the positive ions generated in potassium vapor, which he has been able to assign to K^{40}. Mass spectra of positive thermions emitted from various potassium sources have been obtained in this laboratory which confirm the existence of this isotope.

The potassium ion source in the present experiments was a platinum disk, 2 mm in diameter, held in position 6 mm above the immergent slit by a tungsten filament to which it was spot-welded. The disk was impregnated with potassium by first coating with a potassium-containing material, basalt and K_3PO_4 being used, and then heating to redness in vacuum for about one hour. After the heating the disk was washed in distilled water to remove any of the coating which might distort the accelerating field. During the heating process the platinum dissolves sufficient potassium to become an excellent emitter of K^+ ions.

[1] A. O. Nier, Phys. Rev. **48**, 283 (1935).

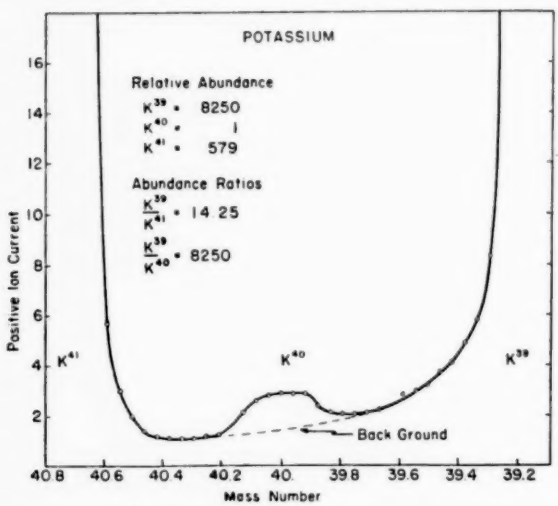

FIG. 1.

The accelerating potential between the disk and slit was maintained at 580 volts. The pressure, as recorded by an ionization manometer, was 3×10^{-6} mm.

A representative analysis of the region between the K^{39} and K^{41} peaks is shown in Fig. 1.

It will be observed that the peak is flat-topped and that the background is comparatively small.

The K^{39}/K^{41} abundance ratio has been measured for a large number of inorganic sources and has been found to be close to 14.25 with a probable error of about 0.03. The K^{39}/K^{40} abundance ratio estimated from curves of the type shown in Fig. 1 lies within the range of 8300 ± 100 in most every instance. The principal source of error is in the estimation of the background. These ratios are close to those obtained by Nier who found $K^{39}/K^{41}=13.96\pm0.1$ and $K^{39}/K^{40}=8600$.

The possibility of the observed peak being due to Ca^{40} is small since large changes in the calcium content of the source had no effect on the observed ratio; the measurements were made at a filament temperature below which a Ca^+ emission could be detected. The possibility of the peak being due to $K^{39}H^+$ is remote. It could not be due to a hydride formed about K^{39} ions in transit between the disk and slit since the chance of such formation is small and since ions so formed give a diffused and not a sharply defined peak. Again it is difficult to ascribe the peak to $K^{39}H^+$ ions emitted from the platinum since fresh filaments gave essentially the same ratio as did those that had been heated for 12 hours at 700°C; the high dissociation pressure of potassium hydride should materially reduce its concentration during this heating period. The fact that the abundance ratio is essentially the same as that obtained by Nier from an entirely different type of ion source strongly suggests the existence of an isotope of potassium of mass 40.

A. KEITH BREWER

Fertilizer Investigations,
Bureau of Chemistry and Soils,
U. S. Department of Agriculture,
Washington, D. C.,
August 30, 1935.

THE AMERICAN INSTITUTE OF PHYSICS

INCORPORATED

GOVERNING BOARD

For The American Physical Society:

KARL T. COMPTON, *Chairman*
Massachusetts Institute of Technology

GEORGE B. PEGRAM, *Secretary*
Columbia University

JOHN T. TATE
University of Minnesota

For The Optical Society of America:

E. C. CRITTENDEN
Bureau of Standards

PAUL D. FOOTE
The Gulf Companies

F. K. RICHTMYER
Cornell University

For The Acoustical Society of America:

HARVEY FLETCHER
Bell Telephone Laboratories

VERN O. KNUDSEN
University of California at Los Angeles

WALLACE WATERFALL
The Celotex Company

For The Society of Rheology:

E. C. BINGHAM
Lafayette College

A. STUART HUNTER
du Pont Rayon Company

S. E. SHEPPARD
Eastman Kodak Company

For The American Association of Physics Teachers:

HOMER L. DODGE
University of Oklahoma

PAUL E. KLOPSTEG
Central Scientific Company

FREDERIC PALMER
Haverford College

ADMINISTRATIVE STAFF

HENRY A. BARTON, *Director* JOHN T. TATE, *Adviser on Publications*

MADELINE M. MITCHELL, *Editorial Secretary*

Office: 11 East 38th Street, New York, New York

JOURNALS

THE PHYSICAL REVIEW

REVIEWS OF MODERN PHYSICS

PHYSICS
JOHN T. TATE, *Editor*
J. W. BUCHTA, *Assistant Editor*
E. C. BINGHAM, *Rheology Editor*

THE JOURNAL OF THE OPTICAL SOCIETY OF AMERICA

THE REVIEW OF SCIENTIFIC INSTRUMENTS
WITH PHYSICS NEWS AND VIEWS
F. K. RICHTMYER, *Editor*

JOURNAL OF THE ACOUSTICAL SOCIETY OF AMERICA
F. R. WATSON, *Editor*

THE JOURNAL OF CHEMICAL PHYSICS
HAROLD C. UREY, *Editor*

THE AMERICAN PHYSICS TEACHER
DUANE ROLLER, *Editor*

The American Institute of Physics is a membership corporation of which five societies are the founding members. These five societies are the principal national societies devoted to pure and applied physics in America. Their names, and those of their representatives who form the Governing Board of the Institute, are given above. The principal work of the Institute is the publication of journals sponsored by the societies or by itself. The names and the editors of the journals are also listed above.

The broad purpose of the Institute is to represent, in all matters of wide or common interest, the five thousand or more members and subscribers associated with the Founder Societies and the journals. It aims to advance the science and profession of physics, and to promote cooperation between pure research, the applied sciences and the industries. To achieve these aims, it is greatly in need of an endowment and is empowered by law to administer grants and funds of any kind.

CONTENTS

PHYS. REV. 48 (1935) OCTOBER 1

Diffuse Scattering of X-Rays by Conduction Electrons . . CLARENCE ZENER 573

Extra Negative Term in the Incoherent Part of the Diffuse Scattering of X-Rays from Neon-Like Crystals. G. E. M. JAUNCEY AND J. H. DEMING 577

On the Structure and Interpretation of the Infrared Absorption Spectra of Crystals . . . . . R. BOWLING BARNES, R. ROBERT BRATTAIN AND FREDERICK SEITZ 582

Spectra of Strontium Hydride . . . . . W. R. FREDERICKSON, M. E. HOGAN, JR. AND WILLIAM W. WATSON 602

$3p^3\Sigma \rightarrow 2s^3\Sigma$ Bands of HD and D_2 . . . . . G. H. DIEKE 606

Triplet $3p$ Complex of the Hydrogen Molecule. . . . . G. H. DIEKE 610

Magnetic Anisotropy of Crystals of Sn, and of Sn with Added Sb, Cd, or Ga. . . . . HAROLD J. HOGE 615

Principal Expansion Coefficients of Single Crystals of Mercury . . . . . DONALD M. HILL 620

Quenching of Cadmium Resonance Radiation by Foreign Gases. . . . . HARRY C. LIPSON AND ALLAN C. G. MITCHELL 625

Intensity of Diffraction of Electrons by ZnO . . . . . H. J. YEARIAN 631

Letters to the Editor:

Further Evidence for the Existence of K^{40} . . . . . A. KEITH BREWER 640

LANCASTER PRESS, INC., LANCASTER, PA.